

**Investigating the Scalability of
Incoherent OCDMA Systems based
on Ultrashort Optical Pulses**

By

Tolulope Babajide Osadola

A thesis submitted for the Degree

Of

Doctor of Philosophy

Centre for Intelligent & Dynamic Communications

Department of Electronic & Electrical Engineering

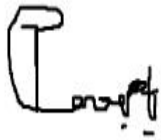
University Of Strathclyde

Glasgow, United Kingdom.

March 2015

Declaration

This thesis is the result of the author's original research. It has been composed by the author and has not been previously submitted for examination, which has led to the award of a degree. The copyright of this thesis belongs to the author under the terms of the United Kingdom Copyright Acts as qualified by University of Strathclyde Regulation 3.50. Due acknowledgement must always be made of the use of any material contained in or derived from this thesis.

A handwritten signature in black ink, appearing to be 'L. Wang'.

Signed:

Date: 30/03/2015

Committee in-charge:

Convenor: Dr Vladimir Stankovic

External Examiner: Dr Xu Wang

Internal Examiner: Dr Craig Michie

Preface

This thesis is submitted to the University of Strathclyde in partial fulfilment of the requirements for the degree of doctor of philosophy.

This doctoral work has been carried out at the Department of Electronic and Electrical Engineering, Centre for Intelligent Dynamic Communications (CIDCOM), with Prof Ivan Glesk as main supervisor and Prof Ivan Andonovic as co-supervisor.

This PhD has been funded by the University of Strathclyde Postgraduate Research Award and Scottish Overseas Research Award Scheme (SORSAS).

Abstract

In a world where bandwidth hungry applications are constantly being churned out to an ever ready sea of consumers most of which are eager to experience the latest means of accessing information of various size and formats, there is an ever growing need for increased network capacity to cope with these demands. Optical code division multiple access (OCDMA) technology has long been researched as a possible solution for high bandwidth multi-access networking. The focus of my investigation is on incoherent OCDMA systems based on two-dimensional wavelength-hopping time-spreading (2D-WH/TS) incoherent OCDMA codes that utilize picosecond multi wavelength pulses. I have conducted experiments to characterise the encoding process of the incoherent optical CDMA transmitter which utilises low cost fibre Bragg gratings (FBG) based all optical encoders and decoders. I have tested the viability and practicality of the incoherent OCDMA system by conducting analysis of its performance under real-life conditions. I have investigated the performance of the picosecond code based optical signal when subjected to temperature variations similar to that experience by most buried fibre systems. I have proposed and demonstrated a novel hybrid system that combined the best of OCDMA and optical time division multiple access (OTDMA) to achieve increased network scalability. The field based demonstration was performed over a fully chromatic dispersion compensated 17-km bidirectional fibre link between Strathclyde and Glasgow University. The compensation of the chromatic dispersion of the link was maintained with sub-picosecond accuracy.

Acknowledgements

I will like to thank the Almighty God who has been with me throughout my PhD programme. Also, the writing of this doctoral thesis would have been more difficult without the help and support of the awesome people around me, some of whom I will give particular mention here.

Firstly, I sincerely appreciate the effort of my supervisor Professor Ivan Glesk who has played a great role in ensuring that I complete my thesis. His encouragement, motivation and passion for excellence was an important factor that helped me pull through.

My immense gratitude goes to my second supervisor, Professor Ivan Andonovic. I also appreciate the intellectual support from my colleague Dr Siti Khadijah Idris, and all other PhD researchers at the centre for intelligent and dynamic communications (CIDCOM) too numerous to mention.

The research I conducted in the course of my PhD would not have been possible without the help of my industrial collaborators in the person of Dr Gwaneshwar Gupta and Kensuke Sasaki, of Oki Electric Company Japan. Special thanks also go to Professor Wing. C. Kwong of Hofstra University New York USA for his expert guidance, advice and efforts in proofreading some of the manuscripts I published in the course of this research. I really enjoyed the time I spent on the research visit to Hofstra University facilitated by him.

Finally, I would like to appreciate my loving wife Olajumoke Osadola, my wonderful son Jeremy Mojolaoluwa Osadola for their extraordinary emotional support and great patience at all times, for always being there to encourage me at those time when I felt like giving up. To my Mum, siblings and in-laws, I say thank you for your prayers and for your

confidence in me. This thesis is dedicated to the memory of my loving father Engineer Albert Osadola who passed away midway into my research programme. I am comforted with the fact that you will be proud of what I have been able to achieve despite all the challenges.

Table of Contents

Declaration	ii
Preface	iii
Abstract	iv
Acknowledgements	v
Table of Contents.....	vii
List of Figures.....	xi
List of Abbreviations	xviii
List of Symbols	xxi
Chapter 1 Introduction.....	1
1.1 Motivation.....	1
1.2 Existing Optical Multiple Access Systems	3
1.3 Merits and Applications of OCDMA.....	4
1.4 Aims of this Research.....	5
1.5 Organisation of this Thesis.....	6
1.6 Summary of Contributions	7

Chapter 2 Optical Code Division Multiple Access Network	12
2.1 Introduction	12
2.2 Concept of OCDMA Systems	14
2.3 Coherent Optical CDMA	15
2.4 Incoherent Optical CDMA	15
2.4.1 1D-OCDMA (Prime) Codes	16
2.4.2 2D-Wavelength Hopping time Spreading (WH/TS) codes	17
2.5 Origin of Multi-Access Interference in a 2D-WH/TS OCDMA System.....	21
2.6 Novel Power Saving Architecture Based on FBG Encoders using 2D-WH/TS OCDMA Codes.....	24
2.7 Chapter Summary	30
Chapter 3 Effect of Variations in Environmental Temperature on 2D- WH/TS OCDMA Code Performance	32
3.1 Introduction	32
3.2 Optical Fibres	33
3.2.1 Single Mode Optical Fibre	34
3.2.2 Multimode Fibre	35
3.3 Optical Fibre Attenuation.....	36
3.4 Dispersion	37

3.5	Temperature Dependence of Fibre Chromatic Dispersion	39
3.6	Impact of Temperature Fluctuations on Autocorrelation of Incoherent 2D-WH/TS OCDMA Codes	40
3.6.1	2D-WH/TS Code Cardinality	41
3.6.2	Analysis of OCDMA Code Propagation.....	41
3.7	Improving System Design for Better Performance.....	52
3.8	Chapter Summary.....	54
Chapter 4 Improving Performance of 2D-WH/TS Optical CDMA with all-Optical Signal Processing		
		56
4.1	Introduction.....	56
4.2	Wavelength Pulse Power Inequality in FBG Encoded OCDMA Codes.....	57
4.3	Single mode-Multimode-Single mode fibre structure.....	58
4.4	Experimental Demonstration of In-Situ Redistribution of Wavelength Power in FBG Encoded OCDMA.....	60
4.5	Chapter Summary.....	70
Chapter 5 Achieving Network Scalability Using OCDMA over OTDM....		
		71
5.1	Introduction.....	71
5.2	Optical TDM.....	73
5.3	OCDMA over OTDM System Architecture	74

5.3.1 Scalability Calculation.....	77
5.3.2 Experimental Demonstration and Results	80
5.4 Chapter Summary.....	85
Chapter 6 Towards Highly Scalable hybrid incoherent OCDMA Systems and Improved Data rates	87
6.1 Introduction.....	87
6.2 Design of Highly Scalable OCDMA over OTDM Hybrid System	89
6.2.1 P x M-Users incoherent OCDMA	90
6.2.2 Scaling to P x M-Users x N channels	91
6.2.3 Proposed Receiver Architecture	92
6.3 Scalability and Power Calculations.....	94
6.4 Chapter Summary.....	97
Chapter 7 Conclusion and Future Work	99
7.1 Conclusion	99
7.2 Future Work	101
References	103

List of Figures

- Figure 1.0 Trend of growth in number of individuals using the internet per 100 inhabitants between 2001 and 2013 [Source: ITU World Telecommunication /ICT Indicators database].
- Figure 2.1 An Optical CDMA Network. Mod-Modulator.
- Figure 2.2 A concept of 2D-Wavelength-Hopping Time-Spreading (2D-WH/TS) OCDMA code, where p_i is number of used time chips and w is number of used wavelengths (a code weight).
- Figure 2.3 2D-Wavelength Hopping Time Spreading OCDMA code generation using arrayed waveguide gratings (AWG).
- Figure 2.4 2D-Wavelength Hopping Time Spreading OCDMA code generation using thin-film filters.
- Figure 2.5 2D-Wavelength Hopping Time Spreading OCDMA code generation using integrated fibre Bragg gratings.
- Figure 2.6 Illustration of a K user OCDMA system showing the output of each user's encoder and the (autocorrelation and cross correlations) output of the decoder matched to a particular user K .
- Figure 2.7 Architecture of a multiuser OCDMA signal generation. The input multi wavelength pulse is splitted N times and distributed to each of the FBG based OCDMA transmitters representing up to N simultaneous users. Where Mod is Modulator.
- Figure 2.8 Illustration of the experiment to determine the percentage of input optical supercontinuum (OSC) power that is converted into an FBG encoded optical CDMA code.

- Figure 2.9 Optical spectrum of (a) multi wavelength signal input from port 1 (b) unreflected signal coming out of port X of the encoder and (c) OCDMA encoded signal output from port 3 of the FBG based OCDMA encoder.
- Figure 2.10 Original architecture of the multiuser FBG based OCDMA signal generation. Showing input and output powers of the OCDMA encoders.
- Figure 2.11 Modified architecture of the multiuser FBG based OCDMA signal generation. The encoders have been cascaded to enable the reuse of unreflected multi wavelength optical. The input optical splitter has also been replaced with a cheaper alternative. Where Mod is Modulator.
- Figure 3.1 Physical geometry of a single mode optical fibre showing the core and the cladding.
- Figure 3.2 Physical geometry of a multimode optical fibre showing a considerably larger core and the cladding.
- Figure 3.3 Illustration using a digital pattern 1011 of pulse broadening as light is transmitted along a fibre: (a) fibre input; (b) fibre output at a distance L (km).
- Figure 3.4 Decoding of the 2D-WH/TS OCDMA code after its propagation in a fully dispersion compensated fibre link under ideal conditions; with no code matrix distortion after code propagation. The resulting autocorrelation signal is undistorted.
- Figure 3.5 Decoding of the 2D-WH/TS OCDMA code after its propagation in a fully dispersion compensated fibre link under practical conditions with code matrix distortion after code propagation when the fibre temperature has changed. The resulted autocorrelation signal is distorted due temperature induced temporal skewing effect.

- Figure 3.6 Plot of autocorrelation signal formed by decoding OCDMA transmission based on 2D-WH/TS OCDMA codes with 2 ps, 8 wavelength pulses after experiencing 20°C temperature variation over a distance of 0 km (back-to-back). The fibre temperature coefficient used for calculation $D_{temp} = 0.0025$ ps/nm • km/°C .
- Figure 3.7 Plot of autocorrelation signal formed by decoding OCDMA transmission based on 2D-WH/TS OCDMA codes with 2 ps, 8 wavelength pulses after experiencing 20°C temperature variation over a distance of 10 km.
- Figure 3.8 Plot of autocorrelation signal formed by decoding OCDMA transmission based on 2D-WH/TS OCDMA codes with 2ps, 8 wavelength pulses after experiencing 20°C temperature variation over a distance of 20 km.
- Figure 3.9 Plot of autocorrelation signal formed by decoding OCDMA transmission based on 2D-WH/TS OCDMA codes with 2 ps, 8 wavelength pulses after experiencing 20°C temperature variations over a distance of 40 km.
- Figure 3.10 Maximum obtainable autocorrelation height for an (8,200), 2D-WH/TS code as temperature increases over a 10 km and 20 km link.
- Figure 3.11 Maximum obtainable autocorrelation height after a (8,200), 2D-WH/TS code propagates in fibre under the influence of environmental temperature swing.
- Figure 3.12 Performance curves for an (8,200) 2D-WH/TS OCDMA system illustrating (a) case where T is constant, (b) case where T changes by 20°C and code propagation distance is 7 km, (c) case where T changes by 20°C and code propagation distance is 10 km.

- Figure 3.13 Minimum obtainable bit error rates as ΔT increases over a 10 km and 20 km fibre link respectively.
- Figure 3.14 Transmission distance against code spectral allocation for a 200 chips OCDMA system using 2D-WH/TS OCDMA codes when the total temperature induced skew is below 1 chip duration. $\Delta\lambda$ is the wavelength spacing. Code spectral allocation is directly related to the code weight.
- Figure 4.1 Architecture of a multiuser OCDMA signal generation. The input multi wavelength pulse is splitted N times and distributed to each of the FBG based OCDMA transmitters representing up to N simultaneous users. Where Mod is Modulator.
- Figure 4.2 Experimental setup to demonstrate wavelength power redistribution in OCDMA transmission using PLC-MMF. Where C is Circulator, Att is Attenuator, OSA is Optical Spectrum Analyser, OSC is Oscilloscope and DDF is Dispersion decreasing fibre.
- Figure 4.3 Optical spectrum of OCDMA signal showing the power distribution among individual wavelengths within the code at the input of PLC-MMF module.
- Figure 4.4 Non equalized optical spectrum of OCDMA signal showing the power distribution among individual wavelengths within the code after passing PLC-MMF module but with polarization settings not optimized.
- Figure 4.5 Optimized optical spectrums of OCDMA signal showing the power distribution among individual wavelengths within the code: after passing PLC-MMF module with different settings of PLC.

- Figure 4.6 OCDMA code modulated with USER 1 data as seen on the oscilloscope via an 11GHz bandwidth limited optical receiver.
- Figure 4.7 Obtained autocorrelation after decoding a single user OCDMA data transmission by decoder matched to USER 1 encoder.
- Figure 4.8 Obtained autocorrelation signal at the USER 1 OCDMA decoder output showing autocorrelation peaks corresponding to received USER 1 data and the MAI resulting from simultaneous users broadcasting on the network without PLC-MMF module implementation.
- Figure 4.9 Obtained autocorrelation signal at the USER 1 OCDMA decoder output showing autocorrelation peaks corresponding to received USER 1 data and the MAI resulting from simultaneous users broadcasting on the network with PLC-MMF module implementation.
- Figure 4.10 BER versus received optical power for case of OCDMA transmission over 17 km long bidirectional fibre optical link between Strathclyde and Glasgow University. Squares: PLC-MMF module used; circles: no PLC-MMF module used.
- Figure 5.1 A sequence of optical time division multiplexed channels forming a periodic frame. Where Ch is channel.
- Figure 5.2 Illustration of a hybrid optical system formed by overlaying multiuser OCDMA into each channel of an OTDM frame to increase scalability.
- Figure 5.3 Architecture of the transmitter for the hybrid OCDMA over OTDM system showing different M-User OCDMA being combined to form a time division multiplexed optical signal. That is launched into the fibre optic link.

- Figure 5.4 Illustration of the receiver showing M-User OCDMA signals being de-multiplexed from different channels /timeslots of the incoming time division multiplexed optical signal. (The demultiplexing stage precedes the per user decoding process).
- Figure 5.5 Performance curves for a standalone M-User OCDMA system showing the changes in error probability as the number of simultaneous users increase. (The first curve is for a system with code weight $w = 4$ and the other curve shows calculations for a system using codes with $w = 8$).
- Figure 5.6 Showing scaling potential of the proposed OCDMA over OTDM network architecture.
- Figure 5.7 Experimental testbed to demonstrate the incoherent OCDMA over OTDM network architecture. Where TG is time gate, EDFA is erbium doped fibre amplifier, FBG is fibre Bragg grating. Att is attenuator, RF is radio frequency, SC is super continuum, ChN is Channel N, TODL is tuneable optical delay line.
- Figure 5.8 Examples of OCDMA traffic over OTDM channels as seen on bandwidth limited oscilloscope; (a) traffic in Ch2 only; (b) traffic in Ch1 and Ch2.
- Figure 5.9 (a) Autocorrelations representing received OCDMA data by the user 1 when is transmitting alone only on OTDM Ch1; (b) only on OTDM Ch 2; (c) both users 1 are transmitting on their channels Ch1 and Ch2, respectively; (d) case in (c) when all other users also transmit on all four OTDM OTDM channels.
- Figure 5.10 Sample eye diagram obtained during the proof of concept experiment to demonstrate the OCDMA over OTDM concept.

- Figure 5.11 BER performance results obtained from the experimental demonstration of incoherent hybrid OCDMA-OTDM OTDM system.
- Figure 6.1 Architecture of the hybrid multi wavelength band OCDMA transmitting over N-Channel OTDM system.
- Figure 6.2 Multiple 2D-WH/TS based OCDMA sub-systems encoded within P individual wavelength bands $\Delta\lambda_P$ to form $P \times M$ Users OCDMA transmitting to the N th OTDM channel.
- Figure 6.3 An N-channel OTDM frame with each channel containing several groups of OCDMA systems in order to increase the system capacity.
- Figure 6.4 Illustration of the stages involved in the demultiplexing of a transmitted $P \times M$ -User \times N channel hybrid 2D-WH/TS OCDMA over OTDM traffic at the receiver. Where is PD photodetector, ps is picosecond, AWG is arrayed waveguide grating with channel spacing $\Delta\lambda$.
- Figure 6.5 Performance curve for OCDMA system with using 2D-WH/TS codes with 5 ps, 8 ps, 10 ps pulse width.
- Figure 6.6 Scalability calculations for the hybrid $P \times M$ -User \times N channel OCDMA over OTDM system.

List of Abbreviations

1D	One-dimensional
2D	Two-dimensional
2D-WH/TS	Two-dimensional wavelength-hopping/time-spreading
Att	Attenuator
AWG	Arrayed waveguide grating
BER	Bit error rate
CDMA	Code division multiple access
DDF	Dispersion decreasing fibre
DSL	Digital subscriber lines
DWDM	Dense wavelength division multiplexing
EDFA	Erbium doped fibre amplifier
FBG	Fibre Bragg gratings
FEC	Forward error correction
FP	Fabry-Perot
FTTB	Fibre to the building
FTTC	Fibre to the cabinet
FTTH	Fibre to the home
FWHM	Full width at half maximum
GF	Galois field
GPON	Gigabit passive optical network
IM/DD	Intensity modulation / direct detection

ISI	Inter-symbol interference
ITU	International telecommunication unit
LAN	Local area network
LED	Light emission diode
MAI	Multi-access interference
MLL	Mode locked laser
MMF	Multimode fibre
MZI	Mach–Zehnder interferometer
O/E	Optical to electrical
OC	Optical circulator
OCDMA	Optical code division multiple access
ODL	Optical delay lines
OOC	Optical orthogonal code
OOK	On-off keying
OSC	Optical supercontinuum
OTDM	Optical time division multiplexing
PC	Prime codes
PD	Photodetector
PLC	Polarisation loop controller
PM	Polarisation-maintaining
PMD	Polarization mode dispersion
PMF	Polarisation-maintaining fibre

PPM	Pulse-positioning modulation
PRBS	Pseudo random binary sequence
RF	Radio frequency
SC	Super continuum
SHG	Second harmonic generation
SMF	Single mode fibre
SPE	Spectral phase encoding
TDM	Time division multiplexing
TFF	Thin film filter
TG	Time gate
TOAD	Terahertz optical asymmetric demultiplexer
TODL	Tuneable optical delay line
VoD	Video on demand
WDM	Wavelength division multiplexing
WH/TS	Wavelength hopping time spreading

List of Symbols

w	Code weight
T_b	Bit period
T_c	Chip width
N_c	Number of chips
τ	Pulse width
Δt	Temperature variation induced temporal skew
$\Delta\tau$	Pulse width shrinking per pulse
D_{temp}	Fibre thermal coefficient
ps	Picoseconds
ΔT	Change in temperature
$\Delta\Lambda$	Spectral spacing
$\Delta\lambda$	Pulse spectral line width
S_t	Autocorrelation signal envelope
P_p	Pulse peak power
P_e	Probability of error
K	Number of simultaneous users
$q_{1,1}$	Hit probability

Δt_{tot}	Total temperature variation induced temporal skew
ε	Spectral efficiency
λ	Wavelength
λ_a	Autocorrelation side lobes
λ_c	Cross-correlation function
T_x	Transmitter
Ch	Channel
t_{ch}	Channel duration (OTDM)
N_{ch}	Number of channels
$\Delta\lambda_P$	Wavelength band
P	Number of wavelength bands
T_s	Sampling window

Chapter 1

Introduction

1.1 Motivation

In the past decade, there has been a phenomenal increase in demand for information and communications technology. Information technology has engulfed almost every aspect of everyday life. Bandwidth hungry applications are constantly being churned out to an ever ready sea of consumers most of which are eager to experience the latest means of accessing information [1].

The explosion of the internet has redefined the way we work, play, and communicate. Traditional methods of television access such as terrestrial broadcasting is giving way to more modern on-demand television in which content is delivered using broadband connection to the home. Businesses are cutting the cost of travel by implementing sophisticated multimedia communication technologies to connect headquarters with other branch offices that may be scattered all over the world thereby improving productivity and enhancing profitability [2].

Figure 1.1 shows the rate of increase in the number of internet users between 2001 and 2013, from the data; we can deduce that the last decade has witness a steady growth in the number of internet users both in developed countries and in developing countries.

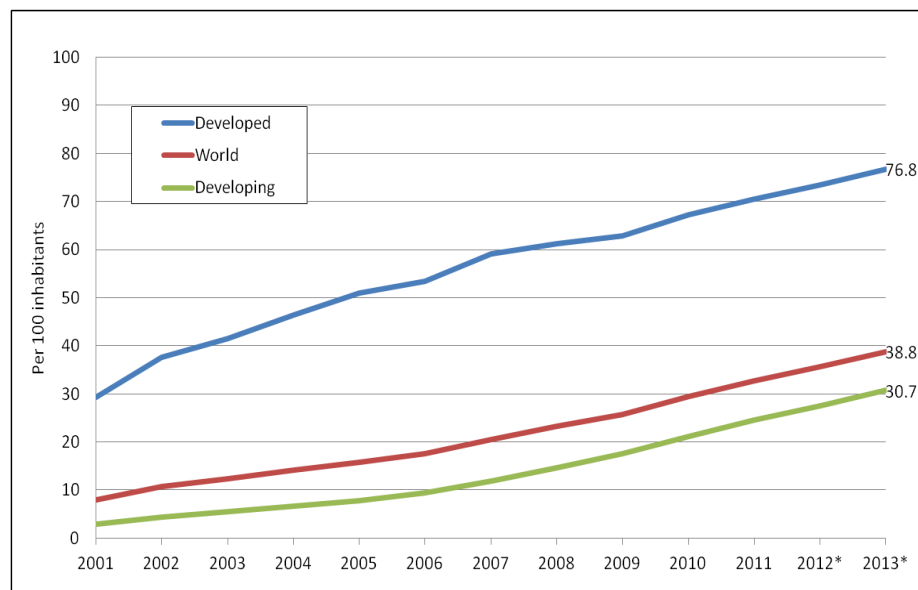


Figure 1.1 Trend of growth in number of individuals using the Internet per 100 inhabitants between 2001 and 2013 [Source: ITU World Telecommunication /ICT Indicators database] [3]

The introduction of cloud computing, text, audio and video based social media, internet based radio and television and need to store large amount of data has revolutionized computing with a gradual shift from the traditional personal computers to the evolution of numerous high capacity datacentres where information is stored and retrieved at any time.

In the midst of these phenomenal changes, the role of telecommunications service providers has also evolved from the traditional voice telephony. All of the above mentioned technologies rely on efficient broadband availability to both homes and business. Therefore telecommunications providers are constantly developing methods of delivering higher broadband speed in a cost effective manner.

At present, the major access network technology being employed by most service providers is the digital subscriber line (DSL) which provides about 1.5 Mbps of bandwidth. This creates a major bottleneck in access network as part of the overall service provider network. No matter the amount of investment in high capacity backbones in the core of the service provider network infrastructure, if the main distribution infrastructure is not capable of delivering the same capacity to end users, it will be difficult to ensure reliable delivery of broadband based services such as video-on-demand (VoD) to the end users.

In the light of these, efficient technologies are now been rolled out in order to maximise the amount of bits of information that can be pushed down to each consumer as fast as possible [4]. This involves redesigning of the telecommunications provider's transport, distribution and access networks and replacing the legacy copper based digital subscriber lines to the consumer premises with fibre optic based technologies like fibre to the cabinet (FTTC), fibre to the building (FTTB) and fibre to the home (FTTH).

1.2 Existing Optical Multiple Access Systems

In order to provide reliable and efficient access solutions in a cost effective manner, service providers must ensure that they maximize the capacity of the existing fibre infrastructure. This has been made possible by the introduction of multiple access techniques in which several users are able to share the same physical infrastructure without compromising security and throughput.

Time division multiplexing (TDM) a technology which allows users to share bandwidth has matured over the years. Several standards for multiple access using TDMA technology already exists [5].

The introduction of wavelength-division multiplexing (WDM) have offered a good solution to increase the capacity of standard passive and active optical networks, this is achieved by assigning different wavelengths to different users [6]. This technology has found wide usage in most backbone and metro networks. However, its adoption in local access networks is still being delayed as a result of its high cost.

Orthogonal frequency division multiplexing (OFDM) is another technique that is being investigated for enhanced optical network throughput. It is a multicarrier technology in which a data stream is carried with many lower-rate subcarriers [7].

Optical code division multiple access (OCDMA) is another alternative technology that can enable multiple users to share the same transmission medium. Considerable attention is being focused on OCDMA because it combines the high bandwidth advantages of the optical fibre with flexibility of CDMA. Instead of assigning one wavelength per user, OCDMA uses the wavelengths to form a code matrix and identifies each user using unique optical codes. OCDMA is not yet standardized as research is still ongoing to determine the best method of implementation.

1.3 Merits and Applications of OCDMA

One of the advantages that OCDMA offers is the capability for asynchronous transmission which greatly simplifies media access control compared to TDMA [8]. In addition, the ability to simultaneously transmit variable code lengths enhances the potential for implementing multi-class traffic.

OCDMA finds potential application in places like local area networks because of its bursty nature. OCDMA can also be potentially deployed in optical interconnects for datacentres. Optical access networking is also another area in which OCDMA could be effectively applied because of the simplicity of asynchronous transmission which it offers.

1.4 Aims of this Research

As a result of the success enjoyed by CDMA technology in the wireless space, several propositions have been made and researched towards replicating similar successful deployment of CDMA technology using optical fibre. In particular the issue of scalability and security have been mentioned as a possible benefit of developing OCDMA as an alternative to WDM or TDM for multiple accesses. However, most of the results earlier reported in the literature have focussed mostly on theoretical calculations that do not take into consideration the peculiar physical characteristics and limitations of the optical fibre medium. The Incoherent approach is the simplest implementation of OCDMA [9] [10]. Incoherent OCDMA systems have been a subject of several investigations since the 1980s. It requires only intensity modulation and direct detection (power summation) of the optical signal pulses. Because only the intensity of the optical pulse can be utilised in incoherent OCDMA schemes, it is not possible to obtain bipolar codes as in coherent OCDMA and this could limit the number of simultaneous users. To somewhat mitigate the above the incoherent two-dimensional wavelength hopping time spreading (2D-WH/TS) coding scheme has been introduced [11].

The incoherent (2D-WH/TS) based OCDMA system offers better cross-correlation properties and can potentially support larger number of simultaneous users [12]. However, to design 2D codes with larger cardinality, a large number of short wavelength pulses must be contained in this coding scheme and the pulse width of these pulses must be accordingly short to fit the code's time chip's width within the bit period used.

It is well known that optical signals propagated in the optical fibre are affected by the properties of the optical fibre. This motivated my intention to study the behaviours of these 2D-WH/TS OCDMA systems with particular focus on codes created using picosecond optical pulses.

In this thesis, the aim is to study practicable aspects of incoherent 2D WH/TS OCDMA implementations with a view to better understand the behaviours of the optically encoded data when they are transmitted in the optical fibre under the effects of the optical fibre impairments. Only incoherent 2D-WH/TS OCDMA will be the subject of focus throughout the thesis.

Another key objective of the research is to investigate novel methods to ensure high quality OCDMA transmission.

OCDMA system scalability will also be investigated. In particular, several hybrid approaches that combines the best of OCDMA with other well-known multiple access techniques will be demonstrated and analysed. This is geared towards achieving increased number of simultaneous users in order to ensure commercial viability.

1.5 Organisation of this Thesis

Chapter 1 summarizes the motivation, the objectives and the main contributions of this research. Chapter 2 then presents an overview of optical code division multiple access systems and current standards; a review of current implementations of OCDMA is also presented in detail with special focus on incoherent 2D-WH/TS OCDMA. Several background topics relevant to the discussions in later chapters were also reviewed. A novel power saving OCDMA code generation architecture was also presented and analysed in-depth.

In chapter 3, a theoretical analysis and a field based performance evaluation of incoherent 2D-WH/TS OCDMA which uses codes based on multi wavelength picosecond pulses under the influence of environmental temperature variations was reported.

Chapter 4 reports a novel in-situ method for wavelength power equalization within OCDMA codes and the resulting improvement in performance of the 2D-WH/TS Optical CDMA by using all-optical signal processing.

A novel architecture for increasing scalability using hybrid OCDMA-over-OTDM is described in chapter 5. Here, field based experimental demonstration and theoretical calculations are presented as well.

In chapter 6, another advanced method for achieving improved scalability of hybrid incoherent OCDMA systems by effectively utilising available wavelength spectrum to achieve increased number of simultaneous users is proposed and analysed.

Chapter 7 presents the conclusion of the thesis and focus on direction for future research opportunities.

It is worth noting that for clarity of expression, the overview of the current state of the art is given at the beginning of each chapter (chapter 2-6) and is relevant to the topic researched in that chapter.

1.6 Summary of Contributions

1. A novel power saving incoherent FBG based OCDMA transmitter architecture has been proposed, demonstrated and analysed.
2. An extensive study was carried out on the performance of incoherent 2D-WH/TS OCDMA codes under the influence of temperature variations resulting from changing environmental conditions.
3. A novel in-situ approach using a novel device for redistribution of power contained in each wavelength pulse for FBG encoded OCDMA has been proposed and demonstrated. The novel device was also

confirmed as an effective tool for improving the performance of the incoherent 2D-WHTS OCDMA systems.

4. A novel network scaling architecture using hybrid OCDMA over OTDM has been proposed and demonstrated.
5. Novel advanced hybrid OCDMA architecture to further increase OCDMA network scalability using incoherent OCDMA over OTDM-WDM was developed, demonstrated and analysed.

List of my publications related to this thesis

In journals:

1. **T. B. Osadola**, S. K. Idris, I. Glesk, “Improving Multi Access Interference Suppression in Optical CDMA by using All-Optical Signal Processing,” *Telfor Journal*, Vol. 5(1), (2013).
2. **T. B. Osadola**, S. K. Idris, I. Glesk, and W. C. Kwong, “Effect of Variations in Environmental Temperature on 2D-WH/TS OCDMA Code Performance,” *Journal of Optical Communications and Networking*, Vol. 5, pp. 68-73, (2013). doi: 10.1364/JOCN.5.000068
3. S. K. Idris, **T. B. Osadola**, and I. Glesk, “Investigation of All-Optical Switching OCDMA Testbed under the Influence of Chromatic Dispersion and Timing Jitter,” *Journal of Engineering Technology (JET)*, Vol. 4 (1), pp. 41-53, (2013).
4. S. K. Idris, **T. B. Osadola**, and I. Glesk, “Towards self-clocked gated OCDMA Receiver,” *Journal of European Optical Society Rapid Publication (JEOS: RP)*, Vol. 8, (13013), pp. 1-6, (2013).
5. S. K. Idris, **T. B. Osadola**, and I. Glesk, “OCDMA Receiver with Built-in All-Optical Clock Recovery,” *Electronic Letters*, Vol. 49 (2), pp. 143-144, (2013). doi: 10.1049/el.2012.3110
6. **T. B. Osadola**, S. K. Idris, I. Glesk, and W. C. Kwong, “Network Scaling Using OCDMA over OTDM,” *IEEE Photonics Technology Letters*, Vol. 24 (5), (2012). doi: 10.1109/LPT.2011.2179924
7. **T. B. Osadola**, S. K. Idris, I. Glesk, K. Sasaki, and G. C. Gupta, “In situ Method for Power Re-Equalization of Wavelength Pulses Inside of OCDMA Codes,” *IEEE Journal of Quantum Electronics*, Vol. 47 (8), pp. 1053-1058 (2011). doi: 10.1109/JQE.2011.2157305

At conferences:

8. **T. B. Osadola**, S. K. Idris, and I. Glesk, "Novel power saving architecture for FBG based OCDMA code generation," *Proc. SPIE 8915*, Photonics North 2013, 89150H (October 11, 2013); DOI: 10.1117/12.2037500; <http://dx.doi.org/10.1117/12.2037500>.
9. S. K. Idris, **T. B. Osadola**, and I. Glesk, "Experimental Investigation of 2D-WH/TS Codes based on PS Multi-Color Pulses," *21th Telecomm.Forum*, pp. 903-906, TELFOR 2013.
10. **T. Osadola**, S. Idris; I. Glesk; W. Kwong "Investigating the influence of thermal coefficients on 2-D WH/TS OCDMA code propagation in optical fiber," CLEO EUROPE/IQEC, 2013, vol.1, no.1, pp. 12-16 May 2013
11. **T. B. Osadola**, S. K. Idris, and I. Glesk, "Novel Method for multi access interference suppression in multi wavelength FBG-encoded OCDMA", *20th Telecomm. Forum*, pp. 907-910, TELFOR 2012.
12. S. K. Idris, **T. B. Osadola**, S. Shaukat, and I. Glesk, "All-Optical Clock Recovery for OCDMA Systems with optical time gating," *20th Telecomm. Forum*, pp. 903-906, TELFOR 2012.
13. S. K. Idris, **T. B. Osadola**, and I. Glesk, "OCDMA Receiver with built-in All-Optical Clock Recovery," Post-deadline submission, *4th European Optical Society Annual Meeting*, EOSAM 2012 , 25-28 September 2012, Aberdeen, Scotland.
14. **T. B. Osadola**, S. K. Idris, I. Glesk, and W. C. Kwong, "Improving Network Scalability Using OCDMA over OTDM" *Optical Fibre Communication Conference and Exhibit, 2012, OFC 2012*.
15. Glesk, **T. B. Osadola**, S. K. Idris, K. Sasaki, and G. C. Gupta, "Demonstration and Analyses of a Hybrid Multiplexing Scheme for

Scaling-Up the ‘Last Mile’,” *14th International Conference on Transparent Optical Networks*, Invited paper, (*ICTON*), 2012.

16. Glesk, **T. B. Osadola**, S. K. Idris, K. Sasaki, and G. C. Gupta, “Evaluation of OCDMA system deployed over commercial network infrastructure,” *13th International Conference on Transparent Optical Networks (ICTON), 2011*, pp. 1-4, 26-30, June 2011.
17. Glesk, M. N. Mohd Warip, S. K. Idris, **T. B. Osadola**, and I. Andonovic, “Towards Green High Capacity Optical Networks,” *7th International Conference on Photonics, Devices and Systems, ARTEMIS Olympik Hotel-Congress Centre, Prague, Czech Republic, August 24 - 26, 2011*.
18. **T. B. Osadola**, S. K. Idris, I. Glesk, I. Andonovic, C. Michie, A. E. Kelly, and M. Sorel, “Strathclyde-Glasgow fibre-optic test bed for testing ultra-high speed communications,” Poster presentation in Scottish Research Partnership in Engineering (SRPe) Conference- Showcasing Engineering Research. Dynamic Earth, Edinburgh, 15th February 2011.

Chapter 2

Optical Code Division Multiple Access Networks

2.1 Introduction

Code division multiple access (CDMA) technique has been extensively studied and exploited for wireless communications [13, 14] [15]. Fundamentally, CDMA allows the random sharing of communications channels by users. There have been a lot of interest and research in optical CDMA (OCDMA) systems over the past few decades, since 1985, several papers have been written in this area [16, 17]. OCDMA has a unique soft blocking property that enables the trade off between performance and number of simultaneous users.

Another advantage of OCDMA is the elimination of centralized control and management associated with time division multiple access (TDMA) and wavelength division multiple access (WDMA) thereby reducing latency [18]. This is because the unique code sequence which serves as the address of each user in the network is used to distinguish information sent to that user. Since the code sequences of all the users are pseudoorthogonal, two or more users can access the optical fiber channel simultaneously as long as they are sending to different receivers. Any user can access the transmission medium whenever there is information to be transmitted. This explains why OCDMA has been suggested as a possible alternative to both TDM and WDM.

There are two major approaches to OCDMA coherent and incoherent. The focus of this work is incoherent OCDMA.

Several techniques have been investigated in the quest for achieving commercially viable optical CDMA technology in both long and short distances communications systems. [19, 20]

Early works relating to incoherent optical CDMA were first reported around 1985 by Hui [20] and Prucnal [21, 16]. Hui's proposed model was based on a broadcast network that utilized tapped delay lines to generate and detect optical patterns. Hui's work also mentioned the use of linear amplification and hard limiting to achieve regeneration of weak coded optical signals. Hard limiting involves setting the value of digital signal to one if the input light amplitude exceeds a certain threshold and zero if the amplitude is below the threshold. At the time of Hui's publication, achieved bandwidth of 1 Mbps was still classified as "extremely high".

While the work of Hui was mostly theoretical, in 1986, Prucnal et al. [16] demonstrated a spread spectrum CDMA local area network by using optical fibres as delay lines for incoherent signal processing. It is here that the foundations of incoherent optical CDMA that will employ all optical signal processing and use devices such as mode-locked laser, optical modulators,

and fibre optic delay lines encoder/decoder and fibre optic transmission medium was laid.

In this chapter, a background and general overview of OCDMA is presented and discussed in detail.

2.2 Concept of OCDMA Systems

Figure 2.1 shows a typical representation of an OCDMA network.

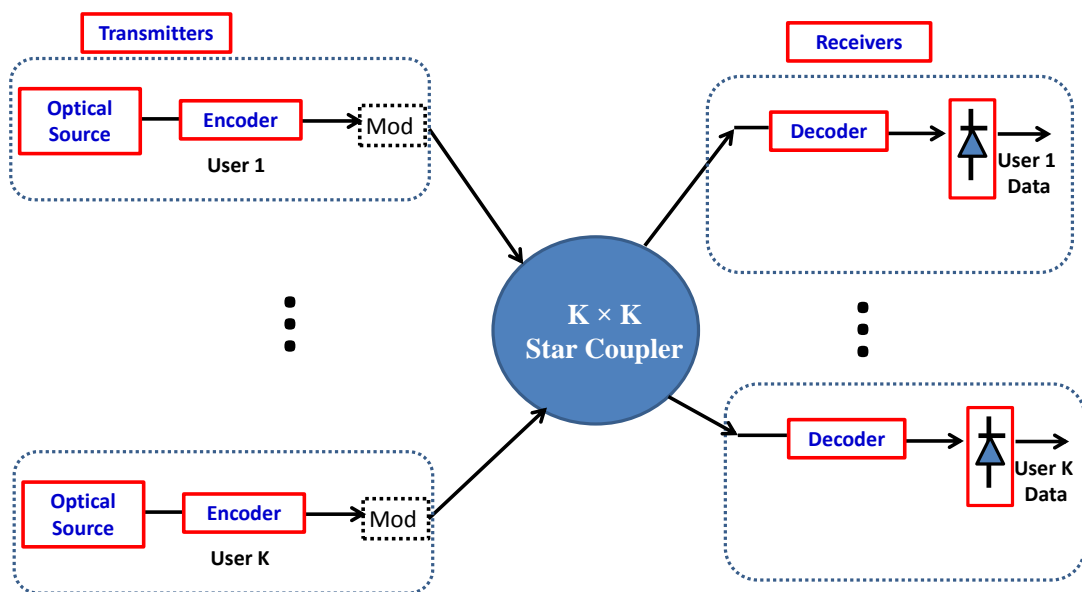


Figure 2.1 An Optical CDMA Network. Mod-Modulator

In the network shown in figure 2.1, M nodes are connected using a passive star coupler. Data from each of the users in the network will be encoded with a unique optical code before being combined with encoded data from other users and thereafter coupled into the fibre optic transmission link for onward broadcast to all receivers. For each user's encoder there is a corresponding unique matching decoder. Therefore all users in the network will receive broadcasted optical signal containing encoded data of all other users, they can only decode data that is specifically matches their decoding sequence. Both coherent and incoherent optical signal processing methods

have been proposed and demonstrated for OCDMA systems [22, 23, 24, 25, 26].

2.3 Coherent Optical CDMA

Coherent OCDMA systems are systems in which the encoding of the optical signal is achieved by the modulation of the phase property. There are several variations of coherent OCDMA code types that have been proposed and previously demonstrated [26]. Examples of such coherent encoding schemes are the spectral phase encoding [17] and the temporal phase encoding [27].

Spectral phase encoded OCDMA systems (SPE-OCDMA) are achieved by the spectral encoding of the broadband spectrum of an optical pulse. In practice, the encoded pulses are usually of very short durations [28]. The code is created by applying different phase shift pattern to each spectral component. In the same way, the decoding is done by applying a phase conjugated pattern to the spectrally encoded signal and the resulting output of the decoder is a recovered spectrum of the original optical pulse. Early experiments on SPE-OCDMA were carried out by Weiner, Heritage and Salehi [28] [29]

Temporal phase optical encoding/decoding [27] is achieved by spreading the input signal in the time domain. To encode a data bit “1” the encoder uses an optical code to generate a sequence of pulses which are relatively phase shifted depending on the sequence of the optical code. Conversely, the decoder reverses the temporal phase shift in order to reproduce the original input optical signal.

2.4 Incoherent Optical CDMA

One of the oldest methods of signal processing is via incoherent manipulation of optical signals. This process involves intensity modulation and direct detection [30, 31]. In the earliest form of incoherent OCDMA proposals, optical delay lines are used to encode fast high intensity optical

pulses into unique code patterns. Each pattern is then multiplexed with other unique code pulses from several other transmitters [31]. At the transmitter, an On/Off keying (OOK) method is used to modulate the optical channel which is a unipolar OCDMA code sequence generated by the encoder. Various methods have been demonstrated for the generation of incoherent OCDMA codes [31, 32].

OCDMA codes are generated based on predefined sequences. Codes can either be one-dimensional (1D) or two-dimensional (2D) [33]. In practice, incoherent one dimensional code can only be defined using one of either time, or wavelength while 2D codes can be defined using a combination of both wavelength (carrier) and time. Key parameters of optical codes include code weight, length, correlation and cardinality. The code weight defines the number of optical carrier wavelength present in the encoded signal. While the code length is the number of timeslots in which optical carrier permutations can be placed. The code length is limited by the signal bit rate and the pulse duration. The cardinality of a code refers to the size of the code set [29]. Ideally larger cardinality, will translate to a larger number of simultaneous OCDMA users. 2D codes are getting much attraction because of its ability to achieve increased cardinality.

2.4.1 1D-OCDMA (Prime) Codes

These are single carrier codes (code weight of 1) in which the spreading pattern is described by a set of unique prime numbered sequence. The first set of prime codes for OCDMA applications was first introduced in 1983 [11]. The prime code is closely related to the extended Reed-Solomon code [34]. The original prime code was constructed using the finite field arithmetic algorithm which is also referred to as the Galois field [35]. In its basic form, to construct a prime sequence $S_i = (s_{i,0}, s_{i,1}, s_{i,2}, \dots, s_{i,j}, \dots, s_{i,p-1})$, each element $s_{i,j}$ can be obtained by the relationship

$$s_{i,j} = i \cdot j \pmod{p}$$

Where p is a prime number, $s_{i,j}$, i, j are all elements of the Galois field $GF(p)$. The maximum achievable cross correlation value of the original prime code is 2 [36]. As a result of this, and other practicality considerations, there exists some strict restriction placed on the original prime code. For example for a prime number p the code weight is restricted to p , the code length should not exceed p^2 and the cardinality cannot exceed p [13, 11].

Other members of the family of prime codes include extended prime code, synchronized prime code, generalized prime code, and modified prime code [11]. The extended prime code [37] was introduced in order to achieve a maximum cross correlation value of 1 which is a 50% reduction when compared to the cross correlation value of the original prime code. The construction of the generalised prime code [38] is done in a manner that will provide greater flexibility of code weight, code length and cardinality without affecting the correlation properties.

2.4.2 2D-Wavelength Hopping time Spreading (WH/TS) codes

The incoherent two-dimensional wavelength hopping time spreading (2D-WH/TS) OCDMA codes are one of several families of OCDMA codes which combine both wavelength and time to form a single code. This coding can potentially support much larger number of codes than the one dimensional codes [39] Figure 2.2 shows a typical wavelength hopping time spreading OCDMA code generated using a 2D algebraic approach.

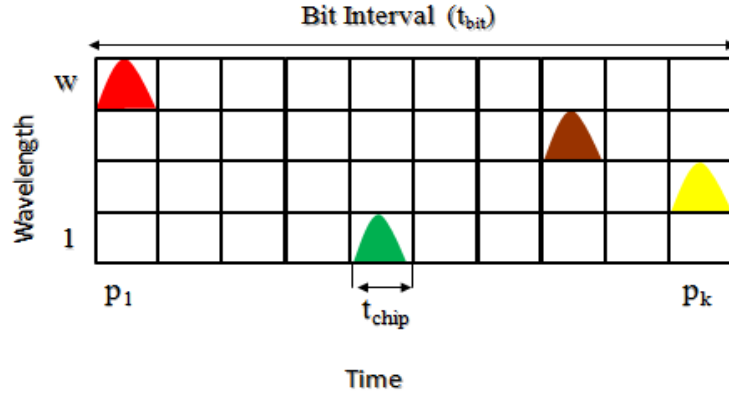


Figure 2.2 A concept of 2D-Wavelength-Hopping Time-Spreading (2D-WH/TS) OCDMA code, where p_i is number of used time chips and w is number of used wavelengths (code weight).

The code sequences are represented as $(p_1 p_2 \dots p_k)$ binary $(0, 1)$ matrices of length $p_1 p_2 \dots p_k$, weight w , and k being a set of prime numbers $\{p_1 p_2 \dots p_k\}$. Note that w is also the number of rows, relating to the number of available wavelengths, and $p_1 p_2 \dots p_k$ is the number of columns, relating to the length of the matrices [31, 33].

Each matrix consists of one pulse (i.e., binary one) per row and each pulse in a matrix is associated with a distinct carrier wavelength, the code has zero autocorrelation side lobes ($\lambda_a = 0$) and cross-correlation function of at most one ($\lambda_c = 1$). Therefore, any 2D-WH/TS code matrix can be described as a set of ordered pairs, where an ordered pair (w, p_k) records the vertical and horizontal position of a binary one from the bottom-leftmost corner of a matrix, w represents the wavelength and t shows the (time or chip) position of a binary one in the matrix [40]. The wavelength hopping time spreading code can thus be denoted as a class of $(w \times p, 0, 1)$ where w is the number of wavelengths and p is the number of chips.

Generation of Incoherent 2D-WH/TS OCDMA Codes

Optical CDMA is made possible by the ability to generate ultrashort light pulses in the picosecond or femtosecond ranges to achieve a uniquely

patterned (coded) pulse train by different bit encoding techniques. One of the most common sources of optical pulses used to generate multi wavelength OCDMA codes is the supercontinuum generation [41]. This method is particularly useful because of its ability to generate picosecond pulses having a very broad spectrum [42].

Another source of multi wavelength optical pulses is by combining multiple pulses from an array of lasers with each laser producing pulses at different wavelengths however the commercial viability of this method is very low because of the high cost of lasers that will be needed to generate the code for each user.

Figure 2.3 shows incoherent OCDMA code generation from supercontinuum (multi wavelength pulse) using arrayed waveguide gratings (AWG) based OCDMA encoding [43].

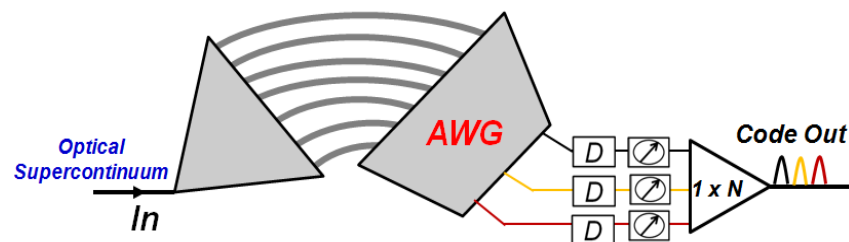


Figure 2.3 2D-Wavelength Hopping Time Spreading OCDMA code generation using arrayed waveguide gratings (AWG) [44].

The AWG is a phased array of optical planar waveguides. Each waveguide in the array provide different wavelength dependent phase shifts to the input signal depending on the length. The code matrix is generated by first passing the input multi wavelength pulse (supercontinuum) through the AWG. Each output port of the AWG produces separate wavelength pulses which then undergo the appropriate delays it needs in order to form the code sequence. The optical attenuator is usually introduced to enable power control between these wavelength pulses. All the individually separated pulses are then combined together to form the OCDMA code.

Another method that can be used to generate OCDMA codes is the use of thin film filters (TFF) [44]. They are basically Fabry-Perot (FP) etalons with cavities surrounded by multiple reflective dielectric thin-film layers. As shown in figure 2.4, the thin film filter performs the same functions as the AWG, in addition, delay and attenuation is needed in order to obtain the required OCDMA code.

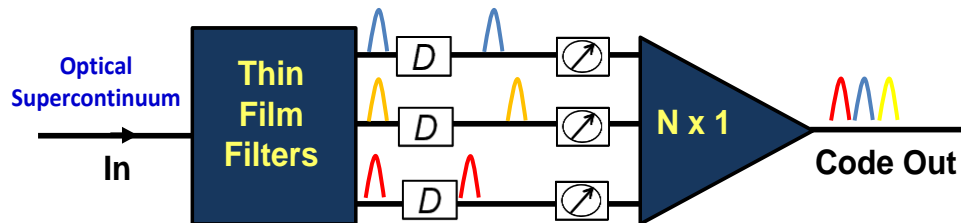


Figure 2.4 2D-Wavelength Hopping Time Spreading OCDMA code generation using thin-film filters [44].

The fibre Bragg grating (FBG) has also been developed for OCDMA encoding and decoding [32] [45]. The advantage of fibre Bragg grating en/decoders is the integrated function of wavelength separation and pulse delay. Also, the fibre Bragg grating can be easy miniaturized to save space. Figure 2.5 shows the process of generating incoherent 2D-WH/TS OCDMA code using fibre Bragg gratings.

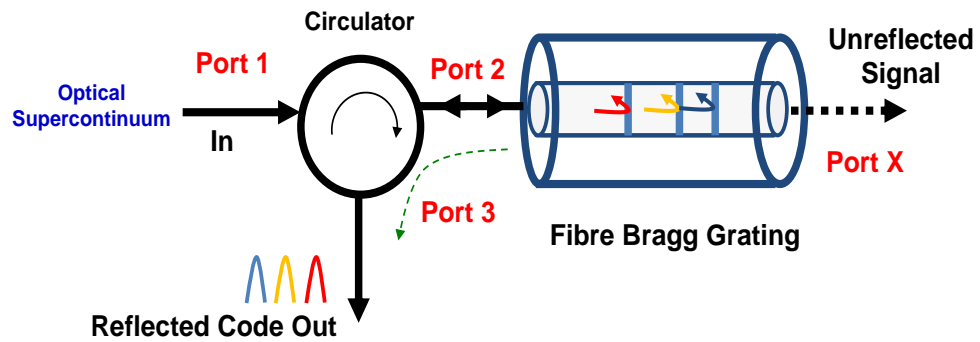


Figure 2.5 2D-Wavelength Hopping Time Spreading OCDMA code generation using integrated fibre Bragg gratings.

At the receiver, the encoded optical pulses are decoded using optical delays to produce the original high intensity optical signal. One of the major drawbacks of intensity modulated systems is the multi-access interference. This can be very severe and is caused by the lack of full orthogonality of intensity modulated signals [10]. The experiments carried out in this thesis was carried out using integrated fibre Bragg grating encoders therefore the next section presents an further study of FBG encoded OCDMA systems.

2.5 Origin of Multi-Access Interference in a 2D-WH/TS OCDMA System

As already known, incoherent OCDMA signals uses intensity modulation to convert electrical data to optical data that can be transmitted through the optical fibre [46, 32]. In the same way, the detection process at the receiver employs direct detection of the optical signal by converting the optical signal to electrical form using the photodetector. However, this conversion is always preceded by the all optical decoding of the received encoded signal.

Figure 2.6 illustrates in detail the process involved in the encoding and decoding process of a 2D-WH/TS OCDMA signal. For a bit period of a digital bit “0”, nothing is transmitted. However every time a digital bit “1” is transmitted, the output of each user’s encoder will be a sequence

wavelength pulses spread within bit period. The encoded traffic of all K users is then combined and launched into the optical fibre.

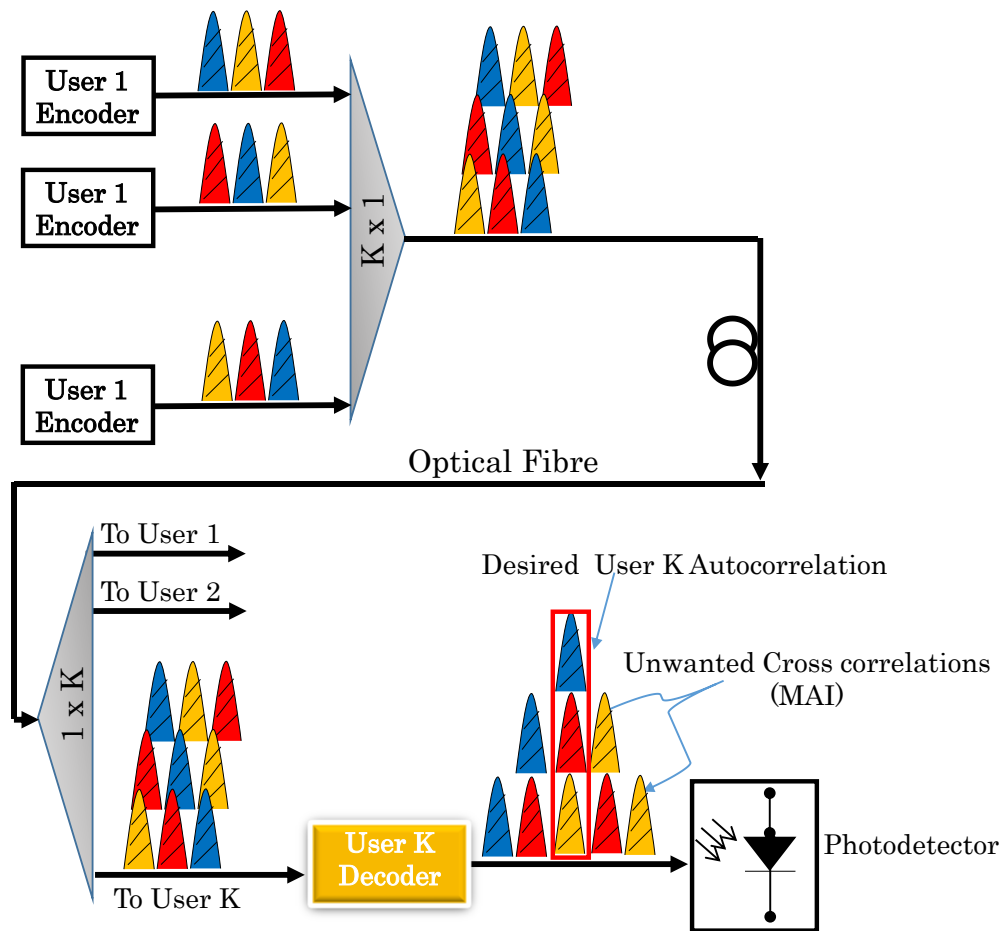


Figure 2.6 Illustration of a K user OCDMA system showing the output of each user's encoder and the (autocorrelation and cross correlations) output of the decoder matched to a particular user K .

At the receiver, the process involves passing the encoded signal which contains optical pulse sequences from multiple users through a reciprocal of the encoding process. This is done in a manner that will ensure that only the pulses corresponding to one single user (desired user) out of the multiple users are completely overlapped to produce an autocorrelation signal. Because of the presence of other transmitting users using different codes, a given user decoder output also consists of cross correlations - pulses formed

by incorrectly decoded codes used by other users on the network, this forms the MAI.

The resulting decoded optical signal (autocorrelation + MAI) is then converted to electrical pulse by a photodiode and sent to a threshold detector. The threshold detector makes the decision whether the signal represents the transmitted bit “1” or bit “0”.

In 2D-WH/TS-based OCDMA systems the proper threshold decision setting is achieved by setting the threshold for detecting the autocorrelation signal (i.e., its height) equal to the code weight w [11].

To improve performance, OCDMA receivers can also employ hard limiting, and time gating, [47, 48]. For a receiver with the hard limiter, if the input light intensity at a time instant is greater than or equal to a fixed decision threshold, th , the intensity of the output is clipped to a fixed level. If the light intensity falls below the threshold, the hard limiter will clip its output to zero. Thus in the event that the threshold of the detector is set equal to the code weight w (usually done for better performance), any autocorrelation signal whose height falls below the code weight is automatically clipped to zero.

Also, the use of time gating [49] can be employed in OCDMA systems in order to minimize the effect of MAI. Usually placed immediately after the decoder, an OCDMA receiver’s time gate (gating window) is tuned to match the time width of the decoded autocorrelation signal. This ensures that only the desired autocorrelation signal is passed onto the detector and cross correlation signal is rejected; thereby reducing errors due to MAI. However, in order to achieve effective time gating, especially in systems where the codes are generated using picosecond pulses, effective and accurate synchronization is required.

Most importantly, it is preferable for the synchronization clock to be recovered directly from the data signal. An all optical method for clock recovery from 2D-WH/TS OCDMA traffic has been reported [49]

In OCDMA systems with coding schemes based on multi-wavelength pulses, in order to achieve the best performance of the OCDMA system, the theory prescribes [39] that these individual wavelengths pulses within the generated OCDMA code should have equal power levels. Fulfilling this requirement is essential towards achieving the desired power relationship between auto and cross-correlation signals in the presence of MAI. This is because during the signal detection, the OCDMA receiver/decoder produces besides the autocorrelation peak carrying data also undesired cross correlations as the result of seeing and incorrectly decoding transmitted codes from simultaneous network users.

It is obvious that depending on relative positions among individual wavelengths pulses within these individual 2D-WH/TS codes, there will be always a non-zero probability that some of these wavelength pulses during decoding process will “accidentally” overlap in such a manner which will result in cross-correlations (MAI) of similar or even taller heights than is the desired correlation peak itself [50, 51]. This will then cause a significant data corruption resulting in undesirable degradation of bit error rate (BER).

The influence of MAI in a multiuser OCDMA system can be very severe especially in incoherent OCDMA implementations that uses simple ON/Off method of data modulation. MAI can cause a significant reduction in the total number of simultaneous users that will be able to transmit conveniently without significant deterioration in performance and this in turn impacts upon the system scalability.

2.6 Novel Power Saving Architecture Based on FBG Encoders using 2D-WH/TS OCDMA Codes

Fibre Bragg grating (FBG) based optical reflectors have been widely used for the purpose of encoding and decoding optical code division multiple

access (OCDMA) data. Both coherent OCDMA and incoherent OCDMA codes can be generated using carefully designed fibre Bragg gratings [43].

In most experiments involving FBG based OCDMA codes, the multi wavelength source signal is usually distributed equally to all users as shown in the transmitter architecture illustrated in figure 2.6. The input multi wavelength pulse is splitted N times and distributed to each of the FBG based OCDMA transmitters corresponding to up to N simultaneous users.

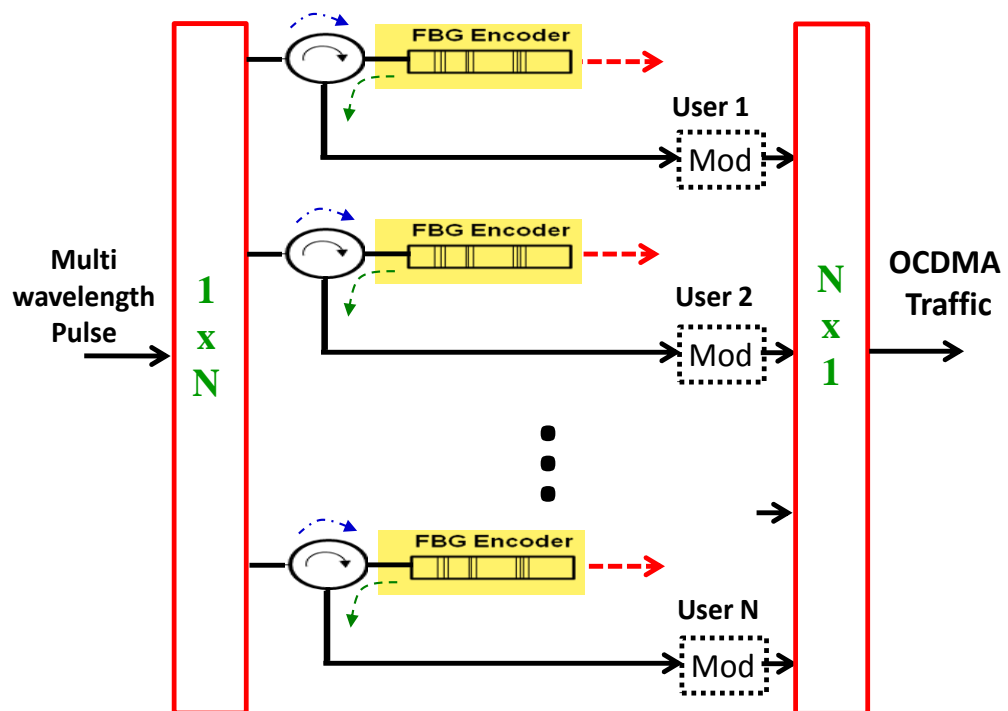


Figure 2.7 Architecture of a multiuser OCDMA signal generation. The input multi wavelength pulse is splitted N times and distributed to each of the FBG based OCDMA transmitters representing up to N simultaneous users. Where Mod is a Modulator.

In this section, an experiment was conducted to determine the ratio of input multi wavelength pulse to the resulting encoded optical signal. In the experiment, an optical super continuum representing multi wavelength pulse with peak power reduced to 0 dBm was passed into an FBG based OCDMA encoder via the input port of an optical circulator (port 1 in figure

2.8) and the output power of the encoded signal was measured (at port 3 of the circulator).

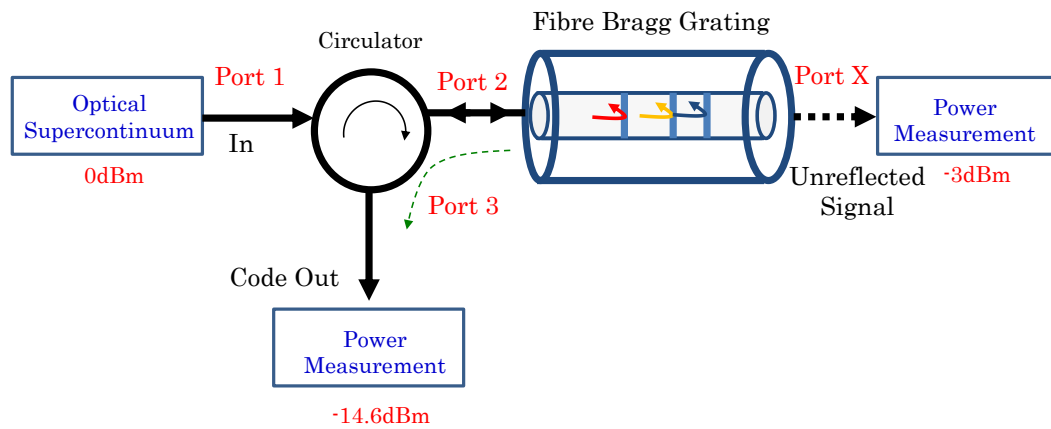


Figure 2.8 Illustration of the experiment to determine the percentage of input optical supercontinuum (OSC) power that is converted into an FBG encoded optical CDMA code.

Also, the power of the unreflected supercontinuum pulse passing through the FBG was measured. Figure 2.9 shows the spectrum of the input optical supercontinuum, the resulting encoded optical signal and unreflected optical supercontinuum that was transmitted through port X (see figure 2.8) of the FBG encoder is also shown.

From the experiment, it was observed that for the 0dBm input optical supercontinuum pulse, the measured average power of the encoded optical signal output (at port 3) is -14.6 dBm and the measured average power that passed through the FBG encoder and exits port X is -3 dBm.

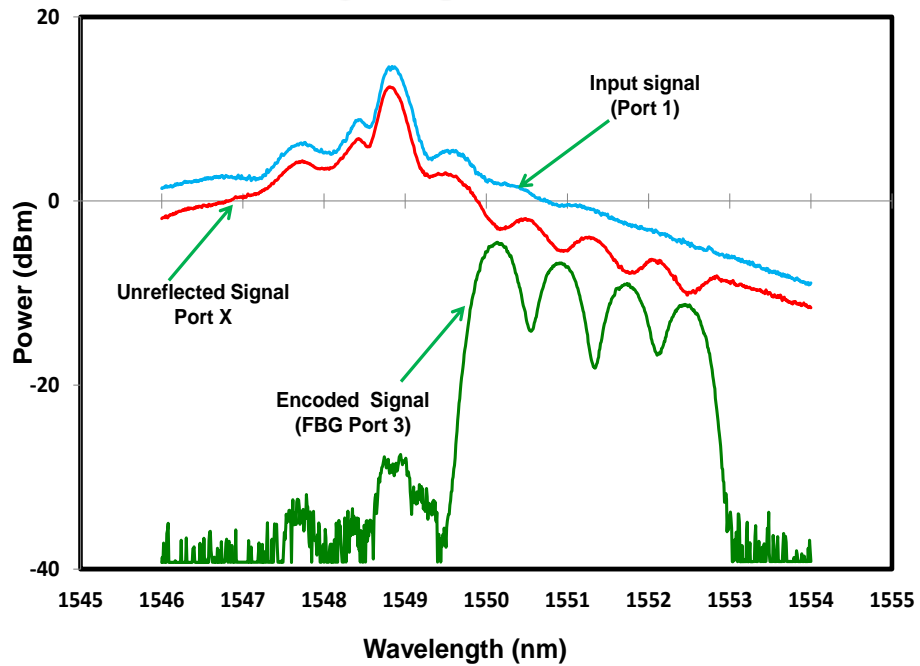


Figure 2.9 Optical spectrum of (a) multi wavelength signal input from port 1 (b) unreflected signal coming out of port X of the encoder and (c) OCDMA encoded signal output from port 3 of the FBG based OCDMA encoder.

This implies that only about 20% of the optical power that enters into the FBG based optical en/decoder is reflected and actually forms part of the encoded signal, while up to 80% of the input optical supercontinuum is not used in the encoding process.

Let us consider a specific application whereby 17 simultaneous users are required, it is not possible to obtain off-the-shelf splitters that will split 17 times, hence going by the “power of 2” splitting rule, a 1×32 optical splitter will be required to distribute the optical supercontinuum to only 17 OCDMA transmitters. Figure 2.10 is a typical OCDMA transmitter architecture which have been used for all the OCDMA experiments described in this thesis. The figure includes calculations of optical power budget for the required 17 User OCDMA system.

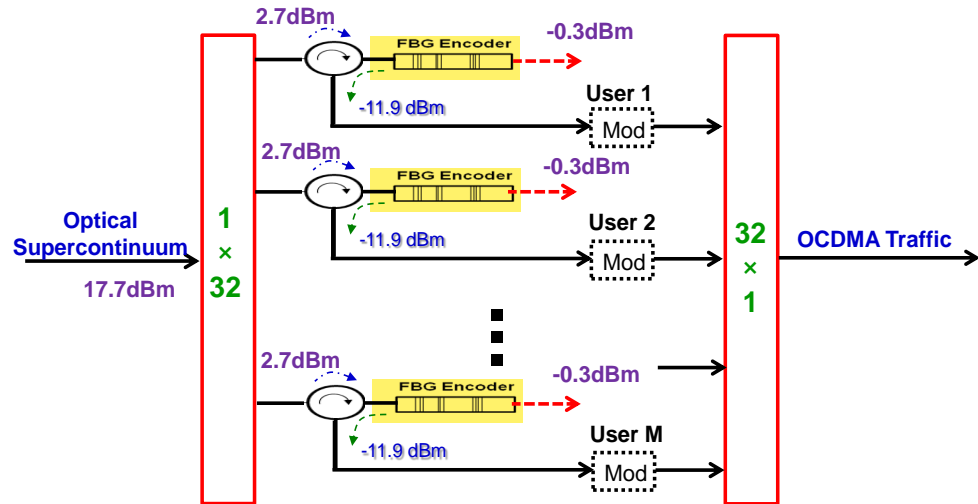


Figure 2.10 Original architecture of the multiuser FBG based OCDMA signal generation. Showing input and output powers of the OCDMA encoders.

For the power calculations shown in figure 2.9, the 17.7dBm input optical supercontinuum which can be realistically sourced from a Pritel Femtopulse optical pulse compressor will be splitted 32 times. The 1 x 32 power splitter will introduce a 15dB loss to each of the 32 splitter branches. This implies that only 2.7dBm of optical power will be available at the input of each FBG encoder. Considering the measured 14.6dB loss in the FBG, the maximum output power of each encoded user signal will not be -11.9dBm as the best case scenario for this architecture in figure 2.10. Also, knowing that majority of the input optical supercontinuum into each encoder is not being converted into OCDMA code; this method of optical power distribution is therefore not the most energy efficient. It is therefore desirable to find new architectures that will enable us to make use of the unutilized optical source signal.

As an alternative to the transmitter architecture in figure 2.10, we developed a new architecture where OCDMA encoders are cascaded as illustrated in the new architecture shown in figure 2.11. In this novel architecture, each OCDMA encoder is supplied with unutilized multi wavelength optical source signal by the encoder preceding it.

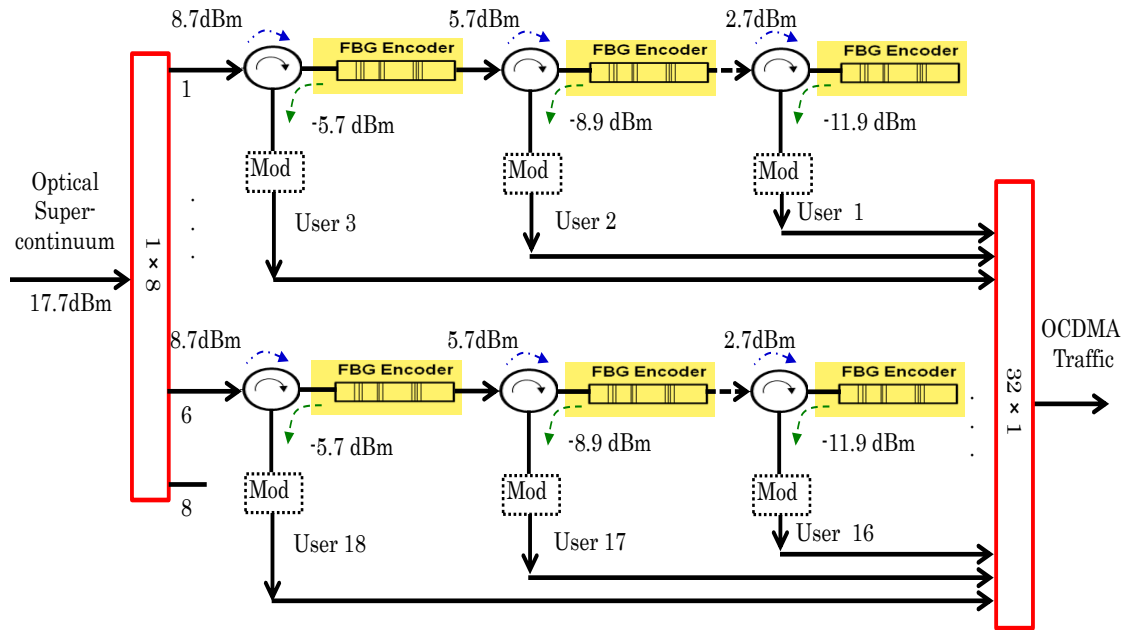


Figure 2.11 Modified architecture of the multiuser FBG based OCDMA signal generation. The encoders have been cascaded to enable the reuse of unreflected multi wavelength optical. The input optical splitter has also been replaced with a cheaper alternative. Where Mod is Modulator

The major difference between the transmitter architecture in figure 2.10 and that of figure 2.11 is that a cheaper 1×8 optical power splitter can now be used to replace the more expensive 1×32 input optical power splitter while up to three separate FBG based OCDMA encoders can be cascaded to reuse the unreflected optical supercontinuum from the preceding FBG based encoder. For the power calculations of the new architecture shown in figure 2.10, the same 17.7dBm input optical supercontinuum will be splitted 8 times using a 1×8 power splitter which will introduce a 9dB loss per output port. This implies that the first encoder in the cascade will have 8.7dBm supercontinuum power at its input. Considering the same 14.6dB measured loss in the gratings, the output power of the user 1 encoded signal in the cascade will be -5.9dBm in the same vein, the next user 2 in the cascade will be presented with 5.7dBm optical power at its input resulting in a -8dBm power output and 2.7dBm unused supercontinuum which will be passed as input for the last user 3 in the cascade.

Note that this is the same power presented to each of the users in the original transmitter architecture that produced the -11.9dBm output encoded signal. This power budget analysis of the new cascaded architecture shows that it is possible to improve the output power of some of the cascaded users by ~6dB. Although, depending on the application, it might be necessary to use appropriate attenuation in order to ensure that all the users have the same power levels. However, the worst case scenario for this new architecture is the same as the best case scenario of the original transmitter architecture. With this new architecture, the targeted 17 users OCDMA system will be achieved with an option to further expand it up to 24 simultaneous users while using the same supercontinuum power level at the input with none of the users transmitting with less than -11.9dBm

2.7 Chapter Summary

This chapter introduces fundamentals of coherent and incoherent OCDMA systems. Concept of Incoherent OCDMA system is explained in more details with focus on encoding methods based on one dimensional (1D) and two-dimensional (2D) codes.

Furthermore, different methods for generating 2D wavelength hopping time spreading codes (2D-WH/TS) were presented.

From experiments I observed that that less than 20% of the optical super continuum that enters the FBG based OCDMA encoder is converted into optical code. Based on this finding, a transmitter architecture that aims to reuse residual optical signal power by cascading several OCDMA encoders was proposed for the first time.

From the analysis, I observed that building a 17 users OCDMA system which would have required a 1×32 optical splitter for distribution of optical supercontinuum to each OCDMA encoder when the newly proposed 17 users system architecture could be implemented with a cheaper 1×8 optical

splitter, this translates to significant savings in both power and cost of implementation.

.

Chapter 3

Effect of Variations in Environmental Temperature on 2D- WH/TS OCDMA Code Performance

3.1 Introduction

This chapter presents a study to quantify the extent to which environmental temperature variations influences the performance of 2D-WH/TS codes used in OCDMA systems if multi wavelength picosecond pulses are utilized. To the best of our knowledge, this is the first time such study will be carried out. Recommendations for 2D-WH/TS code design that will improve the

robustness of these codes, help to better maintain the system performance and at the same time improve spectral efficiency without the need for additional hardware is proposed.

There are several impairments that have been identified as a cause of signal deterioration in optical fibre communication systems these include chromatic dispersion [52], timing jitter [53], and fibre loss [54], just to name a few. All these effects have been extensively studied for various optical systems including wavelength division multiplexing (WDM), [53] and optical time division multiple accesses (OTDMA) and various mitigation techniques have been proposed.

It is well known that the transmission performances of optical communications systems can be manipulated by controlling the optical and geometrical parameters in the fibre structures. Therefore, any undesired variation in the fibre structural parameters, can alter the propagation performances. In terrestrial optical fibre systems, the temperature variation experienced by the buried cable could be several tens of degrees [55]. The dispersion variations that arise from these temperature changes cannot be ignored in high speed systems especially OCDMA systems that are based on multi wavelength picosecond pulses.

3.2 Optical Fibres

The principle of light transmission via dielectric waveguide dates back to the twentieth century. Early experiments using silica glass surrounded by air was deemed impractical until around mid-1960 when the idea of a core and the cladding based waveguide was proposed.

Basically the optical fibre as it is today is of a dielectric structure which consist a core surrounded by a cladding material. The refractive index of the core is slightly greater than the refractive index of the cladding material. This refractive index variation between the core and the cladding makes it possible to guide the electromagnetic wave (light) substantially within the core of the fibre.

Early optical fibres proposed for communications around 1966 had very high attenuation (approx. >1000 dB/km). This prohibitively high attenuation was caused by the presence of impurities in the silicon material used in making the fibre. As research in optical fibres progressed, into the 1980s, it was observed that lower losses and reduced dispersion can be achieved when the light transmitted in the optical fibre is in the 1100 to 1600nm wavelength range.

Typical optical fibre losses at 1550 nm is about 0.2 dB/km. This is a very significant improvement from the initial 1000 dB/km loss of early fibres. Optical fibres can be classified into two main categories; the single mode fibre and the multimode fibre. The mode of a fibre refers to the number of light rays that are allowed to propagate within the core. Each of the two categories will be described below.

3.2.1 Single Mode Optical Fibre

Figure 3.1 shows a geometrical view of the cross section of a single mode fibre. Single mode optical fibres by the reason of their design and manufacturing only allow one mode of optical energy to propagate within the core.

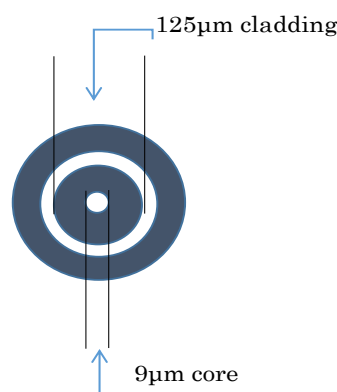


Figure 3.1 Physical geometry of a single mode optical fibre showing the core and the cladding.

The energy of all other light modes is absorbed/attenuated in the geometry of the fibre. The core dimension of most single mode fibres is between 8 to 10 microns. This is very small compared to that of the multimode fibre. For single mode operation, the only mode that exists is the fundamental mode. As a result of this, the single mode fibre theoretically has almost infinite bandwidth. The effective diameter of the cladding is 125 microns.

Single mode fibres find applications mostly in long distance communication because of its ability to transport optical signals over longer distances without significant attenuation.

3.2.2 Multimode Fibre

Compared to single mode fibres, the core diameter of the multimode fibre is significantly larger. Most multimode fibres have core diameters of either 50 or 62.5 microns. The large core diameter enables the propagation of multiple modes of light. The geometry of the multimode fibre is shown in figure 3.2.

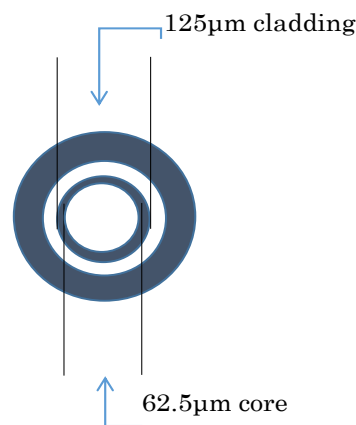


Figure 3.2 Physical geometry of a multimode optical fibre showing a considerably larger core and the cladding.

One of the disadvantages of the large core diameter of the multimode fibre is that dispersion limits the range of signal propagation in the multimode fibres hence they are not suitable for long distance communications. However multimode fibres have found extensive usage in short distance

high bitrates communications because they are relatively inexpensive. Multimode fibres can also be classified as either step index or graded index fibres. This classification is based on the refractive index profile of the core. In graded index multimode fibres, the refractive index reduces gradually from the centre of the core towards the cladding while in step index fibres the refractive index change conforms to a step profile.

3.3 Optical Fibre Attenuation

One of the most important requirements of the optical fibre is the ability to efficiently transmit light waves at the desired frequency over a finite distance. Attenuation is a phenomenon that occurs when the intensity of light becomes reduced as it propagates inside the optical fibre. One important parameter of the optical fibre is the attenuation coefficient. It is referred to as the ratio of the input optical power to the output optical power.

Let the power of a light input of an optical fibre be P_i and the output power after propagation over a unit distance be P_o , the ratio of input to output power can be expressed as [56]

$$\frac{P_i}{P_o} = e^{\alpha} \quad (3.1)$$

where α is the attenuation constant.

Since optical power is mostly expressed in decibel (dB), we can rewrite eqn. 3.1 as

$$\alpha \left(\frac{dB}{km} \right) = 10 \text{Log}_{10} \left[\frac{P_i}{P_o} \right] \quad (3.2)$$

Absorption and scattering are the two major causes of attenuation in optical fibres both of which are wavelength dependent. This explains why typical optical communications systems deploy light sources with wavelength

windows that are capable of reduced attenuation. Historically, three wavelength windows have been exploited for optical communications they are 850nm, 1300nm and 1550 nm in as the first, second and third window respectively.

Fibre attenuation can also occur as a result of subjecting the fibre to a high bending stress. Other sources of fibre attenuation includes leaky mode, mode coupling loss, connector loss and splice loss. All of these losses contribute to the overall degradation in amplitude of the optical signal.

3.4 Dispersion

Dispersion in optical fibres can be described as the mechanism in which light pulses experience a broadening of their pulse width as they propagate along the optical fibre [57].

As shown in figure 3.3 (a), a digital bit pattern 1011 represented by light pulses is input to an optical fibre. After propagation over a fibre length L , dispersion causes the pulses to broaden and therefore the energy of each pulse begins to leak into the neighbouring slots (see figure 3.3 (b)). Also because of the law of energy conservation, pulse broadening causes the amplitude of the pulse power to reduce. As each pulse broadens over the fibre length and overlaps with its neighbours, the bit sequence 1011 eventually become indistinguishable at the receiver input. This is referred to as inter-symbol interference (ISI). Inter symbol interference leads to increase in bit error rate in digital optical communications. Hence dispersion poses a limitation to the maximum possible bandwidth achievable in optical fibre systems [58].

Mathematically, the maximum bit rate B_{max} that may be obtained in an optical fibre link with pulse broadening τ can be given as $B_{max} \leq 1/2\tau$.

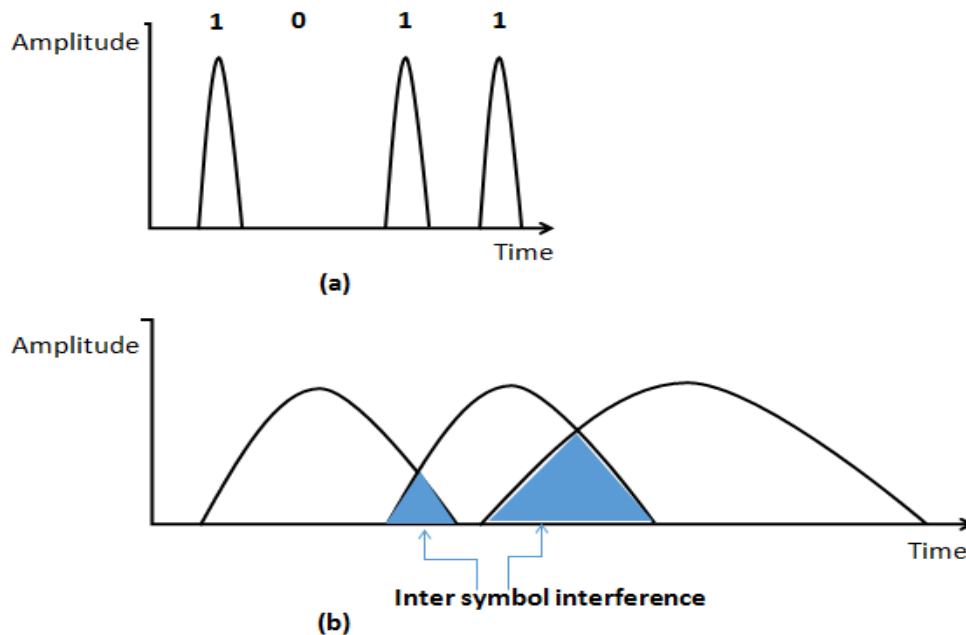


Figure 3.3 Illustration using a digital pattern 1011 of pulse broadening as light is transmitted along a fibre: (a) fibre input; (b) fibre output at a distance L (km).

Dispersion in multimode fibre is more pronounced when compared to single mode fibres. [59] The major dispersive mechanisms that contribute to the overall dispersion in optical fibres include material dispersion, and waveguide dispersion. The combination of material dispersion and waveguide dispersion is referred to as chromatic dispersion.

Various spectral component of light launched into an optical fibre propagate at different group velocities and this results in material dispersion induced pulse broadening. Material dispersion is exhibited mostly by materials in which the second differential of the refractive index with respect to wavelength is non zero. Waveguide dispersion occurs as a result of the variation in group velocity of the fibre mode with wavelength.

Chromatic dispersion accounts for the overall pulse broadening in single mode fibres. This is because only one mode is allowed to propagate. As a

result, single mode fibre bandwidth is limited by the spectral line width of the source.

3.5 Temperature Dependence of Fibre Chromatic Dispersion

Most fibre optic cable installations are usually buried at a depth of about 2-4 feet below the ground. At these depths, it has been shown that they could be exposed to temperature variations up to about 20° C [60].

The temperature variation can cause the quality of transmitted optical signal to degrade under certain circumstances. Because of the dynamic nature of these temperature variations, tuneable compensation schemes that will track and compensate for these unpredictable changes are always preferable. The effect of the impairments caused by the temperature changes has been previously investigated for WDM system transmissions with data rates up to 40Gbits/s [61, 62, 55]. It was established that these impairments can increase the error probability of an optical transmission system, but the effect is not severe until after transmitting over considerably long distances. This is because the bit width (for example 25 ps for 40 Gbits/s systems) is very large when compared to its relative change which results from its distortion via the fibre thermal coefficient.

However, this may not be always true. For example, if an OCDMA system will utilize 2D-WH/Ts codes comprising multi wavelength pulses [63, 64, 65, 66, 67] with the pulse width smaller than 5ps, the effect of temperature fluctuations could be in the order of the pulse width [68] and therefore cannot be anymore neglected even when the transmission link has be fully compensated for chromatic dispersion.

The refractive index variation as a function of temperature (dn/dT) is an important feature in the optical fibre. It determines the temperature characteristics of an optical fibre transmission system. Optical systems are expected to experience changes of temperature in several regions of the planet; this compels the essential demand to investigate the thermal effect in the design of high speed optical communication systems.

Ghosh *et al* developed an empirical model for the temperature-dependent index of refraction of silicon dioxide (SiO₂) a major constituent of most optical fibres. This model can also be used to accurately characterize the temperature dependence of the chromatic dispersion of a wide variety of optical fibres [69]. In [70], an equation for the change in chromatic dispersion of optical fibre with temperature was derived and values for the temperature-dependent coefficients were calculated using the derived equation. However, the analysis in the study using six commercially available fibre types was limited to the transmission of WDM communication systems at speeds up to 40 Gbits/s. This implies that a behaviour of optical pulses that are shorter than 25 ps was not captured in the study.

Incoherent multi wavelength OCDMA pulses can be of the order of a few (<5) picoseconds, therefore it will be of interest to know how these pulses behave under the influence of temperature fluctuations especially since multiple wavelengths are involved in each 2D-OCDMA code.

3.6 Impact of Temperature Fluctuations on Autocorrelation of Incoherent 2D-WH/TS OCDMA Codes

As previously described, 2D-WH/TS codes consist of a wavelength - time matrix representing a logical 1 in a bit sequence. The number of rows in the matrix is determined by the number of available wavelengths (and is called the code weight (w)) and the number of columns of the matrix is the code length. The relationship between the bit period (T_b) and the chip width (T_c) can be given as:

$$T_c = \frac{T_b}{N_c} \quad (3.3)$$

Where N_c represents the number of chips (columns) in the code matrix.

There are rich literatures on the design of 2D-WH/TS codes with various code properties, such as cardinality and correlation values [68, 71, 72]. The

study in this chapter can apply to any incoherent 2D-WH/TS code without restrictions.

3.6.1 2D-WH/TS Code Cardinality

It is well known that an increase in the number of chips N_c enables the generation of larger code sets. This increase in code cardinality will lead to an increase in the number of simultaneous OCDMA users thereby improving scalability [68]. From equation 3.1, in order to increase the number of chips within 2D-WH/TS OCDMA code if the data rate is fixed, the chip width T_c must be reduced. In practical terms, this will require reducing the duration of each wavelength pulse contained within the 2D-WH/TS OCDMA code. Therefore one major requirement for obtaining large code set for the OCDMA system is the provision that short pulses are used to generate the 2D-WH/TS codes.

As will be shown, in the practical implementation of such 2D-WH/TS code based incoherent OCDMA systems, the environmental factors affecting the transmission medium must be considered in order to ensure an effective and robust data transmission.

3.6.2 Analysis of OCDMA Code Propagation

Let us consider the 2D-WH/TS code shown in figure 3.4. The figure illustrates the process involved in the decoding of the 2D-WH/TS code under ideal conditions. By ideal conditions, it means that the codes have been transmitted over a fully dispersion compensated link. Also it is assumed that losses due to fibre attenuation have been fully compensated. The ideal conditions also includes the assumption that the wavelength pulses within the code remain in their time chips, and spaced (in time) as originally designed even after propagating in a fully dispersion compensated fibre link.

It can be seen that after the code has propagated through the decoder, all the wavelength pulses that was originally spread in time has been fully de-spread. The de-spreading of the wavelength pulses has therefore produced a single autocorrelation peak. The height of this autocorrelation peak as shown in the figure is equal to the combined power of all the individual wavelength pulses (code weight (w)) that formed the autocorrelation peak.

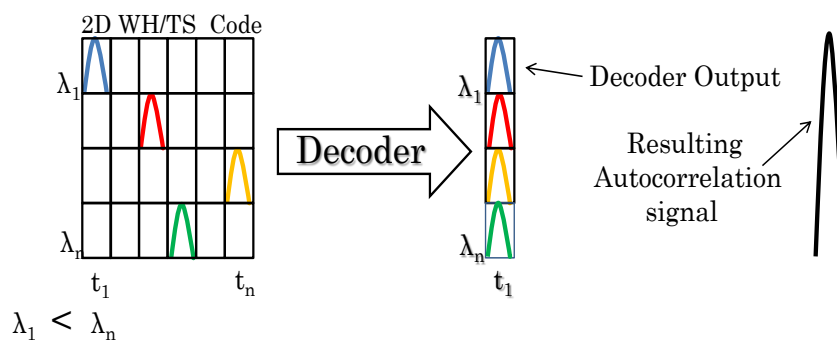


Figure 3.4 Decoding of the 2D-WH/TS OCDMA code after its propagation in a fully dispersion compensated fibre link under ideal conditions; with no code matrix distortion after code propagation. The resulting autocorrelation signal is undistorted.

If however the fibre temperature has changed due to the character of the fibre thermal coefficient, the OCDMA code will be temporally skewed and the decoder will output a distorted autocorrelation (see figure 3.5 for illustration). The severity of this effect is a function of temperature change magnitude (ΔT) and the propagation distance (L).

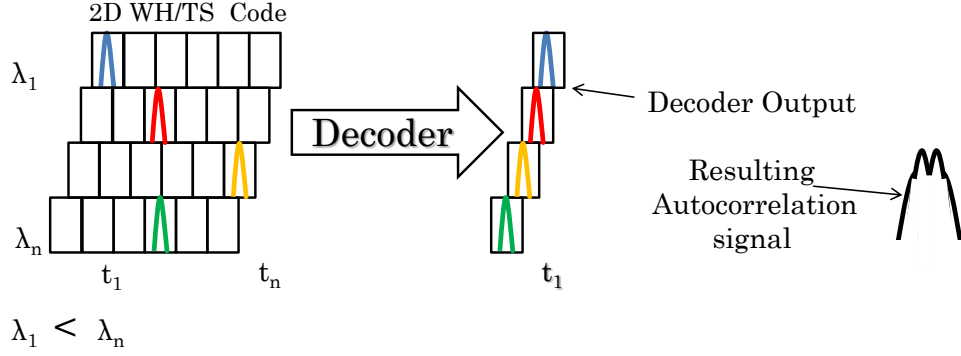


Figure 3.5 Decoding of the 2D-WH/TS OCDMA code after its propagation in a fully dispersion compensated fibre link under practical conditions with code matrix distortion after code propagation when the fibre temperature has changed. The resulting autocorrelation is distorted.

The degree to which temperature induced skewing affects the code and the decoded autocorrelation signal (its height, shape, width) influences the outcome of the thresholding process by the receiver threshold detector. Improper thresholding of the distorted autocorrelation signal will result in an increased bit error rate [73, 74]. This effect may be mitigated via delay lines matched with the skewed-chip duration after certain distances but this will add to the complexity of the system bearing in mind the dynamic nature of the temperature fluctuation. Also, more complexity arises when the OCDMA signal is encoded/decoded using integrated fibre Bragg gratings where there is no direct access to the individual wavelengths. It is important to note that the effect of temperature variation will affect both synchronous and asynchronous OCDMA schemes. This is because the skewing occurs within the codes of individual users therefore causing a misalignment of the pulses at the time of decoding. It is therefore imperative to quantify the effect of the fibre temperature fluctuations on the autocorrelation signal.

Therefore we will now analyse the effect of the varying temperature on the autocorrelation signal resulted from the decoding of an incoherent 2D-WH/TS OCDMA code which consists of w wavelengths pulses of pulse width τ equal to chip width t_c . Let us denote the temperature variation induced

temporal skew as Δt and the amount of pulsewidth shrinking for each wavelength pulse as $\Delta\tau$, then from [67] we can express Δt as

$$\Delta t = D_{temp} \times \Delta T \times \Delta\lambda \times L \quad (3.4)$$

and $\Delta\tau$ as;

$$\Delta\tau = D_{temp} \times \Delta T \times \Delta\lambda \times L \quad (3.5)$$

Where, D_{temp} (ps/nm · km/°C) is the thermal coefficient of the fibre, ΔT (°C) is the average change in temperature experienced by the buried transmission fibre of a length L (km), and $\Delta\lambda$ (nm) is the spectral spacing between 2D-WH/TS OCDMA code wavelengths pulses, and $\Delta\lambda$ (nm) is the pulse spectral line width of each wavelength pulse within the code. In our calculations, $\Delta\lambda$ is assumed to be a constant for all wavelengths pairs.

Next, let us derive the expression for the envelope of the resulting autocorrelation signal S_t . S_t is the incoherent sum of w wavelength pulses present within the code at a decoder output after the code has been propagated in the optical fibre of length L (km) which has been fully compensated for chromatic dispersion over the wavelength slope. Assuming each wavelength pulse has a Gaussian shape with a constant peak power P_p , then the incoherent sum of w wavelength pulses spaced by $(t - k\Delta t)$ whose width has been reduced from the initial pulsewidth value τ to $\tau - \Delta\tau$ (ps) can be expressed as

$$S_t(L) = \sum_{k=0}^{w-1} P_p \exp \left\{ -2.77 \left[\frac{t - k\Delta t}{\tau - \Delta\tau} \right]^2 \right\} \quad (3.6)$$

By setting a code weight $w = 8$ (i.e., eight wavelengths being used in the code), $\tau = 2$ ps, $\Delta\lambda = 0.8$ nm, $\Delta\lambda = 1.4$ nm, and $D_{temp} = 0.0025$ ps/nm · km/°C autocorrelation peaks for four different propagation distances $L = 0$ km, 10 km, 20 km, and 40 km, was calculated respectively . From figure 3.6, it can be seen that the height of a autocorrelation signal S_t for a 2D-WH/TS code

using 8 wavelength pulses is, as the theory predicts for an ideal case [68] (see Figure 3.6).

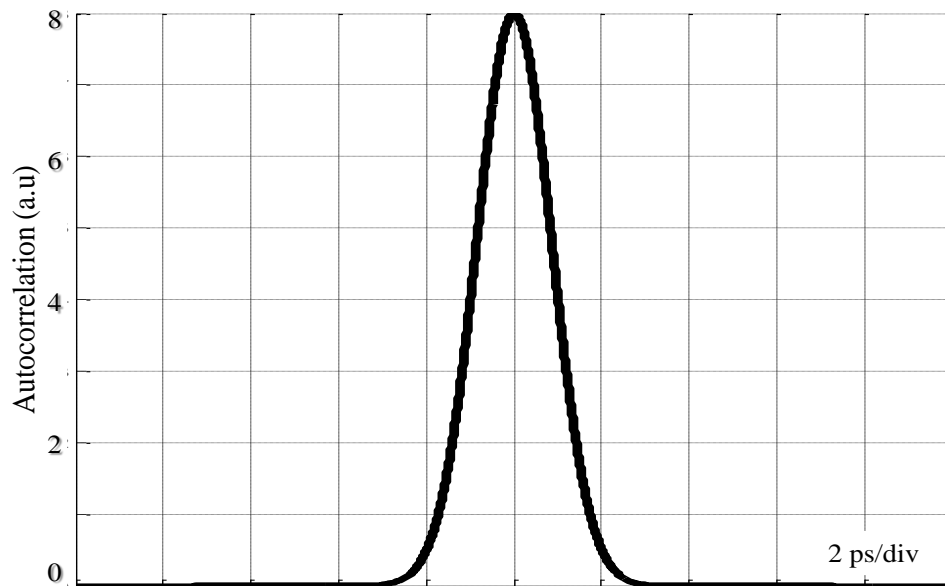


Figure 3.6 Plot of autocorrelation signal formed by decoding OCDMA transmission based on 2D-WH/TS OCDMA codes with 2 ps, 8 wavelength pulses after experiencing 20^o C temperature variation over a distance of 0 km (back-to-back). The fibre temperature coefficient used for calculation $D_{temp} = 0.0025 \text{ ps/nm} \cdot \text{km}/^{\circ}\text{C}$ [69].

However, if this code will propagate 10 km and the fibre experiences the same 20^oC temperature variation, then the autocorrelation signal height would have dropped to below 8 (see figure 3.7).

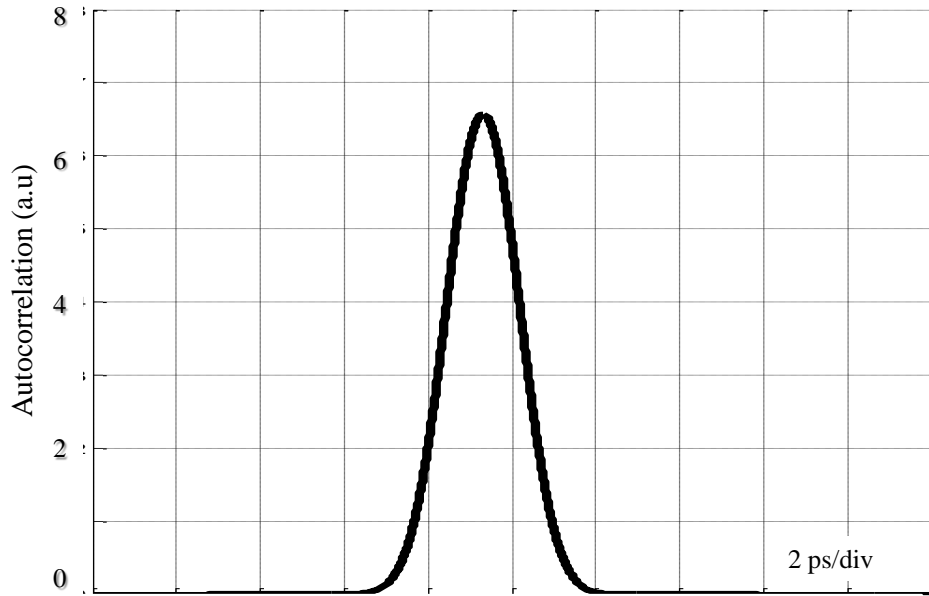


Figure 3.7 Plot of autocorrelation signal formed by decoding OCDMA transmission based on 2D-WH/TS OCDMA codes with 2ps, 8 wavelength pulses after experiencing 20° C temperature variation over a distance of 10 km.

After 20 km of optical fibre propagation, it can be observed that the peak of the autocorrelation signal becomes flattened (see figure 3.8) and at 40 km, peaks of the individual wavelength pulses can be clearly observed (see figure 3.9) this is a result of the discussed time skewing.



Figure 3.8 Plot of autocorrelation signal formed by decoding OCDMA transmission based on 2D-WH/TS OCDMA codes with 2 ps, 8 wavelength pulses after experiencing 20° C temperature variation over a distance of 20 km.

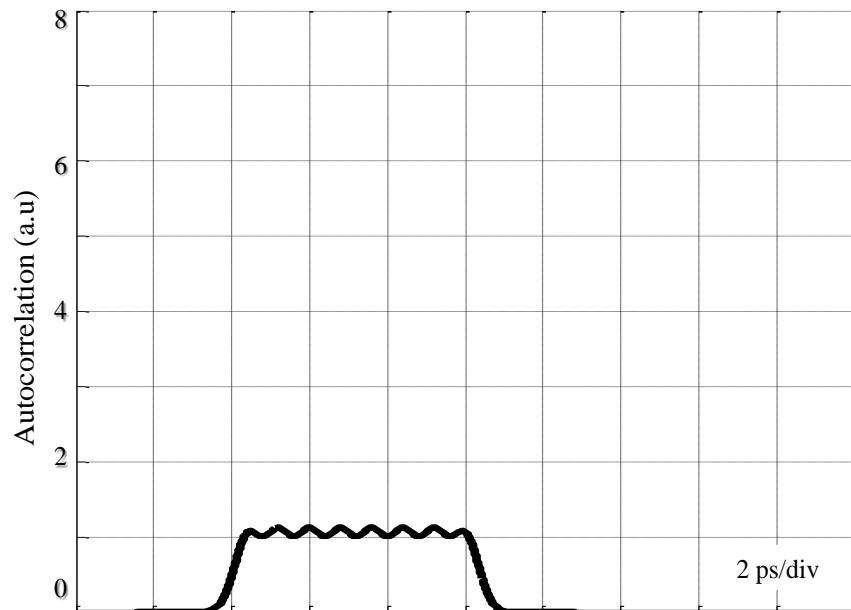


Figure 3.9. Plot of autocorrelation signal formed by decoding OCDMA transmission based on 2D-WH/TS OCDMA codes with 2 ps, 8 wavelength pulses after experiencing 20° C temperature variations over a distance of 40 km.

Figure 3.10 is the plot based on Eq.3.4. It shows the maximum obtainable autocorrelation height S_t as the temperature variation (ΔT) increases for

10km and 20km propagation respectively. It can be observed that as the ΔT increases for a particular distance, the height of the autocorrelation drops more rapidly.

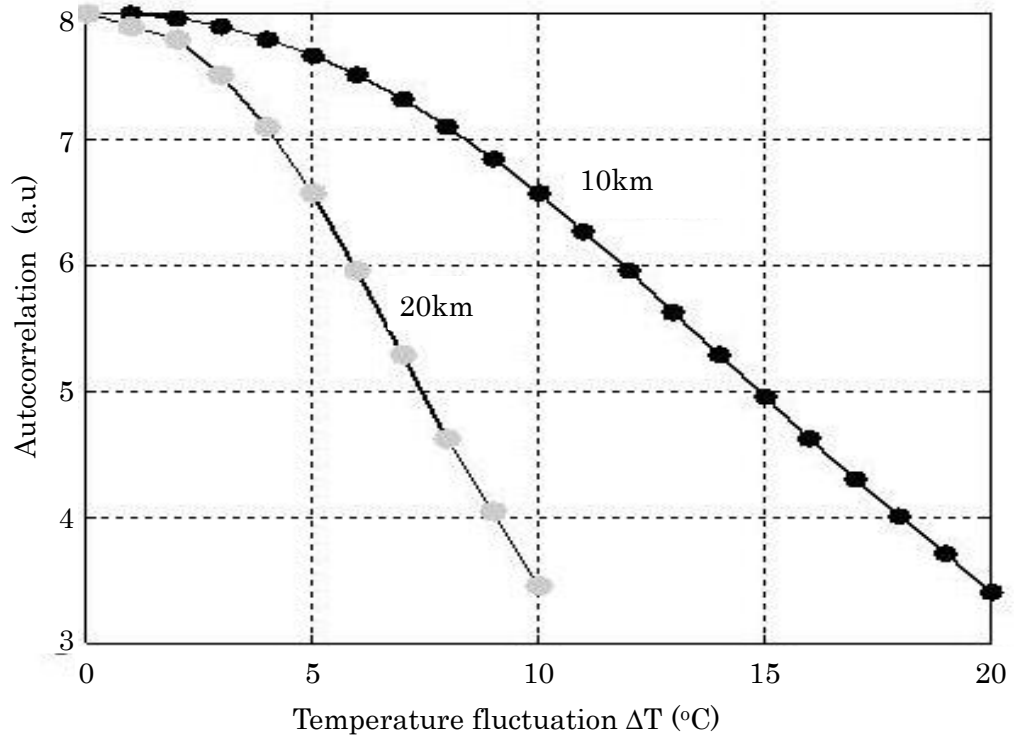


Figure 3.10 Maximum obtainable autocorrelation height for an (8,200), 2D-WH/TS code as temperature increases over a 10 km and 20 km link.

Figure 3.11 illustrates the maximum obtainable autocorrelation height for an (8,200) 2D-WH/TS OCDMA code for the different propagation distances up to 10 km for a case of $D_{temp} = 0.0025 \text{ ps/nm} \cdot \text{km}/^\circ\text{C}$ and $\Delta T = 20^\circ\text{C}$. It can be seen that the maximum achievable autocorrelation height drops from the theoretically value of 8 (expected under the ideal conditions) to a new lower value of 7 in less than 8 km. This implies that the OCDMA receiver designed with a threshold value th set to the code weight of 8 will function incorrectly.

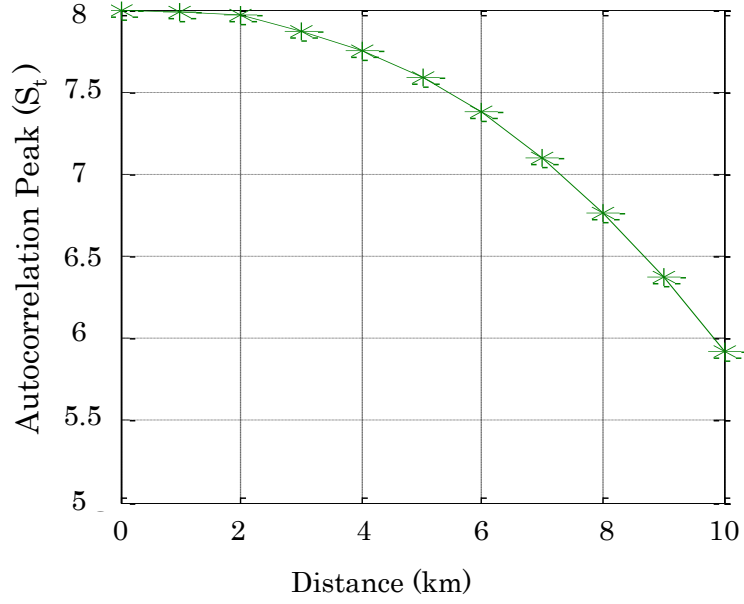


Figure 3.11 Maximum obtainable autocorrelation height after a (8,200), 2D-WH/TS code propagates in fibre under the influence of environmental temperature swing.

To analyse the performance, the relationship between the probability of error P_e and number of simultaneous users (K) for an OCDMA system using 2D-WH/TS codes [68] can be calculated as:

$$P_e = \frac{1}{2} \sum_{j=0}^{th} (-1)^j \binom{w}{j} \left(1 - \frac{j q_{1,1}}{w}\right)^{K-1} \quad (3.7)$$

Where $q_{1,1}$ is the hit probability and is given as

$$q_{1,1} = \frac{w}{2.N_c} \quad (3.8)$$

For an optimum performance, th is usually set to be equal to w .

To obtain P_e , the OCDMA system with (8,200) 2D-WH/TS codes was used. It was assumed to be initially operating at the “designed” temperature T and

then with the temperature changed to the value $T + 20^{\circ}\text{C}$ (because of an environmental temperature swing).

Obtained results are shown in figure 3.12. It should be noted that the results are based on the assumptions that the fibre link has been fully compensated for dispersion and also signal power is assumed to be below levels that can trigger nonlinear effects. These assumptions are used in order to isolate the performance loss due to temperature variations from other losses due to transmissions through optical fibre.

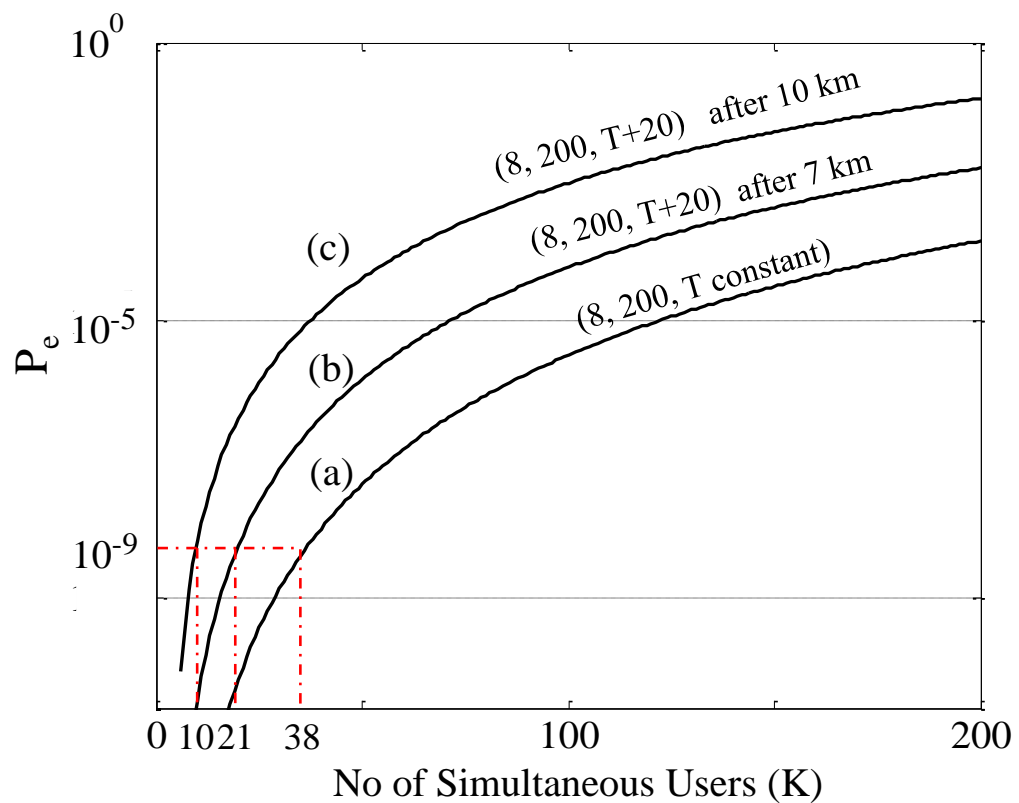


Figure 3.12 Performance curves for an (8,200) 2D-WH/TS OCDMA system illustrating (a) case where T is constant, (b) case where T changes by 20°C and code propagation distance is 7 km, (c) case where T changes by 20°C and code propagation distance is 10 km.

From figure 3.12 it can be seen that for the system to maintain for example the bit error rate of 10^{-9} , the number of simultaneous users will need to be significantly reduced from 38 to 21 users after 7 km of propagation distance and a 20°C temperature change (see figure 3.12(a) and (b)) and to 10 users

after 10 km and 20°C temperature change (see figure 3.12(a) and (c)) respectively.

It is also important to note that if a forward error correction (FEC) is implemented and the error rate of 10^{-4} can be corrected to achieve the value 10^{-9} , then the number of simultaneous users even after the link has been affected by the 20 °C temperature change can be increased from 38 users to 98 users for the case of 7 km propagation distance. Also the number of users for the 10 km case can be improved from 10 users to 51 users. However the implementation of FEC will require additional overhead and processing.

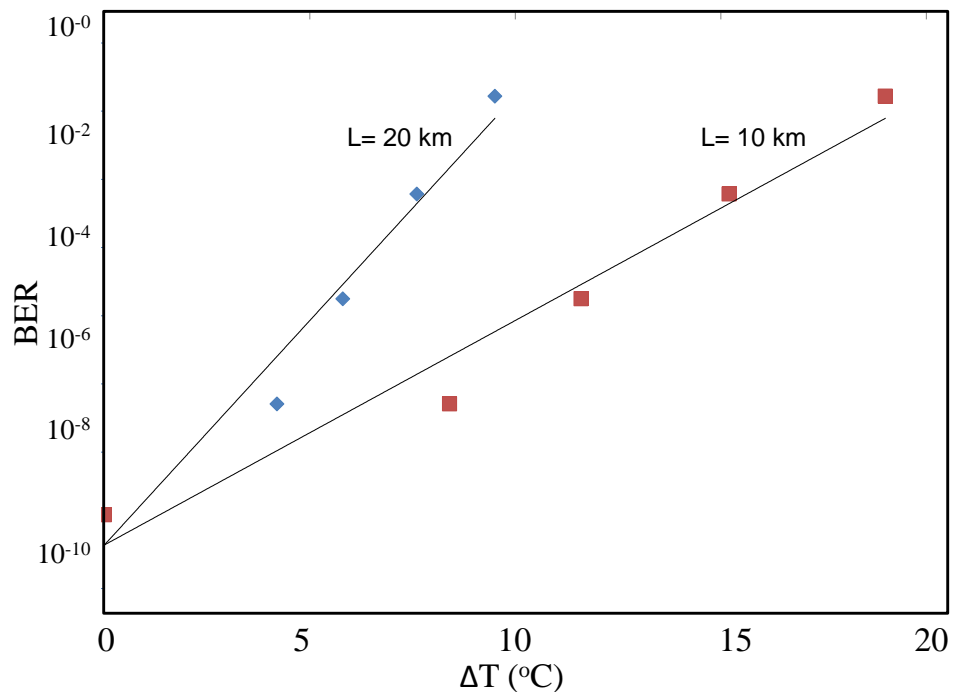


Figure 3.13 Minimum obtainable bit error rates as ΔT increases over a 10km and 20 km fibre link respectively.

The performance can be further analysed by examining figure 3.13 which compares the bit error rate with the temperature fluctuation. The BER worsens as the change in temperature becomes more pronounced over this confirms the results in figure 3.10 and figure 3.11 which compares the height of the autocorrelation peak with temperature change and propagation distance.

3.7 Improving System Design for Better Performance

In view of these significant degradations experienced by the 2D-WH/TS code deploying picosecond (ps) multi wavelength pulses under the influence of temperature changes, let us now analyse if wavelength channel spacing within the code has any effect on the overall OCDMA system performance.

As already shown, the major contributor to the degradation experienced by the codes employing ps pulses is the temporal skew. But the amount of temporal skewing is dependent on the code spectral allocation and the spectral spacing between the individual wavelengths used in the code formation.

Let us define Δt_{tot} as the total temperature variation induced temporal skew, then from Eq. 3.4, Δt_{tot} which is the sum of individual temperature induced temporal skews experienced by the w wavelength pulses that forms the decoded autocorrelation signal can be expressed as $\Delta t_{tot} = w \times \Delta t$. By substituting for $\Delta T = 20^\circ\text{C}$ and $\Delta\lambda = 0.8 \text{ nm}$ in the Eq. 4.2, the maximum transmission distance at which the total temporal skew Δt_{tot} equals one chip width T_c for the (8,200) 2D-WH/TS code used by the OCDMA system running at 2.5Gbits/s was found to be less than 7 km. This would also mean that the height of the autocorrelation signal for the decoded (8,200) system would have dropped from 8 to 7 after propagating in less than 7 km of the temperature affected fibre.

Figure 3.14 shows the data obtained when similar calculations was performed for $\Delta T = 10^\circ\text{C}$ (black), 15°C (light grey), and 20°C (brown) change, respectively for 2D-WH/TS code using $(w, \Delta\lambda)$ values of (8, 0.8nm), (8, 0.4nm), (4, 0.8nm) and (4, 0.4nm), respectively. From the result shown in figure 3.14, it can be observed that for any given transmission performance (say system BER = 10^{-9}), an OCDMA system using 2D-WH/TS OCDMA codes would be able to transmit over two-times longer distances at a temperature increase $T + 10^\circ\text{C}$ (black), compared to temperature increases by $+20^\circ\text{C}$ (dark gray).

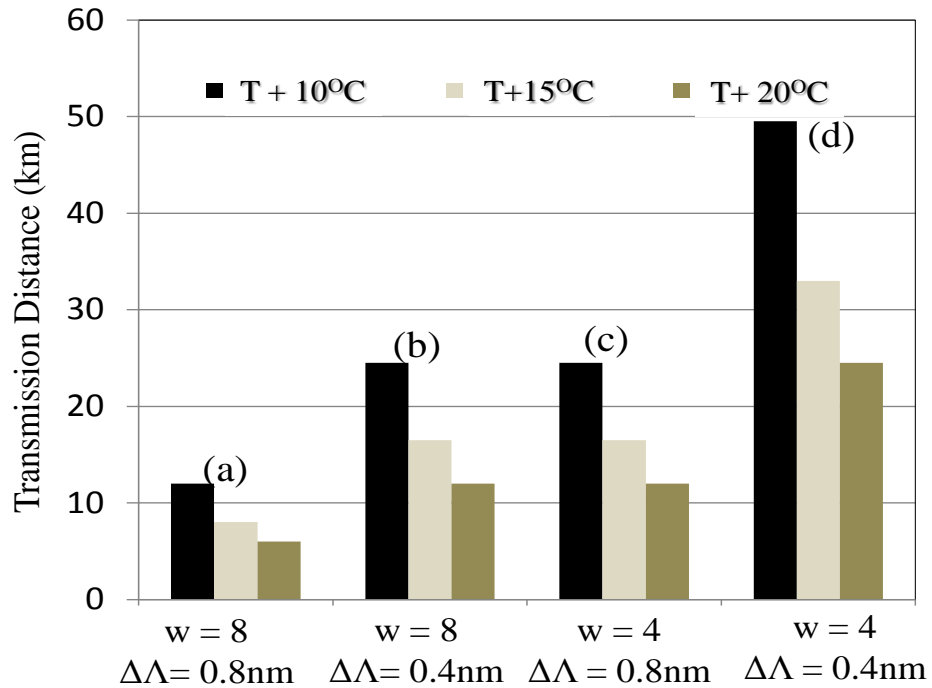


Figure 3.14 Transmission distance against code spectral allocation for a 200 chips OCDMA system using 2D-WH/TS OCDMA codes when the total temperature induced skew is below one chip duration. $\Delta\Lambda$ is the wavelength spacing. Code spectral allocation is directly related to the code weight.

Figure 3.14(b) and 3.14(c) gives the same results for different code weights. This is expected because the wavelength spectrum occupied by these code sets is the same and therefore the autocorrelation signal will experience the same distortion due to the time skewing.

The calculations also show, as can be seen by comparing figure 3.14(a) with figure 3.14(b) [$w = 8$] and figure 3.14(c) with figure 3.14(d) [$w = 4$], that the system transmission distance can be significantly improved when the channel spacing between multi wavelength ps pulses within 2D-WH/TS code is reduced; in this given example from 0.8nm (100 GHz) to 0.4 nm (50 GHz). This is valid for all incoherent wavelength hopping/time spreading OCDMA codes. This reduction in channel spacing will also enhance the spectral efficiency of the system because the used code will occupy less spectral bandwidth.

By calculating the spectral efficiency (\mathcal{E}) of the $w = 8$ wavelength system in figure 3.14 using $\mathcal{E} = K / (t_b \times w \times \Delta\lambda)$ [75], it was found that a fifty percent reduction in the wavelength channel spacing ($\Delta\lambda$) will double the spectral efficiency for a $K = 38$ user OCDMA system at 10^{-9} BER running at 2.5Gbits/s data rate.

It is worthy of note that the OCDMA system parameters relating to the code weight (w) will not be affected by this channel spacing reduction. This means that the cardinality and the number of simultaneous users will remain the same.

3.8 Chapter Summary

An extensive investigation has been carried out on the performance of 2D-WH/TS OCDMA codes under the influence of temperature variations resulting from changing environmental conditions. The codes investigated are based on picosecond multi wavelength pulses. Although the use of picosecond pulses by 2D-WH/TS OCDMA codes helps to increase the number of simultaneous users but as already shown, it will also introduce side effects in terms of overall system performance degradations.

Equations have been derived for the first time to theoretically evaluate the extent to which such temperature changes will degrade the overall OCDMA system performance.

Obtained results have confirmed that temperature changes would adversely affect these codes by causing a reduction in the expected height of the autocorrelation peak thereby resulting in significant performance deterioration of the OCDMA system. This will also limit the reach of these systems. It was also noted that an implementation of FEC will help to significantly increase the number of simultaneous users even under the influence of temperature variation.

Because of the dynamic nature of these temperature changes, tunable compensation schemes are preferable but their implementation may involve an additional cost and a complexity.

To partially mitigate such hardware needs, following certain code design rules was shown to help in minimizing the effect of fibre temperature changes on the OCDMA system.

Therefore the effect of different values of channel spacing occupied by individual wavelength pulses within 2D-WH/TS codes under the influence of the environmental temperature changes on the system performance was investigated. It was found that the codes perform better under the influence of environmental temperature fluctuations if the channel spacing can be reduced. The proposed channel spacing reduction is valid for all incoherent wavelength hopping/time spreading OCDMA codes.

This finding is very important because it also amounts to an improvement in spectral efficiency. For instance, the performance of a 2D-WH/TS code with a 0.4 nm channel spacing will be more robust under a 20°C change temperature swing compared to the code designed with a 0.8 nm channel spacing. It should be noted that the cost of 0.4 nm and 0.8 nm based encoders/decoders are relatively the same hence no additional cost is incurred.

Finally, the reduction in channel spacing will allow the delivery of the same system performance when the transmission distance is doubled.

Chapter 4

Improving Performance of 2D-WH/TS Optical CDMA with all-Optical Signal Processing

4.1 Introduction

This chapter presents the study of a novel all-optical method for processing optical CDMA signals towards improving the suppression of multi access interference (MAI). The main focus is on incoherent OCDMA systems using multi wavelength 2D-WH/TS codes generated using FBG based encoders and decoders.

The MAI suppression capabilities which are based on its ability to eliminate selective wavelength pulse processing is presented. As a result of hardware savings, processing cost will be significantly reduced and power budget improvement resulted in improved performance.

4.2 Wavelength Pulse Power Inequality in FBG Encoded OCDMA Codes

In the process of achieving highly integrated and cost effective OCDMA devices, the fibre Bragg grating (FBG) technology has been harnessed. This involves the use of fibre Bragg grating based optical reflectors for the purpose of encoding and decoding optical code division multiple access (OCDMA) signals. Both coherent OCDMA and incoherent OCDMA codes can be generated using carefully designed fibre Bragg gratings [76, 77, 32].

In most experiments involving FBG based OCDMA codes; the multi wavelength source signal is usually distributed equally to all users as shown in the transmitter architecture illustrated in figure 4.2 [78]. The input multi wavelength pulse is splitted N times and distributed to each of the FBG based OCDMA transmitters representing up to N simultaneous users.

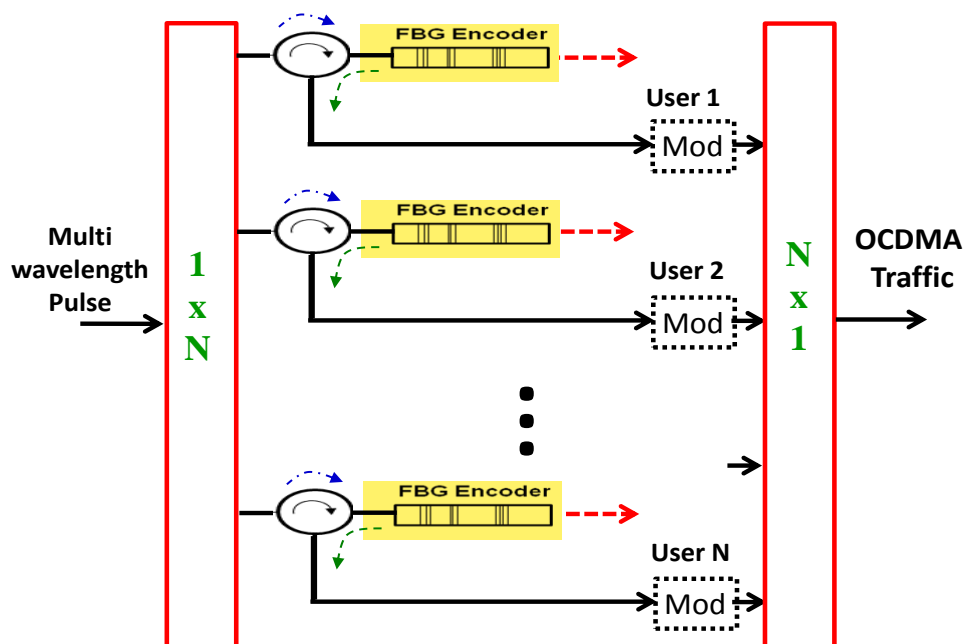


Figure 4.1 Architecture of a multiuser OCDMA signal generation. The input multi wavelength pulse is splitted N times and distributed to each of the FBG based OCDMA transmitters representing up to N simultaneous users. Where Mod is Modulator

It has been observed that imperfections in the fibre Bragg grating or the dispersive properties of the fibre propagating medium, often cause an inequality in the powers of the individual wavelength pulses comprised in an OCDMA code. However, once the signal is encoded and the OCDMA code have been generated by the FBG encoder, the individual wavelengths of the WH/TS OCDMA code cannot be any more easily individually accessed for a selective processing. In current approaches, these individual wavelengths will have to be accessed by first de-multiplexing the multi-wavelength OCDMA code then individually attenuated for the proper power equalization and then multiplexed back in a similar manner to code generation using arrayed waveguide gratings (AWG) and thin film filters while maintaining the original time spreading.

All the above adds additional hardware complexity and also increases the overall system cost. Therefore it is important to find alternative methods by which encoded multi-wavelength OCDMA signals are processed all optically and in a manner that will lead to an improvement in the performance of the system without introducing a distortion to the sequence of the already encoded information.

4.3 Single mode-Multimode-Single mode fibre structure.

The single mode-multimode-single mode fibre structure have been extensively studied [79, 80, 81, 82, 83]. It is achieved by connecting a multimode fibre between two single mode fibres. The SMS arrangement has been found to exhibit the self-imaging principle in which when an input optical field propagating in a single mode fibre is launched into a multimode fibre, a number of guided modes is excited within the core of the multimode fibre. The optical field is later reproduced as a single image at periodic intervals as it propagates within the multimode fibre. The distance at which the optical field is reproduced is referred to as the reimaging distance [80].

This reimaging distance have been shown to be wavelength dependent. Therefore a filter can be obtained by carefully ensuring that the optical field is coupled out of the MMF into the single mode fibre at the reimaging distance [81]. This principle has been widely investigated and adapted in devices such as wavelength selective filters, temperature sensors and optical modulators.

The effect of signal polarization on a single mode fibre transmission link with added section of multimode fibre was noted in [84]. It was shown that manipulating the signal polarization before launching into a single mode fibre via a section of multimode fibre can result in system performance changes. Also it has been previously reported [85] that the transmission characteristics of light in a transmission medium involving the SMS arrangement depends on parameters such as source polarization and because of the imperfections that exist in the connections between the SMF and MMF and connections, mode mixing will occur. It was also observed that if the light source is coherent, such mode mixing leads to interference, which causes fluctuations in the output power and waveforms. However, this study was only limited to a single wavelength being transmitted.

As part of my research in a quest to improve OCDMA system performance this effect of the SMS structure was explored and applied to OCDMA multi wavelengths systems based on two dimensional wavelengths hopping time spreading codes for data communication. An experiment was conducted in which the SMS structure was inserted into the transmission link of an incoherent multiwavelength OCDMA testbed. The conducted experiment

was aimed at investigating the possibility of achieving an in-situ technique to equalize wavelength powers within an FBG generated OCDMA and to study the effectiveness of the proposed in situ technique. A module containing a generic polarization controller from Fibre Control with single mode fiber pigtails followed by a short (60cm) piece of multi-mode fibre was used.

4.4 Experimental Demonstration of In-Situ Redistribution of Wavelength Power in FBG Encoded OCDMA.

To demonstrate the proposed *in situ* technique for wavelength power equalization, the proof of concept experiments were carried out using a field based fibre optic transmission link having a length of 17km. The transmission link is fully compensated for the chromatic dispersion and at its both ends is connected to multiuser OCDMA terminals. The link is part of the advanced bidirectional fibre optic OCDMA test bed connecting CIDCOM research laboratory at University of Strathclyde with the communication laboratory at Glasgow University.

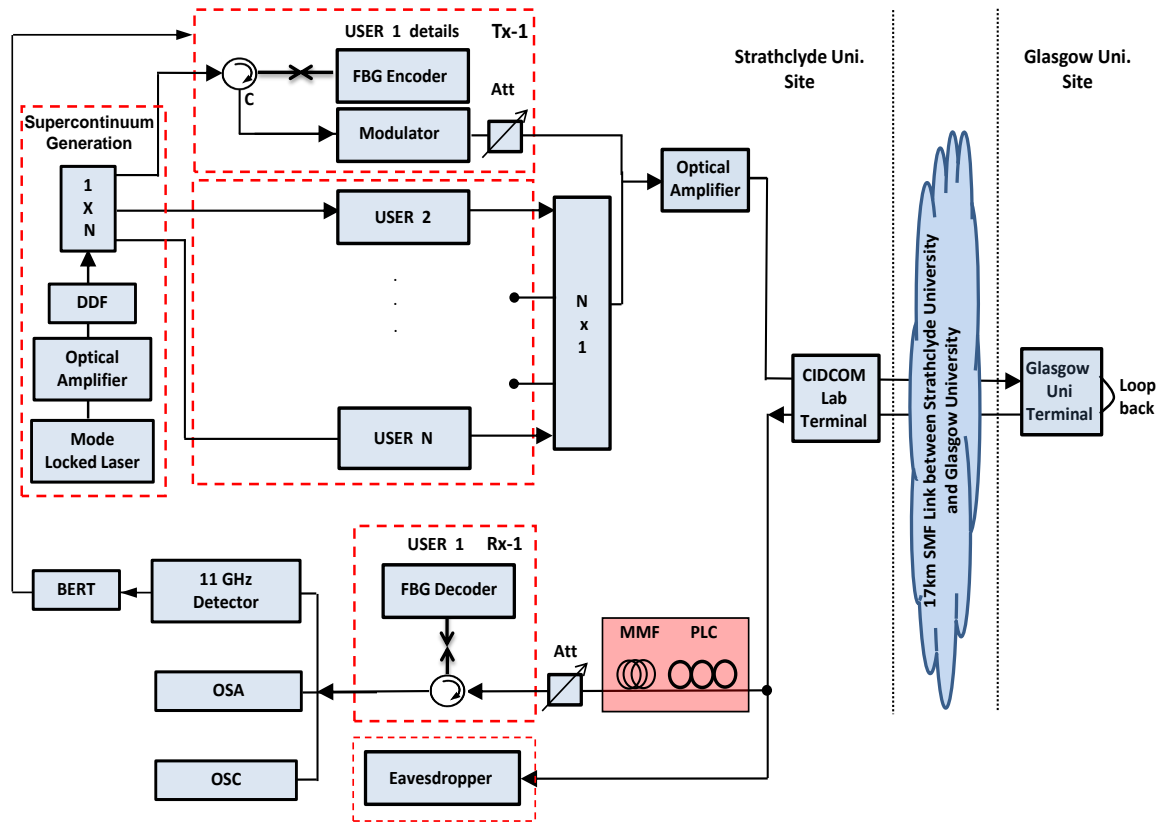


Figure 4.2 Experimental setup to demonstrate wavelength power redistribution in OCDMA transmission using PLC-MMF. Where C is Circulator, Att is Attenuator, OSA is Optical Spectrum Analyser, OSC is Oscilloscope and DDF is Dispersion decreasing fibre.

As shown in figure 4.2, the experimental test bed was populated with four simultaneously transmitting users and two receivers. Each user's data is uniquely encoded using FBG-based encoders with 2D-WH/TS OCDMA codes. Transmitted power level for each user was equalized by the variable optical attenuator at the output of each encoder. USER 1 encoder is matched with the corresponding decoder at the receiving Uni end. The combined traffic when presented to OCDMA decoder matched to USER 1's encoder will produce weight four autocorrelation peak corresponding to decoded transmission from USER 1, while all unmatched codes coming from simultaneous users broadcasting on the network will result in cross correlations thus contributing to the so called MAI.

The OCDMA testbed uses 2D-(4,16) wavelength-hopping time-spreading

prime codes which consist of four wavelengths ($\lambda_1 = 1551.72$ nm, $\lambda_2 = 1550.92$ nm, $\lambda_3 = 1552.52$ nm, $\lambda_4 = 1550.12$ nm) based on 100 GHz ITU grid positioned in 16 time chips each of 25 ps duration. Each code comprises of all four wavelengths. Individual wavelengths are generated by spectral slicing of a 3.2 nm wide optical supercontinuum (OSC) resulting from pulse compression of 1.8 ps full width at half maximum (FWHM) laser pulse from an Erbium doped mode locked fibre laser (MLL) running at 2.5 Gbits/s.

To generate OSC, the laser pulse is passed through an erbium doped fibre amplifier followed by the dispersion decreasing fibre. The optical supercontinuum needed by testbed users for OCDMA codes generation is obtained by its power splitting (see figure 4.3). Each portion is immediately encoded by user's own FBG-based OCDMA encoder. This produces WH/TS OCDMA codes. USER 1 codes are then modulated by Mach-Zehnder data modulator driven by a $2^{31} - 1$ PRBS data from an Agilent N4903A series bit error rate tester.

The encoded sequences from remaining encoders (USER 2-4) are first combined with the USER 1 traffic, amplified and then launched into a 17 km dispersion compensated field fibre link. For the purpose of these experiments, the received signal before it gets decoded was launched into a module containing a polarization controller and a short (60 cm) section of multimode fibre (see PLC-MMF in figure 4.2) and thereafter was presented to USER 1 FBG-based OCDMA decoder using a single mode fiber patch cable. Since the FBG decoder provides reverse wavelength delays compared to the encoder, this results in the strong autocorrelation peak of weight four at the background of cross-correlations.

After OCDMA decoding, the decoded signal was sent via an optical power meter with built in attenuator (Agilent 8157A) to a bit error rate tester with an 11GHz optical receiver (Nortel PP10G) as its frontend. The decoded OCDMA signal was also monitored using an optical spectrum analyzer (Agilent 86146B) and an oscilloscope (Digital communications analyzer - Agilent 86105B equipped with 60GHz optical sampling head).

Figure 4.3 shows optical power spectrum of the received 2D-WH/TS OCDMA code showing an uneven distribution of power among individual wavelengths within the OCDMA code. Figure 4.4 demonstrates that considerable changes of such wavelengths power spectrum was achievable using the proposed in situ technique by simply manipulating signal polarization via the polarization controller inside the MMF-PLC module.

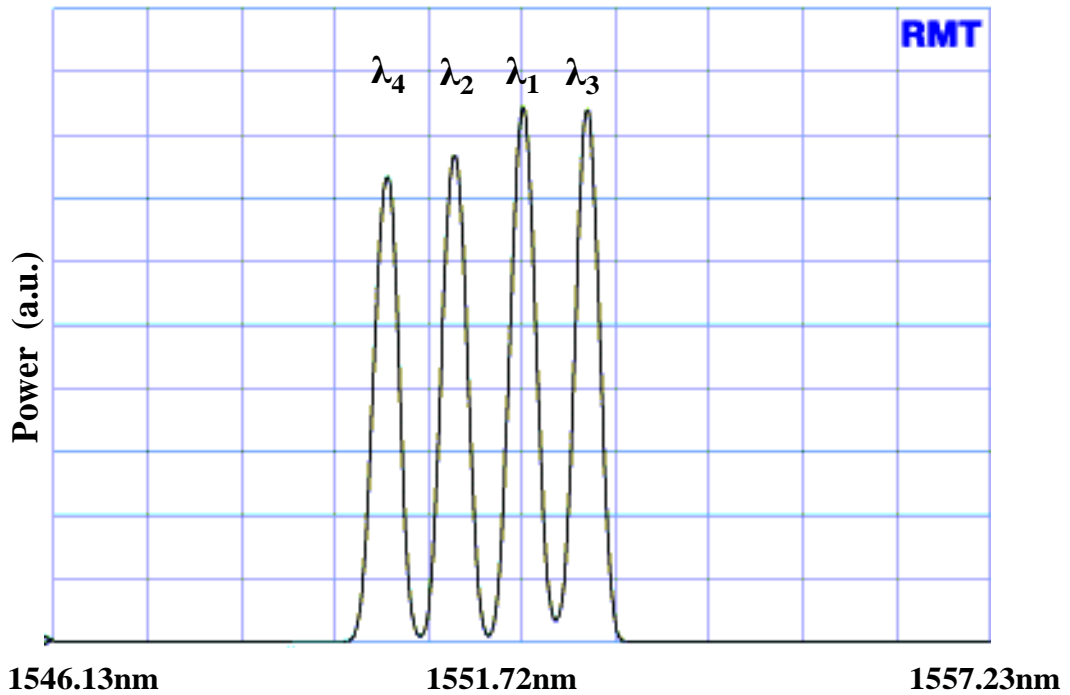


Figure 4.3 Optical spectrum of OCDMA signal showing the power distribution among individual wavelengths within the code at the input of PLC-MMF module.

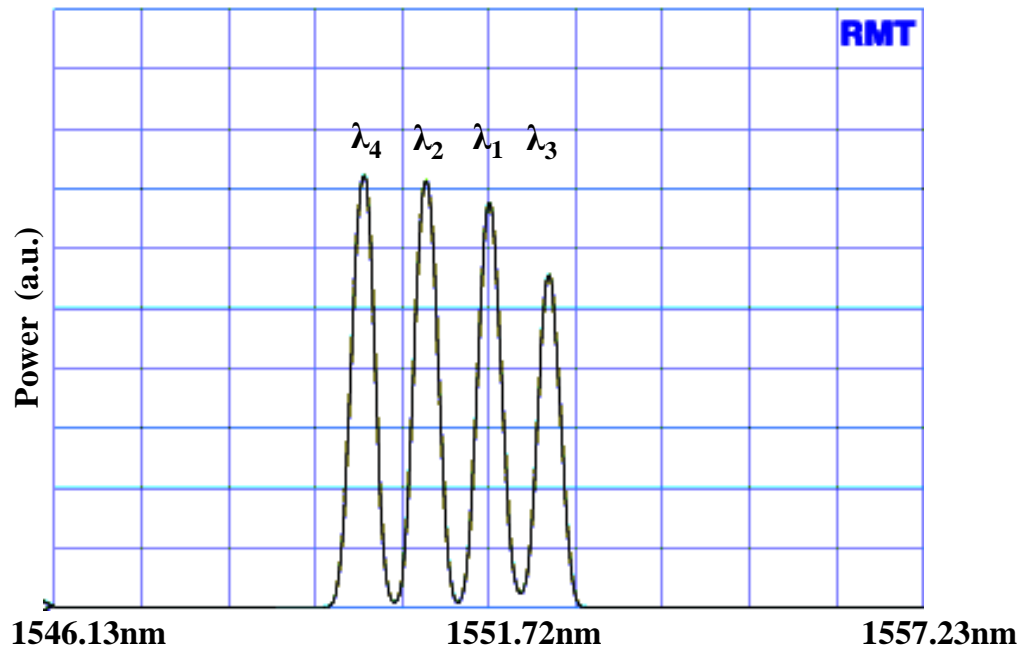


Figure 4.4 Non-equalized optical spectrum of OCDMA signal showing the power distribution among individual wavelengths within the code after passing PLC-MMF module but with polarization settings not optimized.

During these experiments it was also found that regardless of the “undesired influence” of the transmission fibre link on the propagated signal (OCDMA codes) the optical power spectrum (wavelength power distribution) of the OCDMA code always responds to the manipulation of the incoming signal polarization just before the coded sequences were presented to the OCDMA decoder at the receiver end. Figure 4.5 shows a more equalized wavelength pulse sequence compared to figure 4.4 this was achieved after several iterations of polarization settings of the PLC-MMF module.

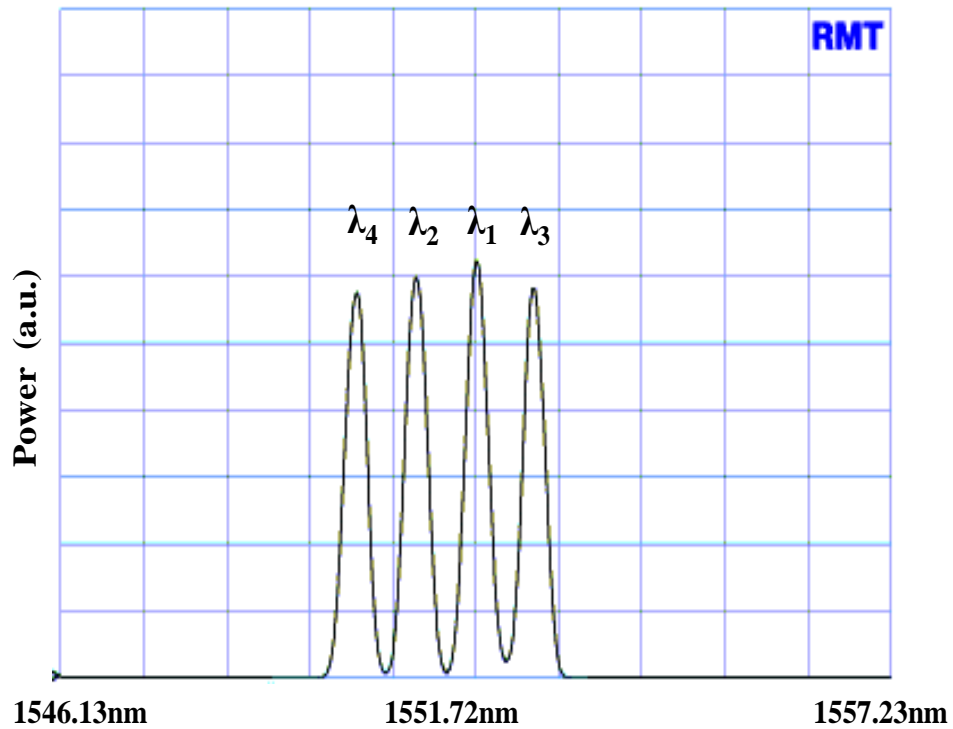


Figure 4.5 Optimized optical spectrums of OCDMA signal showing the power distribution among individual wavelengths within the code: after passing PLC-MMF module with different settings of PLC.

The next set of experiments was designed to verify if the ability to control the optical power spectrum of the OCDMA code can be used for improving the overall OCDMA system performance, in particular, the bit error rate observed by OCDMA users. For the purpose of this demonstration the USER 1 was picked. All measurements were taken in the presence of MAI caused by three additional simultaneous users broadcasting on the network. To conduct these experiments the 17km long bidirectional optical fibre link connecting the CIDCOM research laboratory at University of Strathclyde with the Communication research laboratory at Glasgow University was used.

For an illustration, figure 4.6 is Tx-1 output showing the waveform of OCDMA code 1 modulated with USER 1 data as seen on the oscilloscope via an 11GHz bandwidth limited optical receiver. It is worthwhile to note that

because of an insufficient time resolution of the oscilloscope λ_1 , λ_4 and λ_2 , λ_3 wavelength peaks within the code 1 are not properly time resolved. Figure 4.7 shows the autocorrelation resulting from OCDMA data decoding by USER 1 OCDMA decoder in the absence of MAI, (USERS 2, 3, and 4 are “OFF” and not broadcasting on the network).

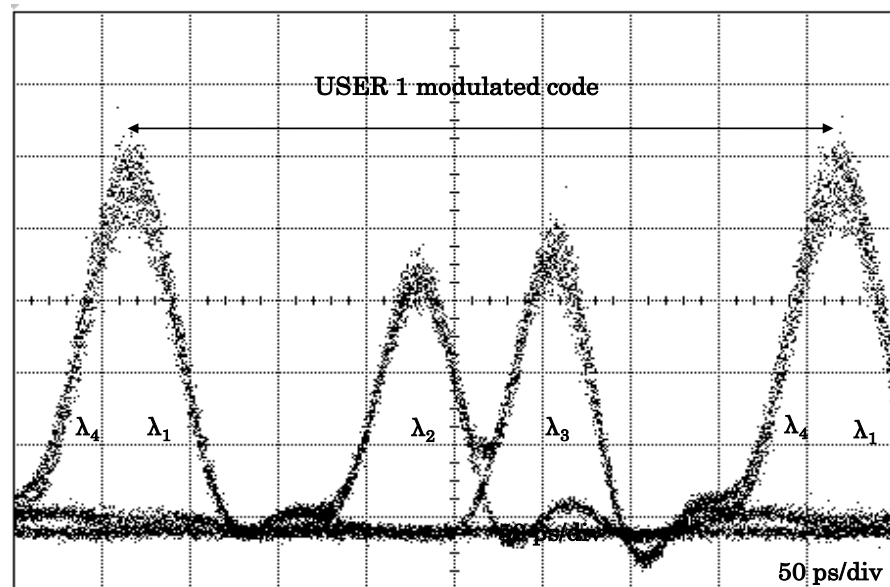


Figure 4.6 OCDMA code modulated with USER 1 data as seen on the oscilloscope via an 11GHz bandwidth limited optical receiver.

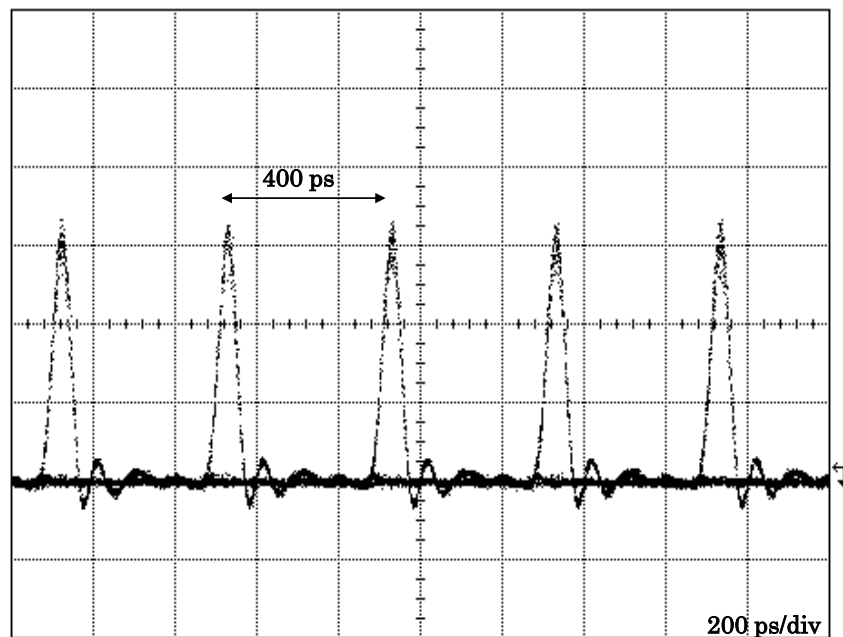


Figure 4.7 Obtained autocorrelation after decoding a single user OCDMA data transmission by decoder matched to USER 1 encoder.

Figure 4.8 shows the decoded OCDMA signal by the USER 1 OCDMA decoder when all users are “ON” without the PLC-MMF module. In this case the decoder output is the combination of an autocorrelation corresponding to the received USER 1 data and cross correlations (MAI) resulting from simultaneous users (USER 2-4) also broadcasting on the network. Figure 4.9 also shows the decoded OCDMA signal by the USER 1 OCDMA decoder when all users are “ON” but this time with the PLC-MMF module implemented. By comparing figure 4.8 and figure 4.9 the contrast ratio between the autocorrelation peak and the “nearby” MAI is lower in figure 4.8 than it is in figure 4.9 where the PLC-MMF module was implemented. This shows that the ratio of the autocorrelation peak to the cross-correlations (signal to noise ratio) has been improved as a result of the in-situ equalization of the wavelength power within the OCDMA code.

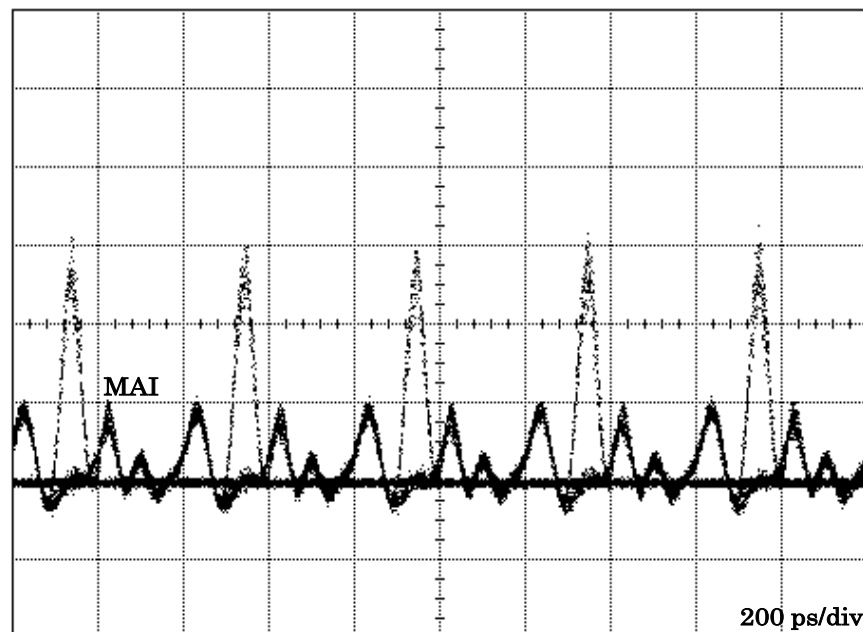


Figure 4.8 Obtained autocorrelation signal at the USER 1 OCDMA decoder output showing autocorrelation peaks corresponding to received USER 1 data and the MAI resulting from simultaneous users broadcasting on the network without PLC-MMF module implementation.

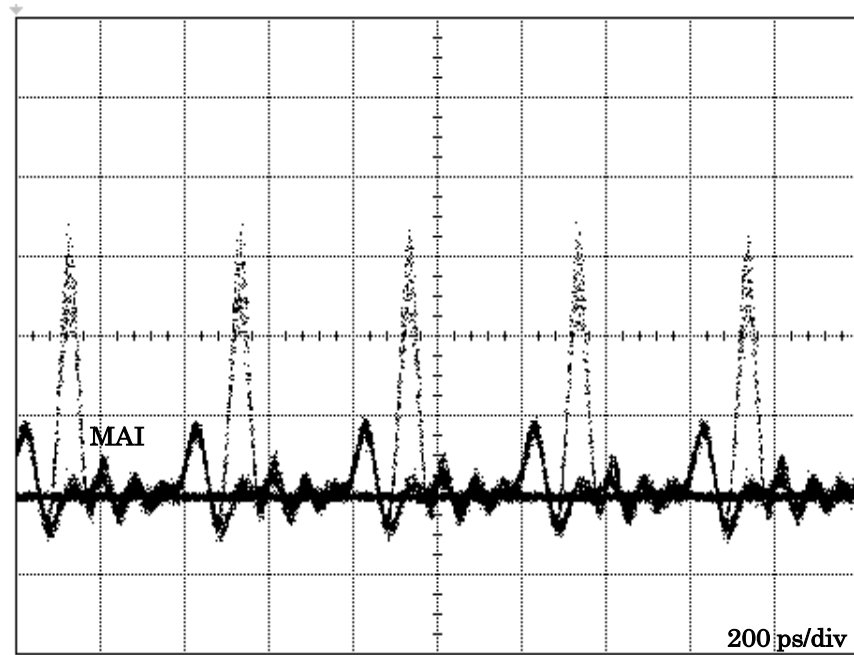


Figure 4.10 Obtained autocorrelation signal at the USER 1 OCDMA decoder output showing autocorrelation peaks corresponding to received USER 1 data and the MAI resulting from simultaneous users broadcasting on the network with PLC-MMF module implementation.

Bit error rate (BER) tests was also conducted in order to effectively quantify the effects of these observed increase in the autocorrelation – crosscorrelation ratio, on the overall system performance. Obtained BER results are summarized in figure 4.10 which shows two sets of data measurements.

The first set of measurements (see squares in figure 4.10) was performed with inserted PLC-MMF module as can be seen in figure 4.2. Then the bit error rate was recorded for varying power levels. Prior to recordings the PLC-MMF module was used to target the most even wavelength power distribution in the OCDMA code (see example figure 4.4 and figure 4.5). This was monitored by an optical spectrum analyser and oscilloscope. It was found that once the proper polarization setting was obtained, it was not necessary to make additional adjustments during subsequent measurements. The second set of measurements (see circles in figure 4.10)

was performed using the same setup but without the PLC-MMF module being inserted.

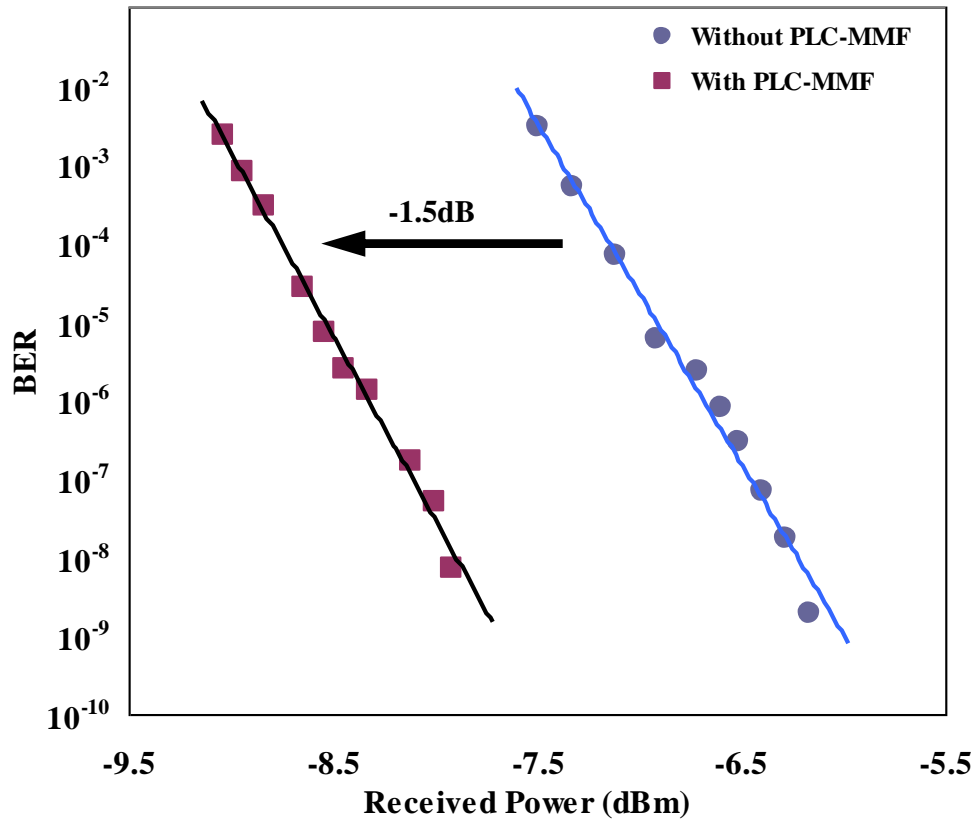


Figure 4.10 BER versus received optical power for case of OCDMA transmission over 17 km long bidirectional fibre optical link between Strathclyde and Glasgow University. Squares: PLC-MMF module used; circles: no PLC-MMF module used.

Comparison of results obtained from both sets of measurements in the form of BER curves can be seen in figure 4.11. The results clearly indicate a 1.5 dB system performance improvement (marked as -1.5 dB power penalty) when the PLC-MMF module was used. It is also worth noting that the control of the polarisation of the incoming signal via the polarisation controller in front of the receiver can contribute to improving the autocorrelation to cross correlation contrast ratio. However, in the present case, since no polarization dependent elements are part of the OCDMA receiver, it was concluded that this was not a contributing factor.

4.5 Chapter Summary

In this chapter, a simple novel in-situ method for re-equalising the power distribution of individual wavelength pulses representing two-dimensional wavelength-hopping time-spreading (2D-WH/TS) OCDMA codes was demonstrated. The method is based on manipulating the polarisation of incoming signal by using a module which combines a polarisation controller and a short section (~60 cm) of multimode fibre in an SMS structural arrangement before it was presented to the OCDMA decoder. The PLC-MMF module was found to affect the power distribution among individual wavelengths pulses of the 2D-WH/TS OCDMA code.

To confirm the effectiveness of these observations, field trials were conducted using 17 km long multiuser OCDMA test bed based on a bidirectional single mode fibre optic transmission link compensated for chromatic dispersion with sub-picosecond accuracy installed between the CIDCOM laboratory at University of Strathclyde and the Communication laboratory at Glasgow University. These experiments confirmed that the proposed in-situ method provides a very effective way to control and equalize the power spectrum of 2D-WH/TS OCDMA codes while propagating in the single mode optical fibre with no need for accessing the code's individual wavelengths to perform such power readjustment if and when necessary.

It was confirmed experimentally that by applying the *in situ* method on the incoming OCDMA signal right before it is presented to the 2D-WH/TS OCDMA decoder the BER system performance improvement can be achieved. A negative 1.5 dB power “penalty” resulting in the left shift of the BER curve as indicated in figure 4.10 was also achieved.

Chapter 5

Achieving Better Network Scalability by Using OCDMA over OTDM

5.1 Introduction

Optical code division multiple access (OCDMA) has been shown to be a possible candidate for broadband access in future optical networks [12, 86]. At present, architectures used for optical data transmission in existing optical networks include wavelength division multiplexing (WDM) [87] and optical time division multiplexing (OTDM) [88]. In WDM networks, each user is assigned a different wavelength, while in OTDM its own channel (timeslot). It is believed that as optical technologies

becomes more mature and advanced optical devices becomes more widely available, WDM standards for last mile access will become more acceptable. However one of the shortcomings of WDM is the fact that the number of available wavelengths might not be adequate to support users in access networks. OTDM on the other hand have been widely standardized for access networks example of existing standard for OTDM is the Ethernet PON which is defined in the IEEE 802.3ha, and ITU-T G.984 standard for gigabit passive optical network (GPON). Also hybrid high-speed networks incorporating WDM and OTDM have been demonstrated as a means of effectively utilizing the bandwidth capacity of the optical fibre [89, 90].

By implementing OCDMA, each user is assigned a unique optical code that is generated by the user's OCDMA encoder. The use of optical coding has been shown to be an attractive way of enhancing data privacy in the physical layer of optical networks [86]. As of today, different architectures have been proposed for possible implementation of either coherent or incoherent approaches to OCDMA [91, 92]. To enhance scalability and to increase the number of simultaneous users that can transmit effectively on the network, hybrid schemes such as WDM-OCDMA and OTDM over coherent OCDMA have been investigated [12, 93, 94]. WDM-OCDMA networks share available bandwidth between end users by deploying OCDMA in each WDM channel. This ensures that the flexibility of OCDMA can be harnessed and all users do not necessarily have to transmit at the same rate [95].

In this chapter, an optical network based on an *incoherent* OCDMA over OTDM network (OCDMA-OTDMA) is proposed and demonstrated.

The demonstration was carried out using already installed fibre link. Based on the overall system analysis which also includes scalability and

power budget calculations, the proposed OCDMA over OTDM architecture can be used to deliver enhanced scalability and a substantial increase in the number of simultaneous users.

The OCDMA implementation and OCDMA-OTDM system analysis is based on implementation of two dimensional wavelength-hopping time-spreading (2D-WH/TS) codes which use multi wavelength picoseconds pulses. The OCDMA encoding/decoding was done using fibre Bragg gratings (FBG) based encoders/decoders [92].

5.2 Optical TDM

Optical time division multiplexed signals are transmitted as a periodic succession of frames. As shown in figure 5.1 each frame consists of N time slots or channels (Ch).

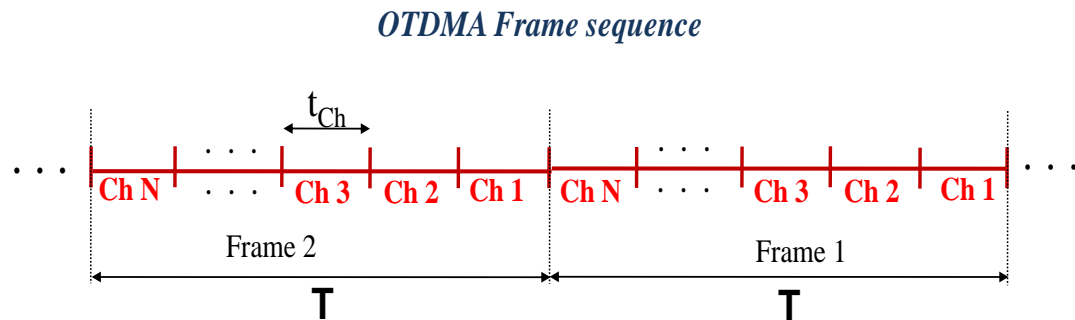


Figure 5.1 A sequence of optical time division multiplexed channels forming a periodic frame. Where Ch is channel.

The length of each OTDM frame (T) is related to the duration (t_{ch}) of each of the N timeslots and is given as:

$$T = N_{ch} \times t_{ch} \quad (6.1)$$

The maximum transmission bit rate per channel is the inverse of the frame length and is equal to $1/T$.

From figure 5.1, it can be observed that the number of users of the OTDM system is limited by the number channels (N_{ch}). There are two approaches by which the number of channels (N_{ch}) can be increased. The first method is by increasing T while keeping t_{ch} constant. However this approach will result in a decrease in bitrate per channel. The other alternative for increasing the number of channels without compromising bitrate is to make t_{ch} smaller. Also, this method is limited by the ability to effectively demultiplex each channel because this will require very fast clock signals. Therefore for a standalone OTDM system, increasing scalability will either be at the expense of speed or it will require faster optical clock and synchronisation schemes.

5.3 OCDMA over OTDM System Architecture

The OCDMA over OTDM is conceptually shown in figure 5.2 where OCDMA systems each capable of supporting M-users is being implemented in each of N time slots (channels) of the OTDM network.

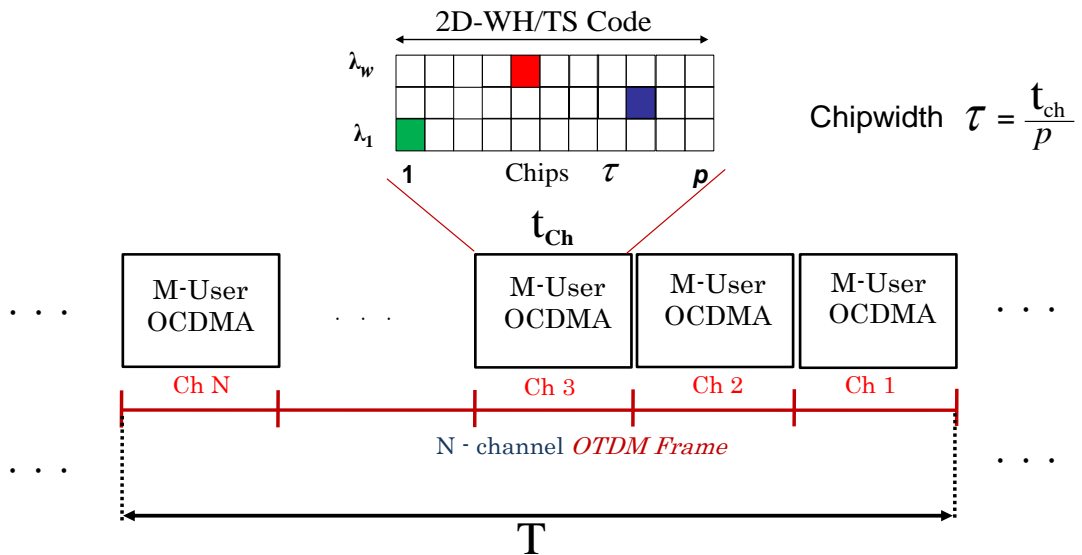


Figure 5.2 Illustration of a hybrid optical system formed by overlaying multiuser OCDMA into each channel of an OTDM frame to increase scalability.

The figure illustrates a typical frame in the hybrid system which is formed by using the each OTDM channel to transmit data belonging to M -OCDMA users. Each transmitting device in an OTDM system is allowed to transmit data for a fixed period t_{ch} . This approach allows N groups of M -users OCDMA system transmit data over OTDM network while reusing the same OCDMA hardware. This also allows OCDMA code reuse which greatly simplifies the OCDMA hardware implementation. This hardware configuration and code reuse are made possible by way of assigning each individual OCDMA transmitting group a separate OTDM timeslot (channel). By so doing, the scalability of the resulting system is N times enhanced when compared to the stand alone OCDMA. In view of this, we can conclude that

$$K = M \times N \quad (6.2)$$

Where

K is the maximum number of simultaneous users (K) of the proposed hybrid OCDMA-OTDM system.

M is the number of simultaneous users of the standalone OCDMA system.

N is the same as N_{ch} which is the number of OTDM timeslots (channels).

Figure 5.3 shows the detailed transmitter architecture for the hybrid OCDMA over OTDM system.

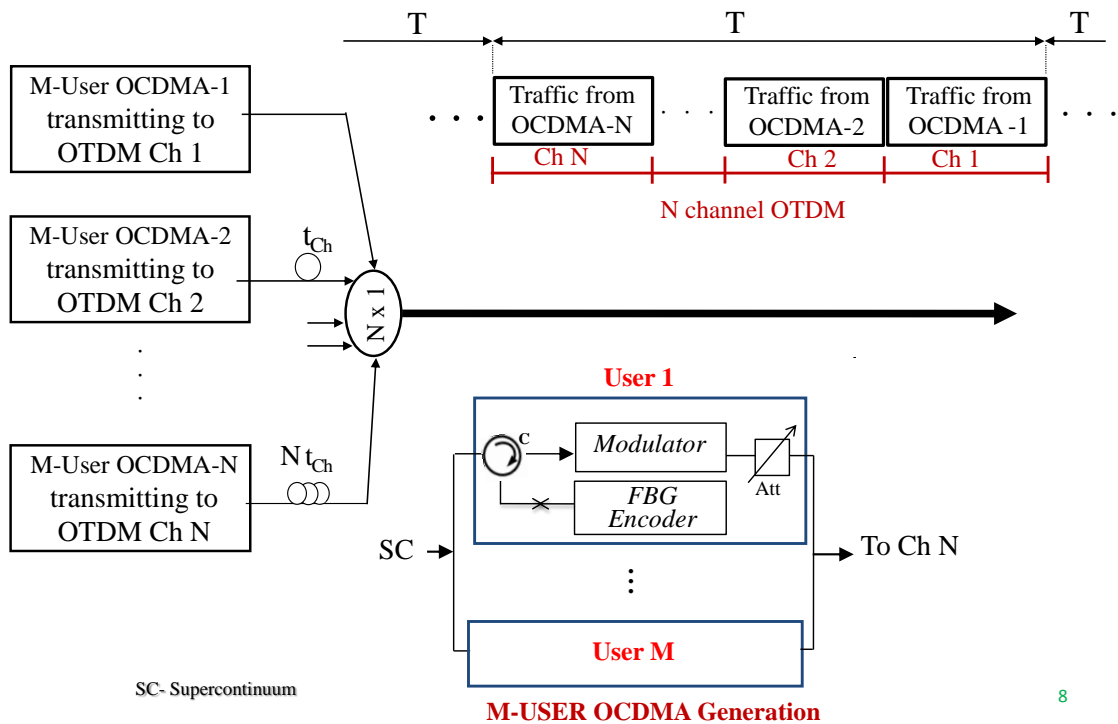


Figure 5.3: Architecture of the transmitter for the hybrid OCDMA over OTDM system showing different M-User OCDMA being combined to form a time division multiplexed optical signal. That is launched into the fibre optic link.

The different M-User OCDMA are seen to be combined to form a time division multiplexed optical signal. The signal that is launched into the fibre optic link is seen as a TDM signal, because all the OCDMA signatures for all users have been encapsulated into the TDM frame. This is an added advantage because it forms another layer of security that need to be broken before an eavesdropper can gain access to a data from a particular OCDMA encoded user [96]

Also, figure 5.4 shows the detailed receiver architecture for the hybrid OCDMA over OTDM system. In order to extract particular user information, it first has to be time division de-multiplexed and thereafter passed through the OCDMA decoding process.

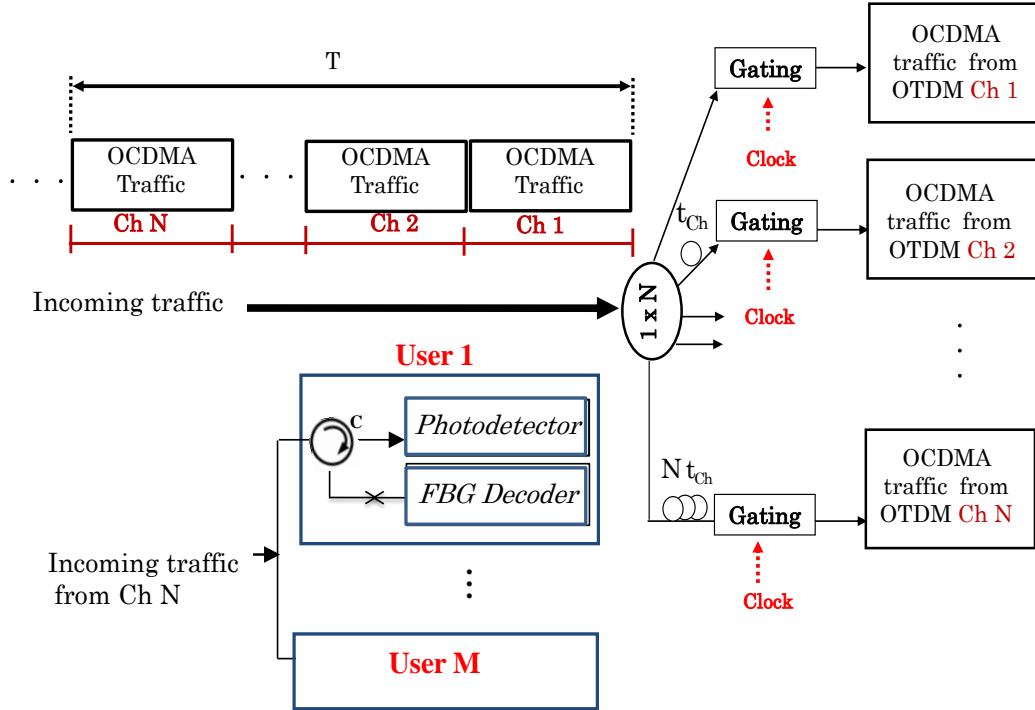


Figure 5.4: Illustration of the receiver showing M-User OCDMA signals being de-multiplexed from different channels /timeslots of the incoming time division multiplexed optical signal. (The demultiplexing stage precedes the per user decoding process).

To optimize the performance of the system it is recommended that the OTDM channel width t_{ch} should not be greater than the OCDMA code length. This will ensure that each group of OCDMA user's encoded data is confined to a specific timeslot. In general, although this hybrid OCDMA over OCDMA enables hardware reuse, it should be noted that this hardware reuse is not a compulsory requirement. Each OCDMA group transmitting into its assigned OTDM time slot may use a different OCDMA hardware uniquely tuned to support any targeted application.

5.3.1 Scalability Calculation

To put into perspective the extent of scalability of an OCDMA system can be improved with the implementation of the proposed OCDMA-over

OTDM, Let us compare the number of simultaneous users of a standalone OCDMA system with the number of simultaneous user of an hybrid OCDMA-OTDM system with the same code parameters (code weight, pulsewidth, chip width and so on). In the proof of concept field demonstrations (later in the chapter), the OCDMA code length was 400ps therefore to deliver OC-12 data rates four OTDM channels were available, i.e. $N = 622\text{Mbits/s}/400\text{ps} = 4$. See figure 5.7 for more detailed diagram of the M-user OCDMA system.

Figure 5.5 and 5.6 presents the calculation results (using equation 3.7) with figure 5.5 showing the relationship between probability of error and the number of simultaneous users for an M-user standalone OCDMA system with the code weight (w) equal to 4 and 8 respectively.

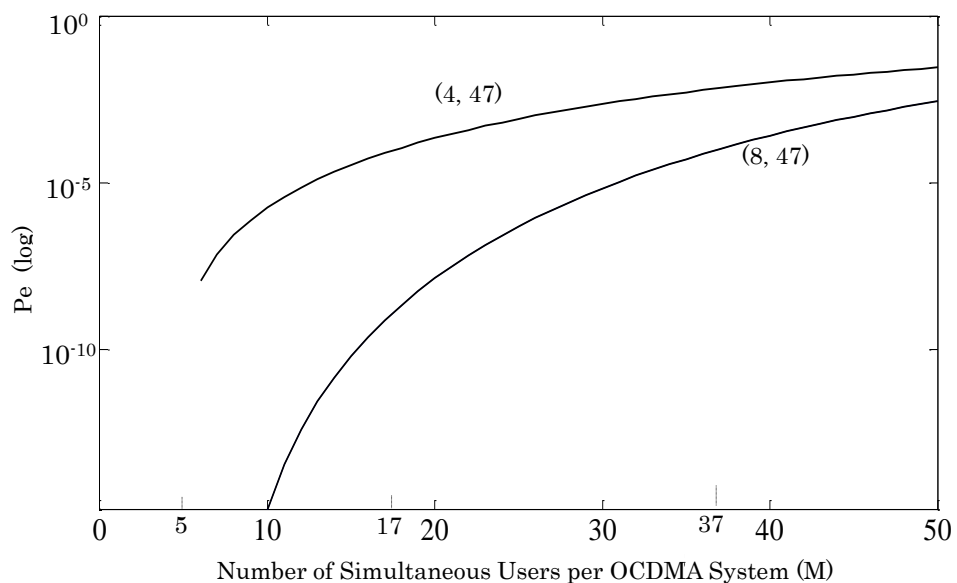


Figure 5.5 Performance curves for a standalone M-User OCDMA system showing the changes in error probability as the number of simultaneous users increase. (The first curve is for a system with code weight $w = 4$ and the other curve shows calculations for a system using codes with $w = 8$)

Figure 5.6 shows the improvement in the number of simultaneous users if an M-user OCDMA system is overlaid over N -channel OTDM system. Based on the above results (see figure 5.5 and 6.6) a “standalone” (8, 47)

OCDMA system can conveniently support 17-users with each user achieving a bit error rate of up to 10^{-9} ; if four of this 17 user standalone system is multiplexed and now overlaid over a four-channel OTDM system, the number of supported simultaneous users will increase to 68 users.

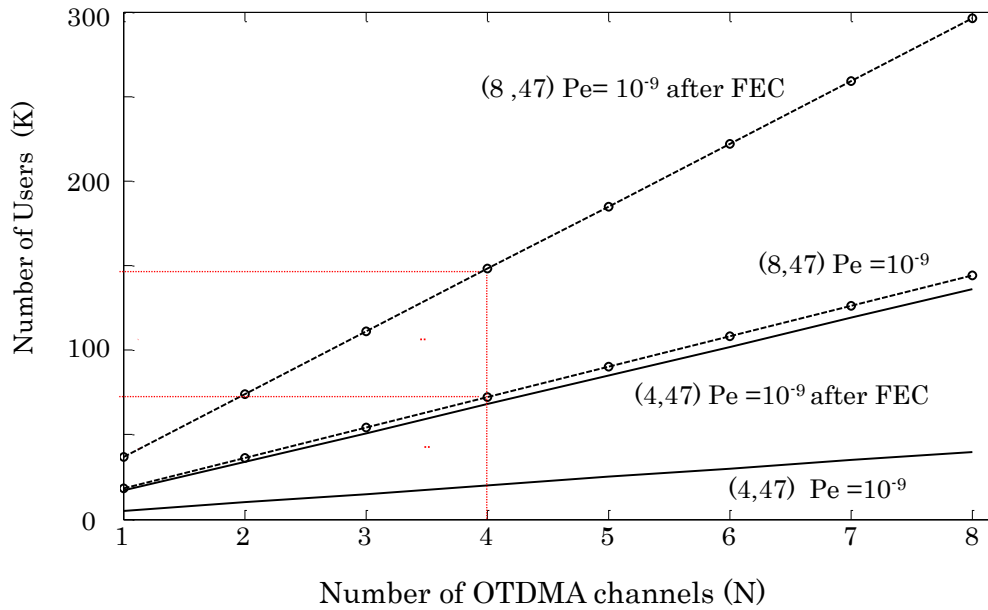


Figure 5.6: Showing scaling potential of the proposed OCDMA over OTDM network architecture.

Thanks to OCDMA soft blocking properties if the same (8, 47) OCDMA is scaled up (designed and build) to support 37 simultaneous users by allowing BER to drop to 10^{-4} (which in turn can be corrected back to 10^{-9} by forward error correction (FEC)) then the OCDMA-OTDM system with four OTDM channels will be able to support up to 148 simultaneous users at the OC-12 data rates.

5.3.2 Experimental Demonstration and Results

The experimental demonstration of the proposed OCDMA over OTDM system was done in a field-based transmission test bed which is a 17km long bidirectional fibre optic link installed between the University of Strathclyde CIDCOM laboratory and University of Glasgow optics laboratory and is fully compensated for chromatic dispersion with sub-picoseconds accuracy.

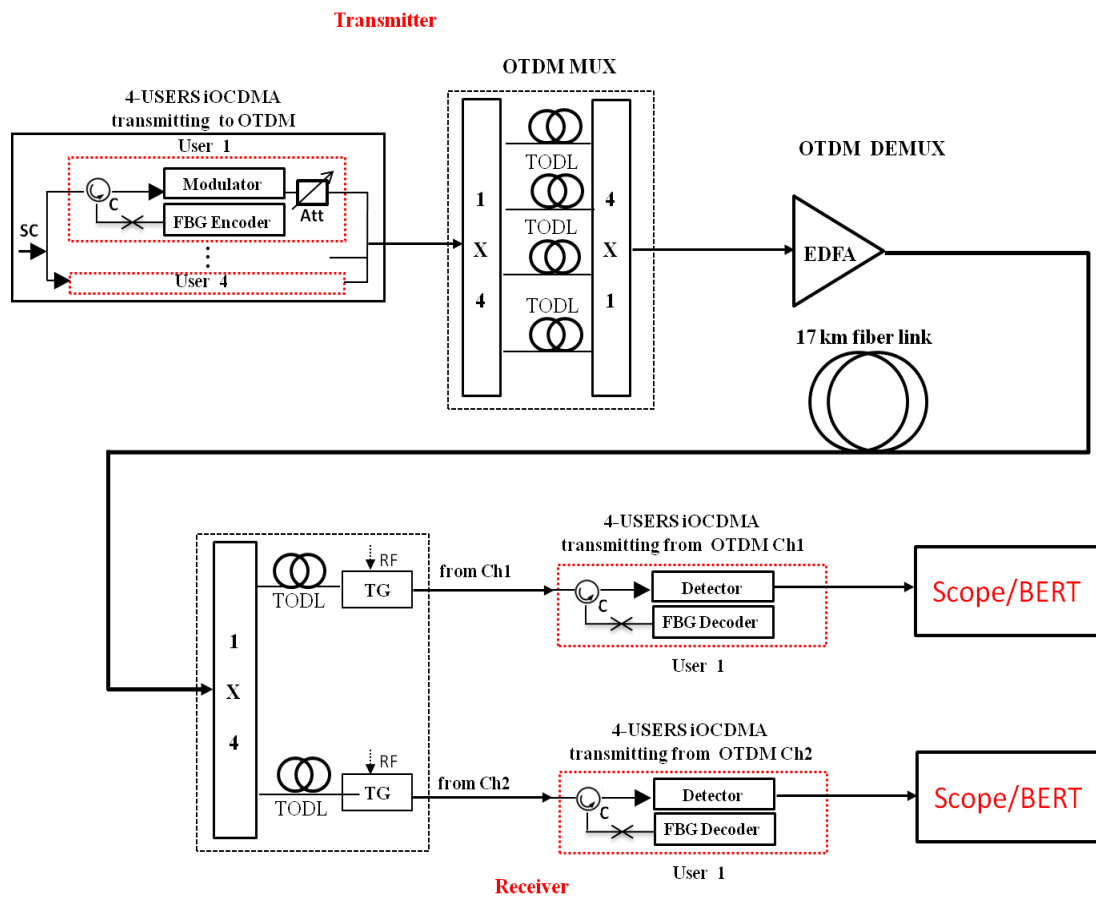


Figure 5.7 Experimental test bed to demonstrate the incoherent OCDMA over OTDM network architecture. Where TG is time gate, EDFA is erbium doped fibre amplifier, FBG is fibre Bragg grating. Att is attenuator, RF is radio frequency, SC is super continuum, ChN is Channel N, TODL is tuneable optical delay line.

The field based experimental test-bed for the OCDMA-OTDM transmission demonstration is shown in figure 5.7. In this proof of concept experiment, a four-user OCDMA system per each of the four OTDM channels at 622 Mbps data rate was used. All users' data were uniquely encoded by FBG-based OCDMA encoders generating 2D-WH/TS codes. The OCDMA systems used 400ps long 2D-(4,47) WH/TS codes consisting of four wavelengths ($\lambda_1 = 1551.72$ nm, $\lambda_2 = 1550.92$ nm, $\lambda_3 = 1552.52$ nm, $\lambda_4 = 1550.12$ nm) based on 100 GHz ITU grid accordingly positioned into 47 time chips each of ~ 8 ps duration. Every code uses all four wavelengths. As an example, chips occupied by the user1 code are (1- λ_3 , 9- λ_2 , 28- λ_4 , 31- λ_1).

Wavelengths are obtained by spectral slicing of a 3.2 nm wide optical super continuum (SC) resulting from pulse compression of 1.8 ps laser pulse from a mode-locked Erbium doped fibre laser. Generated 2D-WH/TS OCDMA codes are then modulated by a Mach-Zehnder modulator driven by a $2^{31}-1$ pseudo-random bit sequence (PRBS) data from an Agilent N4903A series bit error rate (BER) tester.

Transmitted power levels from each user were equalized by optical attenuators placed at each encoder output (see transmitter in figure 5.7). Modulated data from all users within each OTDM channel are first combined by a power combiner and then the traffic from all OTDM channels is time division multiplexed into OC-12 OTDM frame having 400ps channel duration. The resulting signal is amplified by the EDFA and lunched into a field-based optical test bed.

Figure 5.8 shows a temporal trace of the combined OCDMA over OTDM traffic. Here, figure 5.8(a) is a snapshot of OCDMA codes traveling in OTDM Ch2, while figure 5.8(b) in channel Ch1 and Ch2, respectively.

Because of the bandwidth limited oscilloscope used, code weight of 4 is not properly resolved.

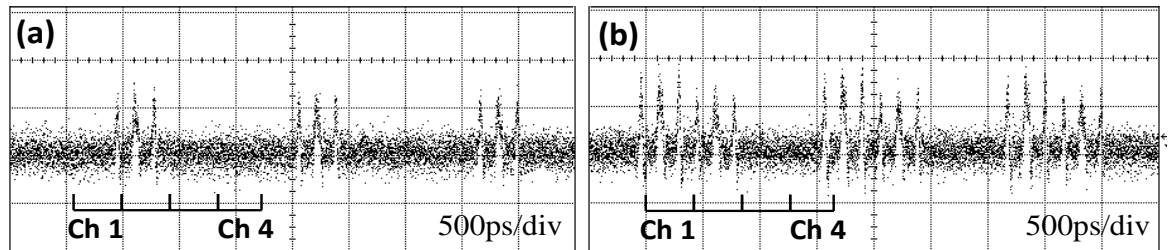


Figure 5.8 Examples of OCDMA traffic over OTDM channels as seen on bandwidth limited oscilloscope; (a) traffic in Ch2 only; (b) traffic in Ch1 and Ch2.

At the receiver, the traffic is first de-multiplexed in time domain into the individual OTDM channels by Mach-Zehnder based gates, TG (see figure 5.7 (receiver)) placed at $1 \times N$ power splitter outputs and as such presented for OCDMA decoding and photo-detection. To decrease the guard band needed by the Mach-Zehnder gate, all optical approach [97] could be implemented. Since OTDM is a synchronous multiplexing technique, the self-clocking enables the synchronization.

The autocorrelations representing received OCDMA data by the user 1 in Ch1 and the user 1 in Ch2 are shown in figure 5.9. For clarity of explanation, a snapshot of data pattern “1” is shown instead of PRBS pattern. Figure 5.8(a) shows autocorrelations of received data over Ch1 by user 1 when transmitting alone on OTDM Ch1; Figure 5.9(b) shows the autocorrelation of the OCDMA user 1 who alone is transmitting on OTDM Ch2.

Figure 5.9(c) shows received autocorrelation from user 1 of OCDMA system transmitting on Ch1 and user 1 of OCDMA system transmitting on Ch2. Figure 5.9(d) shows a scenario similar to one in figure 5.9(c) but with added transmission by all users on all four OTDM channels.

In order to quantitatively evaluate the overall OCDMA-OTDM system performance, the decoded traffic from Ch1 and Ch2 respectively were first sent via an optical attenuator with built in optical power meter (Agilent 8157A) to a bit error rate tester with an 11GHz optical receiver (Nortel PP10G) as its frontend.

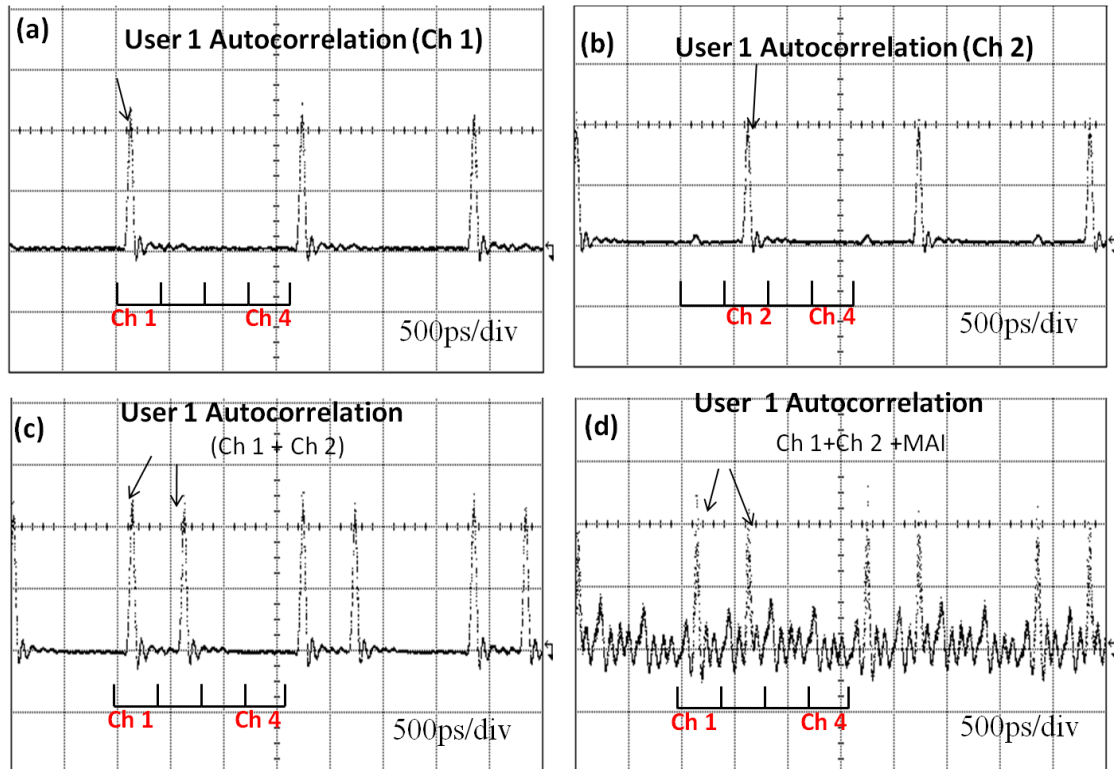


Figure 5.9 (a). Autocorrelations representing received OCDMA data by the user 1 when is transmitting alone only on OTDM Ch1; (b) only on OTDM Ch 2; (c) both users 1 are transmitting on their channels Ch1 and Ch2, respectively; (d) case in (c) when all other users also transmit on all four OTDM channels.

Obtained bit error rate results are shown in figure 5.10 and figure 5.11 shows an example of an eye diagram obtained for OCDMA user 1 transmitting in the OTDM Ch2 in the presence of MAI. The observed wide eye opening indicates good fidelity of the received signal.

The first set of BER curves corresponds to the transmission when only user 1 in OTDM Ch1 and user 1 in the adjacent Ch2 transmit (see figure 5.9(c)). The second set of curves reflects BER of the user 1 in Ch1 and user 1 Ch2 with the presence of all OCDMA users in all four OTDM channels (see figure 5.9(d)).

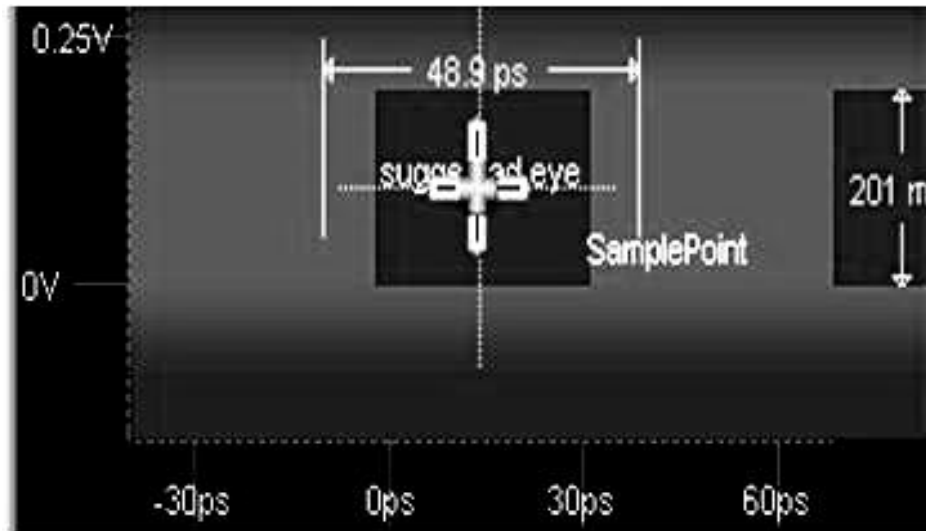


Figure 5.10 Sample eye diagram obtained during the proof of concept experiment to demonstrate the OCDMA over OTDM concept.

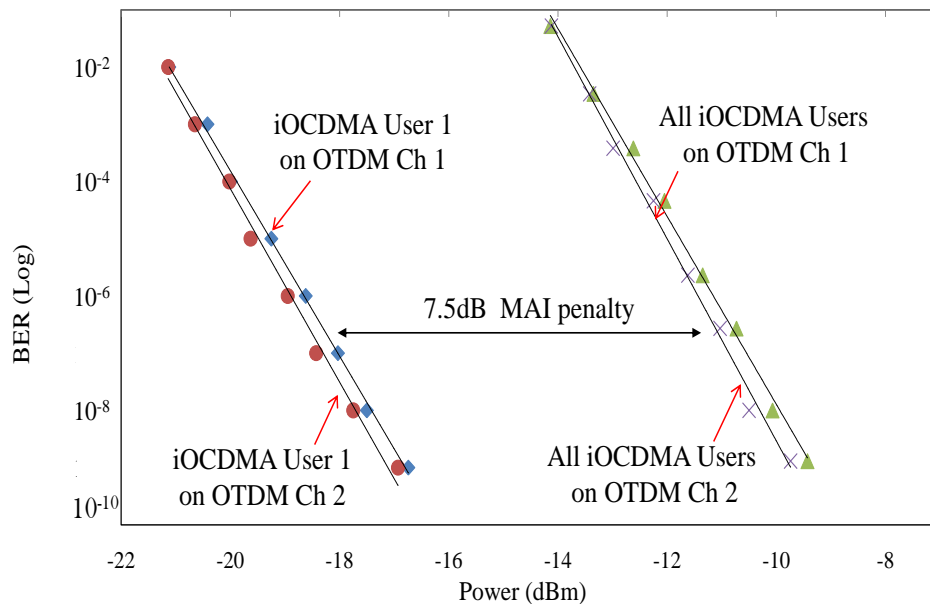


Figure 5.11 BER performance results obtained from the experimental demonstration of incoherent hybrid OCDMA-OTDM system.

5.4 Chapter Summary

In this chapter, a novel approach for increasing the number of simultaneous network users by way of overlaying M-USER *incoherent* OCDMA system over N -channel OTDM architecture was proposed and demonstrated. The field demonstration of this hybrid system was successfully done over a 17km fibre optic link connecting University of Strathclyde and Glasgow with achieved BER better than 10^{-9} , no error floor was observed.

From results obtained, the following was concluded:

- Within the experimental error the obtained BER curves are nearly identical for the demonstrated transmission on OTDM Ch1 and Ch2. This outcome indicates no or very low crosstalk between OTDM channels and high ON/OFF contrast ratio achieved by Mach-Zehnder gates, TG performing de-Mux operation of OTDM signal into individual channels.
- ~7 dB of power penalty per user was incurred as the consequence of detrimental effects of MAI on OCDMA users transmitting on OTDM channel.

Based on system scalability calculation results, it can be observed that a 17-users “standalone” (8,47) OCDMA system will achieve BER = 10^{-9} ; if now overlaid over four-channel OTDM, will support up to 68 users. Thanks to OCDMA soft blocking properties if the same (8, 47) OCDMA is scaled up (designed and build) to support 37 simultaneous users by allowing BER to drop to 10^{-4} (which in turn can be corrected back to 10^{-9} by forward error correction (FEC)) then the OCDMA-OTDM concept with four OTDM channels will be able to support up to 148 simultaneous users

at the OC-12 data rates. Power budget calculations were also conducted. The power budgeting included splitting losses, transmission loss over the demonstrated distance, and the losses incurred by individual devices.

Results of the power budget shows that an EDFA with 30 dB gain and 10dBm saturation power and a photo-receiver with the -30 dBm sensitivity will be sufficient to support 64-users based on (8, 47) OCDMA over 4-channel OTDM system, (BER = 10^{-9} no FEC) and 128-users with (8, 47) OCDMA over 4-channel OTDM system when adopts the FEC approach. The drop in the number of simultaneous users resulted from adopting power of two splitting “rule” which is important in system design. If the OCDMA-OTDM system employs a (4, 47) OCDMA over 4 channels OTDM and adopts the FEC approach it will scale up from 18 to 64 simultaneous users.

It is worth nothing that the hybrid system proposed here is an important step towards achieving commercially viable OCDMA technologies. Most of the argument against OCDMA has been that it has not been possible to achieve the required scalability in terms of large number of simultaneous users promised in theoretical analysis of OCDMA systems. However this novel hybrid approach will make it possible to reduce the number of simultaneous OCDMA users which eventually leads to improved performance. The reduction in the number of users for the standalone system will be offset by the fact that several standalone systems could be combined using the hybrid architecture without compromising performance.

Chapter 6

Towards Highly Scalable hybrid incoherent OCDMA Systems and Improved Data rates

6.1 Introduction

In the previous chapter, the architecture for increasing the scalability of an optical fibre based incoherent OCDMA system was proposed and demonstrated. The proposed system employs the technique of OCDMA code reuse that enables different groups of OCDMA users to transmit in separate OTDM channels. It was shown that the scalability of such hybrid system is increased by a factor of $M \times N$ where N is the number of OTDM channels

and M is the number of simultaneous OCDMA users per the OTDM channel.

The main emphasis of the system architecture described in chapter six was on increasing the number of simultaneous users. The proposed network architecture is useful for implementations in which there is less emphasis on increasing bitrates per user and where more emphasis is laid on increasing revenue by adding more users to the network. However, when the main focus is shifted to enhancing the scalability of optical systems without compromising on capacity and bandwidth, the system proposed in the previous chapter might not be able to tick both boxes. This is because increasing the scalability by increasing the number of OTDM channels will result in lowering data rates.

This chapter focuses on a novel approach that is aimed to further increase the scalability of the previously demonstrated OCDMA-OTDM system described in Chapter 6. The scalability improvement will be achieved via adding a third dimension to the original OCDMA-OTDM architecture and allowing the multiple OCDMA user-groups broadcast in parallel and simultaneously in different wavelength bands within each OTDM channel.

This approach allows OCDMA code reuse in every wavelength band without adding detrimental MAI within the OTDM channel. (Note that, in general, it is possible to implement coherent or incoherent OCDMA schemes in any or all OTDM channels).

As in previous cases, the analysis and discussions presented in this chapter assume the use of multi wavelength two-dimensional wavelength-hopping time-spreading (2D-WH/TS) OCDMA codes [98, 99] in all OCDMA sub-systems operating within the OTDM channels. The OCDMA implementation and the overall system performance analysis also reflect the use of picosecond pulses in 2D-WH/TS coding scheme.

6.2 Design of Highly Scalable OCDMA over OTDM Hybrid System

Figure 6.1 shows the concept of a hybrid transmission system based on the OCDMA over OTDM, which was described in details in chapter six. The newly proposed scheme will retain the hybrid concept but now with a major modification to the design of the OCDMA sub-systems “residing” in the individual OTDM time slots. As previously discussed, each M -User OCDMA system transmitting into the corresponding channel of the OTDM system could be built to use a varying number of wavelengths in the 2D-WT/TS codes in order to achieve the desired code weight for the targeted performance.

However, because of the limitations imposed by higher bitrate rates on the number of chips N_c it might not be practically feasible to achieve very large system scalabilities much beyond the numbers already reported [8].

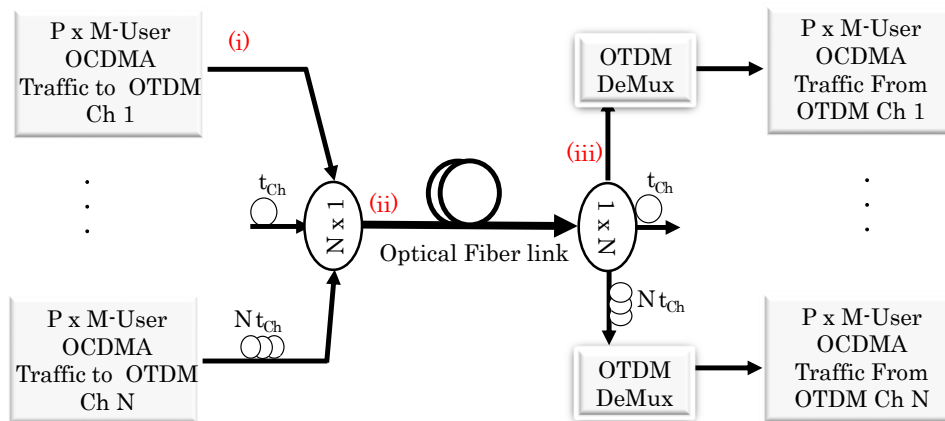


Figure 6.1 Architecture of the hybrid multi wavelength band OCDMA transmitting over N-Channel OTDM system.

The limitation arises from the fact the code duration (t_{ch}) depends on the number of chips (N_c) and the pulse width (T_c). However, because of the inverse relationship between N_c and T_c , to obtain large values of N_c the pulse width T_c needs to be sufficiently short (in the order of picoseconds).

Although technologies exist today for generating stable optical pulses with up to femtoseconds in duration [100], it is still in the early stage of commercialization.

6.2.1 $P \times M$ -Users incoherent OCDMA

To overcome this scalability bottleneck, and still be able to offer users higher bitrates another solution is to add a third dimension to the hybrid OCDMA over OTDM. Instead of using available wavelengths spectrum to form a single 2D-WH/Ts code set, the proposal is that the available wavelength spectrum be split into P groups of wavelength sub-bands [99]. Each one of the wavelength groups may have equal bandwidths allocation or in special cases have unequal bandwidths as will be required [101].

The architecture of the $P \times M$ -Users OCDMA (labelled as (i) in figure 6.1) is shown in figure 6.2.

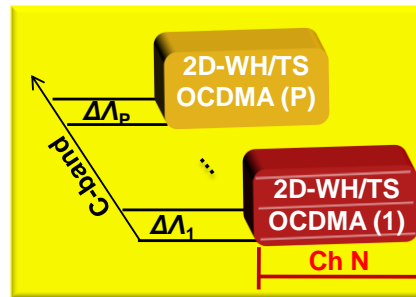


Figure 6.2: Multiple 2D-WH/Ts based OCDMA sub-systems encoded within P individual wavelength bands $\Delta\lambda_P$ to form $P \times M$ Users OCDMA transmitting to the N th OTDM channel.

Here each user-group consists of multi wavelength 2D-WH/Ts codes with code weight w . The code configuration may or may not be reused in each user-group. For a specific band of wavelengths $\Lambda(\text{nm})$, the length $\Delta\Lambda(\text{nm})$ of each of the P sub bands can be defined as

$$\Delta\Lambda_i = \frac{\Lambda}{P} \quad (7.1)$$

where $i = \{1, 2, \dots, P\}$.

$$\text{Also,} \quad \Delta\lambda_i = \delta\lambda \times w \quad (7.2)$$

where $\delta\lambda$ denotes the line width of each individual wavelength pulse that formed the 2D-WH/TS code. As before, the code weight (w) is the number of wavelengths per OCDMA code group if 2D-WH/TS codes of one pulse per wavelength (e.g., carrier-hopping prime codes [98]) are used.

6.2.2 Scaling to $P \times M$ -Users $\times N$ channels

Several groups of M -User OCDMA can be combined without interfering with each other in a manner similar to wavelength-division multiplexing (WDM) systems. The combined $P \times M$ -User OCDMA traffic group from all OTDM channels is then time-division multiplexed into OTDM frame. The OTDM channel duration will not exceed the longest code length of any of the M -User OCDMA. The multiplexing can also be done using appropriate delay lines and arrayed waveguide grating (AWG) which will introduce less loss compared with using simple power combiners' [102, 103, 104].

The OTDM traffic is then amplified and launched into the fibre-optic transmission link. In the new architecture, provided that each of the P groups of M -User OCDMA has equal bandwidth, the total number of simultaneous users will therefore be equal to $P \times M$ -Users of the OCDMA \times number of OTDM channels N .

The optical carriers for the $P \times M$ -User OCDMA traffic transmitting to each OTDM channel can be generated by slicing the spectrum of an optical super continuum by OCDMA encoders based on fibre Bragg grating (FBG), arrayed waveguide grating (AWG) [105], or thin film filter (TFF) [106]. The optical carriers can also be obtained from a set of multi wavelength laser arrays [107].

Figure 6.3 shows schematically the resulting traffic of the modified hybrid system as it propagates in optical fibre. At this point (labelled as (ii) in

figure 6.1), different sets of $P \times M$ -User OCDMA can be encapsulated into each of the N channels of the OTDM frame.

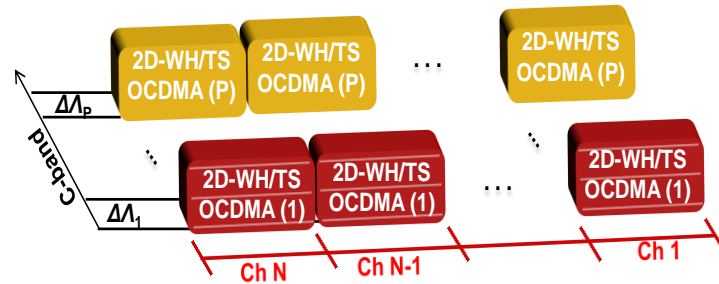


Figure 6.3 An N -channel OTDM frame with each channel containing several groups of OCDMA systems in order to increase the system capacity.

Depending on the application, the code set of each OCDMA code group can either be the same (thereby achieving code reuse) or separate code sets can be chosen for each code groups within the same time slot. Similarly, the coding scheme employed for the OCDMA groups within the different OTDM channels can either be the same or different. If the coding scheme is the same, then hardware reuse will be possible and this will lead to significant cost savings. As noted in the introduction, the analysis and discussions in this thesis assumes that the same multi wavelength 2D-WH/TS OCDMA codes are reusable in all groups and all channels.

6.2.3 Proposed Receiver Architecture

At the receiving end of the transmission link, a power splitter is used to split the OTDM signal into N outputs. Figure 6.4 shows the process of receiving each user's data from the hybrid transmitted OTDM traffic. There are three stages involved.

In the first stage, the incoming optical signal containing the combined traffic of all users is time demultiplexed and separated into individual $P \times M$ -User OTDM channels.

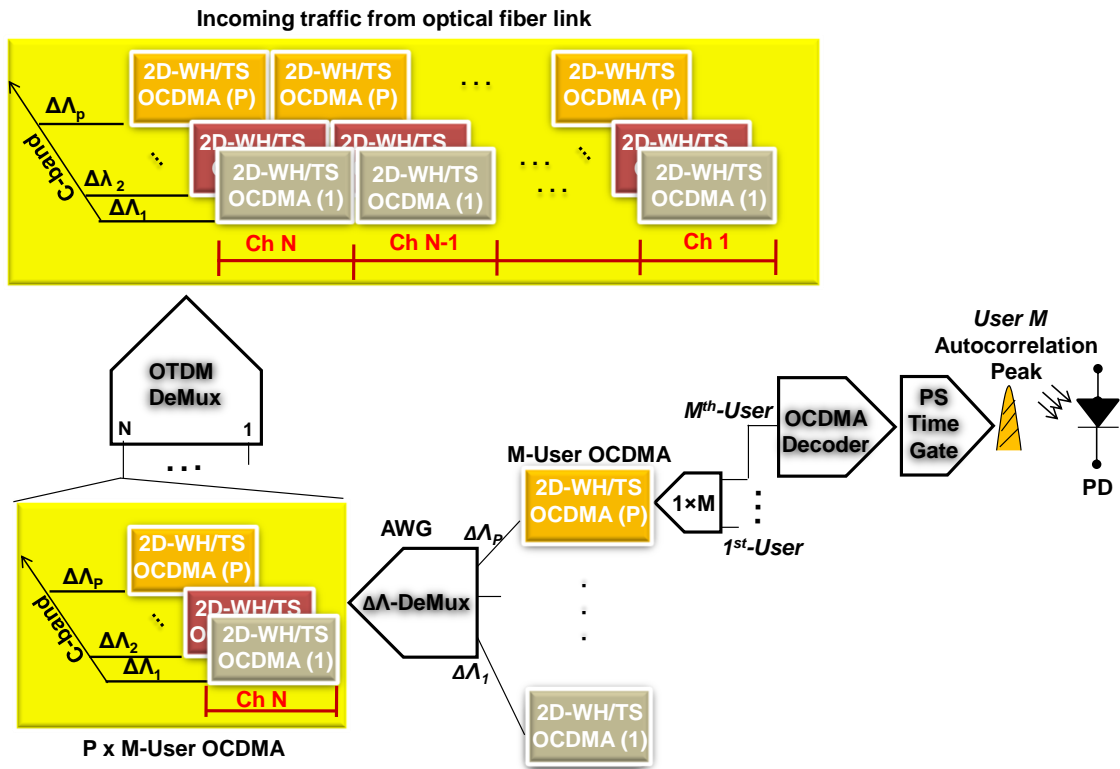


Figure 6.4 Illustration of the stages involved in the demultiplexing of a transmitted $P \times M\text{-User} \times N$ channel hybrid 2D-WH/TS OCDMA over OTDM traffic at the receiver. Where is PD -photodetector, ps is picosecond, AWG is arrayed waveguide grating with channel spacing $\Delta\lambda$.

This demultiplexing can be achieved using all optical Mach-Zehnder-based time gates, driven by a clock signal that is precisely tuned to the channel (timeslot) in which the desired signal is located.

The second stage involves separation of the $P \times M\text{-User}$ OCDMA traffic into standalone $M\text{-User}$ OCDMA traffic. This is done by simple waveband separation (filtering). As shown in figure 6.4, each $M\text{-User}$ OCDMA group can be obtained by passing the demultiplexed signal through an AWG with each output port capable of passing all of the wavelengths in the band $\Delta\lambda_i$.

The final stage is the conventional decoding stage. The $M\text{-User}$ OCDMA traffic signal is splitted M times and the autocorrelation-peak signal for User M can thereafter be extracted when the encoded signal is passed it

through a decoder matched to User M (desired user) encoder. The transmitted signal at high data rates may suffer from timing jitter, depending on the link length. The effect of timing jitter may significantly cause problems relating to receiver synchronization. Synchronization can be achieved using a clock signal that is either generated from the incoming signal or by sending a separate clock signal from transmitter.

In order to achieve the required performance levels, sampling of the autocorrelation peak is required as will be defined in the calculations in later sections. Because the width of the autocorrelation peak is in the order of few picoseconds, picosecond sampling must also be implemented. One advantage of extracting the clock signal from the incoming signal is the possibility of reducing timing jitter and obtaining pulses that are fast enough to create picosecond sampling window. All-optical clock recovery from OCDMA signal was previously demonstrated in [108] [109], showing that it was possible to extract a picosecond clock signal from the autocorrelation output of an OCDMA decoder.

6.3 Scalability and Power Calculations

In fibre-optic communications, standard erbium doped fibre amplifiers EDFA are capable of operating in the C band and L band (ranging from 1528 nm to 1605 nm). Here the calculations focus on the C-band optical spectrum band Λ ranging from 1535 nm to 1565 nm. Thus, if the 30 nm optical spectrum band is divided using ITU-standard 100 GHz ($\delta\lambda = 0.8$ nm) filters, $w = 8$, and $\Delta\lambda_i = 6.4$ nm, from Eq. 6.1, $P = 4$ wavelength sub bands can be conveniently obtained.

The calculation of number of simultaneous users presented here is in line with previous system scalability calculations in chapter 5. The chip-asynchronous, hard-limiting performance of a $(P \times \Delta\lambda, w, N_c)$ 2D-WH/TS OCDMA system can be modified from [Eq. (1.6), [10]] as

$$\begin{aligned}
P_e &= Pr(1 - copyerror|data bit 1) Pr(data bit 1) \\
&\quad + Pr(1 - copyerror|data bit 0) Pr(data bit 0) \\
&= \frac{1}{2} Pr(1 - copyerror|data bit 0)
\end{aligned}$$

$$P_e = \frac{1}{2} \sum_{j=0}^w (-1)^j \binom{w}{j} \left(1 - \frac{j q_{1,1}}{w}\right)^{K-1} \quad (7.3)$$

Where w is the code weight, and K is the number of simultaneous users, The factor $\frac{1}{2}$ is due to on off keying (OOK) with equal probability of transmitting data bit 1s and 0s. For a code with length N_c , The hit probabilities of the 2D-WH/TS codes with the maximum cross-correlation value of one (e.g., carrier-hopping prime codes [98]) is given by

$$q_{1,1} = \frac{w}{2N_c} \quad (7.4)$$

It is important to note that Eq. 7.3 is valid for an OCDMA system for which sampling of the autocorrelation peak is implemented. The sampling window T_s is incorporated into Eq. 7.4 as $T_s = T_b/N_c$ where T_b is the bit period. The case of $P = 1$ is referred to as a “standalone” M -User 2D-WH/TS OCDMA system.

Figure 6.5 shows the performance curve for the standalone OCDMA system with $w = 8$, three curves showing the performance of the standalone system when the 2D-WH/TS codes are formed using pulses with 5 ps, 8 ps and 10 ps pulse width respectively are presented.

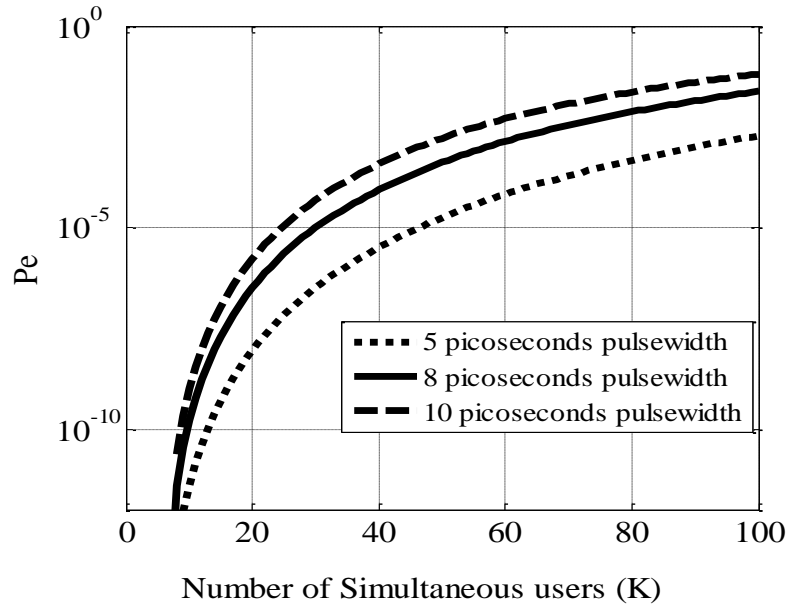


Figure 6.5 Performance curve for OCDMA system with using 2D-WH/TS codes with 5 ps, 8 ps and 10 ps pulse width.

From the figure, the standalone system with $P = 1$ will support 19, 17, and 15 simultaneous users with pulse width of 5ps, 8ps and 10ps respectively having bit error probability $P_e = 10^{-9}$.

Results in figure 6.6 show that a system with four OCDMA groups will have $P = 4$ and as such the number of simultaneous users (for codes with 8ps pulse width) will increase from 17 to 68 simultaneous users. It can be observed that this (without OTDM) is comparable to the scalability obtained for the OCDMA over OTDM reported in the previous chapter.

If such system is then overlaid over every channel of a four-channel OTDM system, up to 272 simultaneous users will be supported (see figure 6.5) without deterioration in performance.

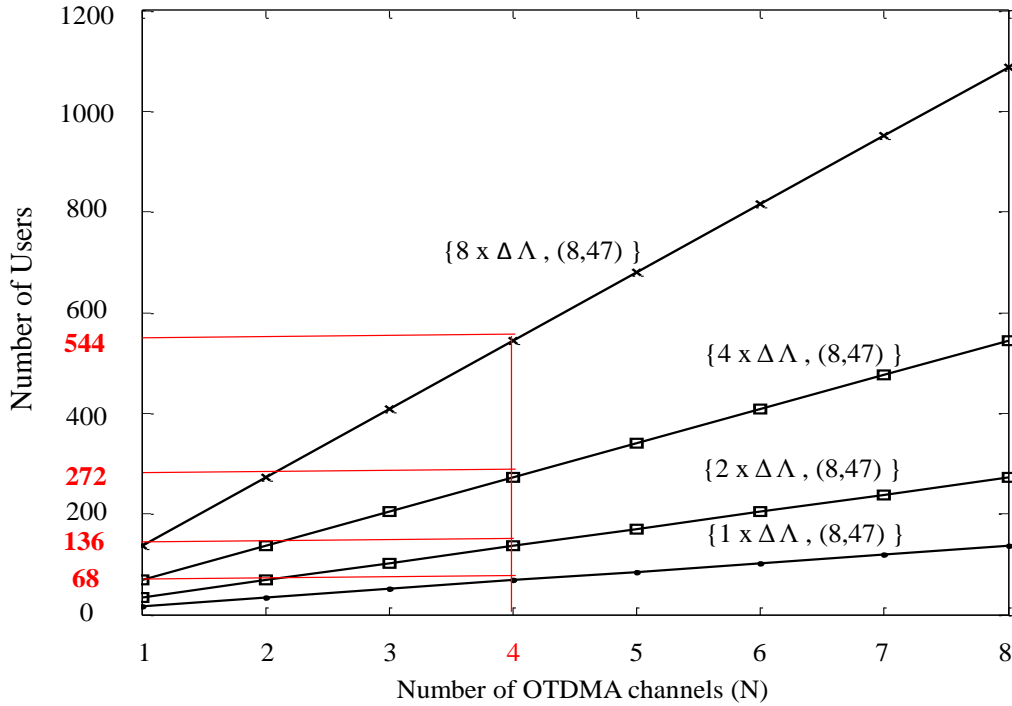


Figure 6.6 Scalability calculations for the hybrid $P \times M$ -User $\times N$ channel OCDMA over OTDM system.

Also as seen from figure 6.6, the number of simultaneous users can be scaled up to 544 when the number of OCDMA groups per OTDM channel is increased to $P=8$.

Power budget calculations include splitting losses, transmission loss over the demonstrated distance, and the losses incurred by individual devices. It is estimated that a 30 dB/10 dBm erbium doped fibre amplifier (EDFA) is needed to amplify the coded signals in each OCDMA group (within a band of wavelengths $\Delta\lambda_i$ over four timeslots) when a photo-receiver with 30dBm sensitivity is used in each user. This EDFA will be capable of supporting 128 simultaneous users, based on ($w = 8, N_c = 47$)-OCDMA over 4-channel OTDM ($P_e = 10^{-9}$).

6.4 Chapter Summary

In this chapter a novel architecture to further improve the scalability of the demonstrated hybrid OCDMA–OTDM system has been proposed and

analysed. This new architecture was designed to increase the number of simultaneous users without necessarily causing a reduction in bitrate per user.

To achieve this goal, a third dimension was added to the original OCDMA-OTDM scheme by allowing multiple OCDMA user-groups be assigned to different wavelength bands, and they all were transmitted simultaneously within each OTDM time slot channel.

The 2D-WH/TS codes (based on multi-wavelength picosecond pulses) were reusable in P wavelength bands and each band supported one of $P M$ -User OCDMA user-groups operating in each of N OTDM channels. This novel approach also supports code and hardware reuses and can therefore offer cost savings. The OCDMA-OTDM system performance analysis, that was conducted based on $P=8$, $N=4$, $M=17$, showed that up to 544 users could be transmitting simultaneously. (Compared to only 68 simultaneous users in our original hybrid scheme)

Chapter 7

Conclusion and Future Work

7.1 Conclusion

The study of the scalability of incoherent OCDMA implementations was the main focus of my research presented in this thesis. In particular, attention was directed at understanding the behaviours of optically encoded data using incoherent two-dimensional WH/TS OCDMA based on picosecond optical pulses.

The major contributions of the thesis will be summarised in the following paragraphs in the order of appearance within the thesis.

After an extensive discussion on the fundamental OCDMA concepts with special emphasis on code generation, an experimental analysis of an integrated 2D-WH/TS incoherent OCDMA encoder was conducted in chapter three. This then led to the demonstration of a novel power saving OCDMA transmitter architecture. The chapter was concluded with a discussion on the effects of multiple access interference in OCDMA systems.

For the first time to our knowledge, the investigation of the effect of temperature fluctuations on the integrity of 2D-WH/TS OCDMA signals in which the optical code was generated using picosecond pulses have been carried out. Analysis conducted in the course of the research, showed that proper attention is required when designing such systems because the picosecond pulse based optical codes are very sensitive to thermally induced fibre dispersion. By deriving the relationship between thermally induced pulse broadening and fibre transmission distance, It was found that even after conventional dispersion compensation methods have been implemented, temperature induced pulse broadening can significantly degrade system performance thereby reducing the number of users that can simultaneously be served using the same transmission media when propagating over few kilometres of optical fibre.

Also, an extensive investigation of a novel method to ensure high quality OCDMA transmission by developing new methods for mitigating multiple access interference which is prevalent in multi-wavelength OCDMA systems was conducted in chapter 5. To the best of my knowledge, this is the first time this technique has been proposed and experimentally demonstrated for OCDMA systems. The proposed method enables in-situ power equalization of the wavelength pulses contained in an OCDMA code without having to selectively process the individual wavelength pulses. The experimentally verified equalization works by manipulating the polarisation of OCDMA signal using a module combining a polarisation controller followed by a short section (~60cm) of multimode fibre inserted right before the OCDMA decoder.

For OCDMA to be a viable alternative to other well developed multiple access technologies like WDM, and OTDM, it has to be able to support more simultaneous users without compromising performance. In chapter 6 and 7 of this thesis, two novel solutions were proposed for improving the scalability of OCDMA. The first solution in chapter 6 described a hybrid combination of OCDMA and OTDMA. For the first time to the best of my knowledge, a proof of concept experiment was conducted which verified the possibility of successfully transmitting multiuser OCDMA signals in different channels of an OTDM system. The novel experiment was conducted as a real life field trial over a fully dispersion compensated 17 km fibre optic transmission link between university of Strathclyde and Glasgow university.

The second solution proposed and comprehensively analysed for improving the scalability of OCDMA is the hybrid combination of OCDMA-OTDM-WDM. This solution was shown in chapter 7 to significantly increase the number of simultaneous users. To the best of my knowledge, this is the first time this technique has been proposed for OCDMA systems. It was observed that as OCDMA was fundamentally prone to multi-access interference because of its method of encoding and decoding, combining an OCDMA system that have reduced number of simultaneous users but superior performance with techniques like OTDM and WDM whose methods for effective inter-channel interference mitigation are well developed, will significantly enhance the take up and penetration of OCDMA technology.

7.2 Future Work

The investigation presented in this thesis was primarily focussed on incoherent OCDMA. There are a number of areas for further research based on the results obtained in this thesis.

Firstly, due to the unavailability of specially fabricated fibre Bragg grating en/decoder pairs, the proposed power saving architecture was not experimentally demonstrated. Therefore it will be interesting in future to

experimentally verify the novel OCDMA transmitter architecture and the associated power savings.

Also, it will be worthwhile to investigate the thermal behaviour of the 2D-WH/TS codes taking into consideration the randomness of the temperature fluctuations and also to further study these codes when utilised for applications similar to optical interconnects in datacentres. This is of interest because the temperature conditions under which datacentre equipment operate is different from what applies when the optical fibre is buried under ground.

Another possible area of future research is to investigate the possibility of all optical clock recovery from the hybrid OCDMA-OTDM system described in this thesis with a view to utilizing the recovered clock in the time demultiplexing of the individual channels. Although all optical clock recovery from OCDMA signal and OTDM signals have been investigated and demonstrated separately it will be interesting to further conduct a study of the possibility, behaviour and stability of clock recovered from the hybrid signal.

References

- [1] P. Z. Dashti, C. F. Lam, R. Urata, H. Liu, M. Medin, “Optoelectronic integration for broadband optical access networks,” in *IEEE Photonics Conference (IPC)*, 2012.
- [2] Z. Drago, K. Visnja, G. Kresimir, “Business case assessments of fixed and mobile broadband access networks deployments,” in *20th International Conference on Software, Telecommunications and Computer Networks (SoftCOM), 2012*, 2012.
- [3] International Telecommunication Union, “World Telecommunication /ICT Indicators database,” 04 July 2013. [Online]. Available: http://www.itu.int/en/ITU-D/Statistics/Documents/statistics/2013/ITU_Key_2005-2013_ICT_data.xls. [Accessed 22 April 2014].
- [4] G. Kramer, M. D. Andrade, R. Roy, P. Chowdhury, , “Evolution of Optical Access Networks: Architectures and Capacity Upgrades,” in *Proceedings of the IEEE*, 2012.
- [5] S. Kartalopoulos, Understanding SONET/SDH and ATM: Communications Networks for the Next Mellennium, Wiley-IEEE Press, 1999.

- [6] J. Zheng, H. Mouftah, *Optical WDM Networks: Concepts and Design Principles*, Wiley-IEEE Press, 2004.
- [7] Y. Benlachtar, P.M. Watts, R. Bouziane, P.A. Milder, R.J. Koutsoyannis, J.C. Hoe, M. Püschel, M. Glick, R.I. Killey, "Real-Time Digital Signal Processing for the Generation of Optical Orthogonal Frequency-Division-Multiplexed Signals," *IEEE Journal of Selected Topics in Quantum Electronics*, vol. 16, no. 5, pp. 1235-1244, 2010.
- [8] C - S. Brès, Y - K. Huang, I. Glesk, and P. R. Prucnal, "Scalable asynchronous incoherent optical CDMA," *J. Opt. Net.*, vol. 6, no. 6, pp. 599-615, June 2007.
- [9] I. Andonovic, L . Tancevski, "Incoherent optical code division multiple access systems," in *Proceedings of IEEE 4th International Symposium on Spread Spectrum Techniques and Applications*, 1996.
- [10] I. Glesk , P. R. Prucnal and I. Andonovic, "Incoherent ultrafast OCDMA receiver design with a 2 ps all-optical time gate to suppress multiple access interference," *IEEE Journal of Selected. Topics in Quantum Electronics*, vol. 14, no. 3, pp. 861-867, 2008.
- [11] G. C. Yang, W. C. Kwong, *Prime codes with applications to cdma optical and wireless networks*, Boston: Artech House, 2002.
- [12] I. Glesk, Y. -K. Huang, C. S. Brès, and P. R. Prucnal, "Design and demonstration of a novel Optical CDMA platform for avionics

- applications,” *Opt. Communications*, vol. 271, pp. 65-70, March 2007.
- [13] A. C. Chen, “Overview of code division multiple access technology for wireless communications,” in *Proceedings of the 24th Annual Conference of the IEEE Industrial Electronics Society*, 1998.
- [14] A. J. Viterbi, *CDMA*, New York: Addison-Wesley, 1995.
- [15] N. Donmez, “A game-theoretic approach to efficient power control in CDMA data network,” in *International Symposium on Innovations in Intelligent Systems and Applications (INISTA)*, 2011.
- [16] P. R. Prucnal, M. A. Santoro and S. K. Sehgal, “Ultrafast All-Optical Synchronous Multiple Access Fiber Optical Networks,” *IEEE Journal on Selected Areas in Communications*, vol. 4, no. 9, pp. 1484-1493, 1986.
- [17] Z. Gao, X. Wang, N. Kataoka, N. Wada, “Stealth transmission of time domain spectral phase encoded OCDMA signal over WDM system,” in *Optical Fiber Communication (OFC), collocated National Fiber Optic Engineers Conference*, 2010.
- [18] M. A. Santoro, P . R. Prucnal, “Asynchronous fiber optic local area network using CDMA and optical correlation,” *Proceedings of the IEEE*, vol. 75, no. 9, pp. 1336-1338, 1987.
- [19] P. R. Prucnal, M. F. Krol, J. L. Stacy, “Demonstration of a rapidly tunable optical time-division multiple-access coder,” *IEEE Photonics*

Technology Letters, vol. 3, no. 2, pp. 170-172, 1991.

- [20] J. Y. Hui, "Pattern Code Modulation and Optical Decoding – A Novel Code-Division Multiplexing Technique for Multifiber Networks," *IEEE Journal on Selected Areas in Communications*, vol. 3, no. 6, pp. 916-927, Nov. 1985.
- [21] P. R. Prucnal, M. A. Santoro and T. R. Fan, "Spread Spectrum Fiber-Optic Local Area Network Using Optical Processing," *Journal of Lightwave Technology*, vol. 4, no. 5, pp. 547-554, May 1986.
- [22] X. Wang, Z. Gao, B. Dai, X. Wang, N. Kataoka, N. Wada, "Fast optical code reconfigurable technique for secure optical communication," in *13th International Conference on Transparent Optical Networks (ICTON)*, 2011.
- [23] G. Cincotti, N. Kataoka, N. Wada, K. Kitayama, "Perspectives of optical coding/decoding techniques in OCDMA networks," in *Asia Communications and Photonics Conference and Exhibition (ACP)*, 2009.
- [24] X. Wang, N. Wada, K. Kitayama, "Performance degradation in coherent OCDMA due to receivers's bandwidth limit and improvement by using optical thresholding," in *The 18th Annual Meeting of the IEEE Lasers and Electro-Optics Society*, 2005.
- [25] V. Baby, C. S. Brès, L. Xu, I. Glesk, and P. R. Prucnal, "Wavelength

- aware receiver for enhanced 2D OCDMA system performance,” *Electronics Letters*, vol. 40, no. 6, pp. 385-387, 2004.
- [26] P. Toliver, S. Etemad, R. Mendenez, “Coherent Optical CDMA Systems,” in *Optical Code Division Multiple Access: Fundamentals and Applications*, Boca Raton, CRC Press, 2006, pp. 165-196.
- [27] S. Tainta, W. Amaya, R. Garcia, M. J. Erro, M. J. Garde, S. Sales, M. A. Miguel, “Experimental demonstration of a FBG-based temporal optical pulse shaping scheme dual to spatial arrangements for its use in OCDMA systems,” in *Asia Communications and Photonics Conference and Exhibition (ACP)*, 2009.
- [28] A. M. Weiner, J. P. Heritage, J. A. Salehi, “Encoding and Decoding of Femtosecond Pulses,” *Optics Express*, vol. 13, pp. 300-303, 1989.
- [29] J. A. Salehi, “Emerging optical code-division multiple access communication systems,” *IEEE Network*, vol. 3, no. 2, pp. 31-39, 1989.
- [30] H. Ghafouri-Shiraz, M. Karbassian, “Incoherent Temporal OCDMA Networks,” in *Optical CDMA Networks: Principles, Analysis and Applications*, WILEY-IEEE PRESS EBOOK CHAPTERS, 2011, pp. 171- 212.
- [31] C. S. Brès, I. Glesk, P. R. Prucnal, “Experimental demonstration of a 2D incoherent transparent OCDMA path router,” in *Digest of the LEOS Summer Topical Meetings*, July 2005.

- [32] C. Michie, R. Atkinson, I. Andonovic, I. Glesk, P. R. Prucnal, K. Sasaki, and G. Gupta, "Interferometric Noise Characterisation of a 2-D Time spreading Wavelength Hopping OCDMA Networks using FBG Encoding/Decoding," in *International Conference on Transparent Optical Networks (ICTON)*, 2007.
- [33] L. Tancevski, I. Andonovic, "Wavelength hopping time spreading code-division multiple-access systems," *Electronic Letters*, vol. 30, pp. 1388-1390, 1994.
- [34] D. Sarwate, "Reed-Solomon Codes and the Design of Sequences for Spread Spectrum Multiple access Communications," in *Reed-Solomon Codes and their Applications*, NJ, IEEE Press, 1994, pp. 175-204.
- [35] T. Conway, "Galois field arithmetic over GF(pm) for high-speed/low-power error-control applications," *IEEE Transactions on Circuits and Systems I: Regular Papers*, vol. 51, no. 4, pp. 709-717, 2004.
- [36] G. C. Yang, W. C. Kwong, "Performance analysis of optical CDMA with prime codes," *Electronics Letters*, vol. 31, no. 7, pp. 569-570, 1995.
- [37] J. G. Zhang, W. C. Kwong, S. Mann, "Construction of $2n$ extended prime codes with cross-correlation constraint of one," *IEE Proceedings on Communications*, vol. 145, no. 5, pp. 297-303, 1998.
- [38] W.C. Kwong, G. C. Yang, "Construction of $2n$ prime-sequence codes for optical code division multiple access," *IEE Proceedings*, vol. 142, no. 3,

pp. 141-150, 1995.

- [39] G. -C. Yang and W. C. Kwong, Prime codes with applications to cdma optical and wireless networks, Boston: Artech House, 2002.
- [40] N. Bin, J. S. Lehnert, "Performance of an incoherent temporal-spreading OCDMA system with broadband light sources," *Journal of Lightwave Technology*, vol. 23, no. 7, pp. 2206-2214, 2005.
- [41] C. S. Brès, I. Glesk, P. R. Prucnal, "Demonstration of an eight-user 115-Gchip/s incoherent OCDMA system using supercontinuum generation and optical time gating," *IEEE Photonics Technology Letters*, vol. 18, no. 7, pp. 889-891, 2006.
- [42] P. Horak, K. K. Chen, S. Alam, S. Dasgupta, D. J. Richardson, "High-Power Supercontinuum generation with picosecond pulses," in *12th International Conference on Transparent Optical Networks (ICTON)*, 2010.
- [43] C. S. U. Wang, N. Wada, K. I. Kitayama, "Multi-user asynchronous coherent OCDMA system," in *Optical Fiber Communication and the National Fiber Optic Engineers Conference*, 2009.
- [44] R. Sargent, "Recent advances in thin film filters," in *Optical Fiber Communication Conference*, 2004.
- [45] N. Minato, H. Tamai, H. Iwamura, S. Kutsuzawa, S. Kobayashi, K. Sasaki, A. Nishiki, "Demonstration of 10Gbit/s-Based Time-Spreading

- and Wavelength-Hopping Optical-Code-Division Multiplexing Using Fiber-Bragg-Grating En/Decoder,” *IEICE Transactions on Communications*, vol. E88, no. 10, pp. 3848-3854, 2005.
- [46] I. Glesk, V. Baby, C. S. Bres, P. R. Prucnal, W. C. Kwong, “Design and demonstration of a novel incoherent optical CDMA system,” in *IEEE Military Communications Conference, (MILCOM 2005)*, 2005.
- [47] I. Glesk, V. Baby, C. -S. Brès, Y. -K. Huang, and P. R. Prucnal, “Performance Enhancement of Optical CDMA Systems Using Ultrafast All-Optical Sampling,” in *In proceedings IEEE-LEOS 2005 Avionics Fiber-Optics Conference*, Minneapolis, MN, 20-22 Sept. 2005.
- [48] V. Baby, C. -S. Bres, I. Glesk, L. Xu, P. R. Prucnal, “Wavelength aware receiver for enhanced 2D OCDMA system performance,” *Electronics Letters*, vol. 40, no. 6, pp. 385- 387, 18 March 2004.
- [49] S. K. Idris, T. B. Osadola, I. Glesk, “OCDMA receiver with built-in all optical clock recovery,” *Electronic letters*, vol. 49, no. 2, pp. 143,144, January 2013.
- [50] W. Zou, H. Ghafouri-Shiraz, “Proposal of a novel code for spectral amplitude coding optical CDMA systems,” *IEEE Photonics Tech. Letters*, vol. 14, no. 3, pp. 414-416, 2002.
- [51] C. Goursaud, A. Julien-Vergonjanne, C. Aupetit-Berthelemot, J. P. Cances, J. M. Dumas, “MAI Impact Suppression with Parallel

- Interference Cancellation in DS-OCDMA Systems using Prime Codes,” in *International Conference on Acoustics, Speech and Signal Processing (ICASSP) 2006*, 2006.
- [52] N. Kataoka, N. Wada, Xu Wang, G. Cincotti and K. Kitayama, “Demonstration of 10Gbps, 4-user, OCDMA transmission over 59km single mode fiber without inline dispersion compensation,” in *Optical Fiber Communication (OFC)*, 2010.
- [53] J. Santhanam, C. J. McKinstrie, T. I. Lakoba, G. R. Agrawal, “Effects of pre- and post-compensation on timing jitter in dispersion-managed systems,” in *Conference on lasers and Electro Optics Technical Digest*, 2001.
- [54] B. Olsson and P. A. Andrekson, “A simple method for loss and coupling ratio determination in fused fiber couplers,” *IEEE Photonic Technology Letters*, vol. 8, no. 3, pp. 399-401, March 1996.
- [55] H. C. Ji, J. H. Lee, Y. C. Chung, “System outage probability due to dispersion variation caused by seasonal and regional temperature variations,” in *Optical Fiber Communication Conference Technical Digest*, 2005.
- [56] D. J. G. Mestdagh, *Fundamentals of Multiaccess Optical Fiber Networks*, Boston: Artech House, 1995.
- [57] G.D. Brown, “Chromatic dispersion measurement in graded-index

- multimode optical fibers,” *Journal of Lightwave Technology*, vol. 12, no. 11, pp. 1907-1909, 1994.
- [58] J. Hamp, M. J. Wright, M. Hubbard, B. Brimacombe, “Investigation into the temperature dependence of chromatic dispersion in optical fiber,” *IEEE Photonics Technology Letters*, vol. 14, no. 11, pp. 1524-1526, 2002.
- [59] K. H. Kim, H. K. Lee, S. Y. Park, E - H. Lee, “Calculation of dispersion and nonlinear effect limited maximum TDM and FDM bit rates of transform-limited pulses in single-mode optical fibers,” *Journal of Lightwave Technology*, vol. 13, no. 8, pp. 1597-1605, 1995.
- [60] A. Walter, G. S. Schaefer, “Chromatic dispersion variations in ultra-long-haul transmission systems arising from seasonal soil temperature variations,” in *Optical Fiber Communication Conference and Exhibition*, 2002.
- [61] T. Kato, Y. Koyano, M. Nishimura, “Temperature dependence of chromatic dispersion in various types of optical fiber,” *Optical Letters*, vol. 25, pp. 1156-1158, 2000.
- [62] E. K. H. Ng, G. E. Weichenberg, E. H. Sargent, “Dispersion in multi-wavelength Optical Code Division Multiple Access Systems: impact and remedies,” *IEEE Trans. Communication*, vol. 50, no. 11, pp. 1811-1816, Nov 2002.

- [63] C. S. Brès, I. Glesk, P. R. Prucnal, "Demonstration of a transparent router for wavelength-hopping time-spreading Optical CDMA," *Optical Communications*, vol. 254, pp. 58-66, 2005.
- [64] C. S. Brès, Y. K. Huang, I. Glesk, P. R. Prucnal, "Scalable asynchronous incoherent Optical CDMA," *Journal of Optical Networking*, vol. 6, no. 6, pp. 599-615, June 2007.
- [65] V. Baby, C. S. Brès, L. Xu, I. Glesk, P. R. Prucnal, "Demonstration of differentiated service provisioning with 4-node 253Gchip/s fast frequency hopping time spreading OCDMA," *Electron Lett. vol. 40 no. 12, pp. 755-756, 2006.*, vol. 40, no. 12, pp. 755-756, 2006.
- [66] N. Minato, H. Tami, H. Iwamura, S. Kutsuzawa, S. Kobayashi, K. Sasaki, and A. Nishiki, "Demonstration of 10Gbit/s-based time-spreading and wavelength-hopping optical-code-division-multiplexing using fiber-bragg-grating en/decoder," *IEICE Trans. Communication*, Vols. E88-B, no. 10, pp. 3848-3854, Oct 2005.
- [67] V. Jyoti, R. S. Kaler, "Design and implementation of 2-dimensional wavelength/time codes for OCDMA," *Int. J. Light Electron Opt*, vol. 122, no. 10, pp. 851-857, 2010.
- [68] G. C. Yang, W. C. Kwong, Prime codes with applications to cdma optical and wireless networks, Norwood: Artech House, 2002.
- [69] G. Ghosh, M. Endo, T. Iwasaki, "Temperature-dependent Sellmeier

- coefficients and chromatic dispersions for some optical fiber glasses,” *IEEE Journal of Lightwave Technology*, vol. 12, no. 8, pp. 1338-1342, August 1994.
- [70] M. J. Hamp, J. Wright, M. Hubbard, B. Brimacombe, “Investigation into the temperature dependence of chromatic dispersion in optical fiber,” *IEEE Photonics Technology Letters*, vol. 14, no. 11, pp. 1524-1526, Nov 2002.
- [71] P. R. Prucnal, *Optical CDMA: Fundamentals and Applications*, New York: Taylor & Francis Books, 2006.
- [72] C. H. Hsieh, G. C. Yang, C. Y. Chang, W. C. Kwong, “Multilevel prime codes for optical CDMA systems,” *J. Opt. Commun. Netw.*, vol. 1, no. 7, pp. 600-607, December 2009.
- [73] V. Baby, C. S. Bres, I. Glesk, L. Xu, P. R. Prucnal, “Wavelength aware receiver for enhanced 2D OCDMA system performance,” *Electronics Letters*, vol. 40, no. 6, pp. 385-387, March 2004.
- [74] X. Wang and K. Kitayama, “Analysis of beat noise in coherent and incoherent time-spreading OCDMA,” *Journal of Lightwave Technology*, vol. 22, no. 10, pp. 2226-2235, Oct 2004.
- [75] M. Rochette, L. A. Rusch, “Spectral efficiency of OCDMA systems with coherent pulsed sources,” *Journal of Lightwave Technology*, vol. 23, no. 3, pp. 1033-1038, March 2005.

- [76] Y. Zhang, H. Chen, Z. Si; H. Ji, and S. Xie, "Design of FBG en/decoders in coherent 2d time-wavelength OCDMA systems," *IEEE Photonics Technology Letters*, vol. 20, no. 11, pp. 891-893, June 2008.
- [77] N. Minato, H. Tamai, H. Iwamura, S. Kutsuzawa, S. Kobayashi, K. Sasaki, and A. Nishiki, "Demonstration of 10Gbit/s-Based Time-Spreading and Wavelength-Hopping Optical-Code-Division-Multiplexing Using Fiber-Bragg-Grating En/Decoder," *IEICE Trans. Comm.*, Vols. E88-B, no. 10, pp. 3848-3854, Oct. 2005.
- [78] L. Tancevski and I. Andonovic, "Wavelength hopping time spreading code-division multiple-access systems," *Electronic Letters*, vol. 30, pp. 1388-1390, 1994.
- [79] L. B. Soldano, E. C. M. Pennings, "Optical multi-mode interference devices based on self-imaging: Principles and applications," *IEEE Journal of Lightwave Technology*, vol. 13, no. 4, pp. 615-627, 1995.
- [80] Q. Wang, G. Farrell, "All-fiber multimode-interference-based refractometer sensor: Proposal and design," *Optics Letters*, vol. 31, no. 3, pp. 317-319, 2006.
- [81] Q. Wang, G. Farrell, W. Yan, "Investigation on Single-Mode–Multimode– Single-Mode Fiber Structure," *Journal of Lightwave Technology*, vol. 26, no. 5, pp. 512-519, 2008.
- [82] A. M. Hatta , G. Farrell , Q. Wang , G. Rajan , P. Wang and Y.

- Semenova, "Ratiometric wavelength monitor based on singlemode-multimode-singlemode fiber structure," *Microwave Optics Technology Letters*.
- [83] W. S. Mohammed , P. W. E. Smith and X. Gu , "All-fiber multimode interference bandpass filter," *Optical Letters*, vol. 31, no. 17, pp. 2547-2549, 2006.
- [84] S. S. -H. Yam, F. -T. An , M. E. Marhic and L. G. Kazovsky, "Polarization sensitivity of 40 Gb/s transmission over short-reach 62.5 μm multimode fiber using single-mode transceivers," in *Opt. Fiber Commun. Conference*, 2004.
- [85] T. Itoh, H. Fukuyama, S. Tsunashima, E. Yoshida, Y. Yamabayashi, M. Muraguchi, H. Toba, H. Sugahara, "1-km transmission of 10 Gbit/s optical signal over legacy MMF using mode limiting transmission and incoherent light source," in *Optical Fiber Communication Conference*, 2005.
- [86] M. B. Othman, J. B. Jensen, X. Zhang, and I. T. Monroy, "Performance evaluation of spectral amplitude codes for OCDMA PON," in *15th International Conference on Optical Network Design and Modeling (ONDM)*, 2011.
- [87] G. -K Chang, A. Chowdhury, J. Zhensheng, H. -C Chien, M. -F Huang, Y. Jianjun, and G. Ellinas, "Key Technologies of WDM-PON for Future Converged Optical Broadband Access Networks [Invited]," *J. Opt.*

Net., vol. 1, no. 4, pp. C35-C50, Sept 2009.

- [88] S. Kimura, "10-Gbit/s TDM-PON and over-40-Gbit/s WDM/TDM-PON systems with OPEX-effective burst-mode technologies," in *OFC 2009*, 2009.
- [89] C. Bock, J. Prat, S. D. Walker, "Hybrid WDM/TDM PON using the AWG FSR and featuring centralized light generation and dynamic bandwidth allocation," *IEEE Journal of Lightwave Technology*, vol. 23, no. 12, pp. 3981-3988, Dec 2005.
- [90] C. Bhar, G. Das, A. Dixit, B. Lannoo, D. Colle, M. Pickavet, P. Demeester, "A Novel Hybrid WDM/TDM PON Architecture Using Cascaded AWGs and Tunable Components," *Journal of Lightwave Technology*, vol. 32, no. 9, pp. 1708-1716, May 2014.
- [91] C. -S. Brès, Y. -K. Huang, I. Glesk, and P. R. Prucnal, "Scalable asynchronous incoherent optical CDMA," *J. Opt. Net.*, vol. 6, no. 6, pp. 599-615, June 2007.
- [92] S. G. Park and A. M. Weiner, "Performance of Asynchronous Time-Spreading and Spectrally Coded OCDMA Systems," *Journal of Lightwave Technology*, vol. 26, no. 16, pp. 2873-2881, Aug 2008.
- [93] L. Zhou, X. Cheng, Y. -K. Yeo, and L. H. Ngoh, "Hybrid WDM-TDM PON architectures and DWBA algorithms," in *5th International ICST Conference on Communications and Networking in China*

(*CHINACOM 2010*), 2010.

- [94] S. Yoshima, N. Nakagawa, J. Nakagawa, and K. Kitayama, "10G-TDM-OCDMA-PON systems," in *15th OptoElectronics and Comms Conference (OECC 2010)*, 2010.
- [95] P. C Teh, M. Ibsen, J. H. Lee, P. Petropoulos, D. J. Richardson, "Demonstration of a four-channel WDM/OCDMA system using 255-chip 320-Gchip/s quaternary phase coding gratings," *IEEE Photonics Technology Letters*, vol. 14, no. 2, pp. 227-229, Feb 2002.
- [96] N. W. G. C. K. K. N. Kataoka, "2.56 Tbps (40-Gbps \times 8-wavelength \times 4-OC \times 2-POL) asynchronous WDM-OCDMA-PON using a multi-port encoder/decoder," in *European Conference and Exhibition on Optical Communication (ECOC)*, 2011.
- [97] I. Glesk, K. I. Kang, and P. R. Prucnal, "Demonstration of Ultrafast All-Optical Packet Routing," *Electron Letters*, vol. 33, no. 9, pp. 794-795, 1997.
- [98] G. -C. Yang and W. C. Kwong, *Prime Codes with Applications to CDMA Optical and Wireless Networks*, Norwood: Artech House, 2002.
- [99] W. C. Kwong and G. -C. Yang, *Optical Coding Theory with Prime*, NY: CRC Press, 2013.
- [100] D. T. Nguyen, A. Muramatsu, A. Morimoto, "Femtosecond pulse generation by actively modelocked fibre ring laser," *Electronics*

Letters, vol. 49, no. 8, pp. 556-557, 2013.

- [101] I. Glesk, P. R. Prucnal, and I. Andonovic, "Incoherent ultrafast OCDMA receiver design with 2 ps all-optical time gate to suppress multiple-access interference," *IEEE J.Sel. Topics Quantum Electronics*, vol. 14, no. 3, pp. 861-867, May 2008.
- [102] I. Tsalamanis, E. Rochat, S. D. Walker, M. C. Parker, "Polarization orthogonality preservation in DWDM cascaded arrayed-waveguide grating network," in *Optical Fiber Communication Conference (OFC)*, 2004.
- [103] C. Bock, J. Prat, S. D. Walker, "Hybrid WDM/TDM PON using the AWG FSR and featuring centralized light generation and dynamic bandwidth allocation," *IEEE Journal of Lightwave Technology*, vol. 23, no. 12, pp. 3981-3988, Dec 2005.
- [104] G. -K Chang, A. Chowdhury, J. Zhensheng, H. -C Chien, M. -F Huang, Y. Jianjun, and G. Ellinas, "Key Technologies of WDM-PON for Future Converged Optical Broadband Access Networks [Invited]," *J. Opt. Net.*, vol. 1, no. 4, pp. C35-C50, Sept. 2009.
- [105] C. Bhar, G. Das, A. Dixit, B. Lannoo, D. Colle, M. Pickavet, P. Demeester, "A Novel Hybrid WDM/TDM PON Architecture Using Cascaded AWGs and Tunable Components," *Journal of Lightwave Technology*, vol. 32, no. 9, pp. 1708-1716, May 2014.

- [106] I. Glesk, V. Baby, C. S. Bres, P. R. Prucnal, and W. C. Kwong, "Design and demonstration of a novel incoherent optical CDMA system," in *IEEE Military Commun. Conf.*, 2005.
- [107] N. Sambo, A. D' Errico, C. Porzi, V. Vercesi, M. Imran, F. Cugini, A. Bogoni, L. Potì, P. Castoldi, "Sliceable transponder architecture including multiwavelength source," *IEEE/OSA Journal of Optical Communications and Networking*, vol. 6, no. 7, pp. 590-600, 2014.
- [108] S. K. Idris, T. B. Osadola, and I. Glesk, "OCDMA receiver with built-in all-optical clock recovery," *Electron. Lett.*, vol. 49, no. 2, pp. 143-144, Jan 2013.
- [109] S. K. Idris, T. B. Osadola, and I. Glesk, "Towards self-clocked gate OCDMA receiver," *J. Europ. Opt. Soc.: RP*, vol. 8, no. 13013, pp. 1-6, Jan 2013.